Genetic and Biochemical Characterisation of Light Signalling Events during Arabidopsis Seedling and Stomata Development

Inaugural-Dissertation

zur

Erlangung des Doktorgrades

der Mathematisch-Naturwissenschaftlichen Fakultät

der Universität zu Köln

vorgelegt von

Martin Balcerowicz

aus

Neuss

Berichterstatter:	Prof. Dr. Ute Höcker
	Prof. Dr. Martin Hülskamp
Prüfungsvorsitzender:	Prof. Dr. Wolfgang Werr
Tag der mündlichen Prüfung:	17. Oktober 2013

Table of Contents

List of Figures

List of Tables

List of Abbreviations

°C	degree(s) Celsius
A	adenine
ADP	adenosin-5'-diphosphate
APS	ammonium persulfate
ATP	adenosin-5'-triphosphate
AuxRE	auxin response element
B	blue light
bHLH	basic helix loop helix
bp	basepair(s)
BR	brassinosteroid
BSA	bovine serum albumine
bZIP	basic leucine zipper
C	cytosine
C-terminal	carboxy-terminal
cDNA	complementary DNA
CLS	cytoplasmic localisation sequence
d	day(s)
ddH_2O	double-distilled water
DEX	dexamethasone
DMSO	dimethyl sulfoxide
DNA	deoxyribonucleic acid
DNase	deoxyribonuclease
dNTP	deoxynucleoside triphosphate
dpg	day(s) post germination
DTT	1,4-dithiothreitol
e.g.	exempli gratia (for example)
EDTA	ethylenediaminetetraacetic acid
EMS	ethylmethanesulfonate
ERf	ERECTA family
et al.	et alii (and others)
EtOH	ethanol
FAD	flavin adenine dinucleotide
FMN	flavin mononucleotide
FNB	fast neutron bombardment
FR, FRc	far-red light,continuous far-red light
G	guanine
g, kg, mg, µg, ng	gram(s), kilogram(s), milligram(s), microgram(s), nanogram(s)
g	gravity

GA	gibberellin
GC	guard cell
GFP	green fluorescent protein
GMC	guard mother cell
h	hour(s)
HA	human influenza hemagglutinin
HIR	high irradiance response
HRP	horseradish peroxidase
Hz	Hertz
i.e.	id est (that is)
IAA	indole-3-acetic acid
IAM	indole-3-acetamide
IAOx	indole-3-acetaldoximine
IPyA	indole-3-pyruvic acid
kb	kilobasepair(s)
kDa	kilodalton(s)
L, ml, µl	litre(s), millilitre(s), microlitre(s)
LB	Luria-Bertani
LFR	low fluence response
LOV	light oxygen voltage
LRE	light response element
LRR	leucine-rich repeat
m, cm, mm, µm, nm	meter(s), centimeter(s), millimeter(s), micrometer(s), nanometer(s)
M, mM, µM, nM	molar, millimolar, micromolar, nanomolar
mA	milliampere
MAPK	mitogen-activated protein kinase
mbar	millibar
MeOH	methanol
min	minute(s)
MKK	MAPK kinase
MKKK	MAPK kinase kinase
MMC	meristemoid mother cell
mol, mmol, µmol	mole(s), millimole(s), micromole(s)
mRNA	messenger RNA
MS	Murashige and Skoog
N-terminal	amino-terminal
NAA	1-naphthaleneacetic acid
NLS	nuclear localisation sequence
NPA	1-N-naphthylphthalamic acid
OD	optical density
ORF	open reading frame
oxIAA	2-oxoindole-3-acetic acid
P	probability value
PAGE	polyacrylamide gel electrophoresis
PCR	polymerase chain reaction
PI	propidium iodide

PIPES	piperazine-N,N'-bis(2-ethanesulfonic acid)
PVDF	polyvinyledene difluoride
R, Rc	red light, continuous red light
RNA	ribonucleic acid
RNAi	RNA interference
RNase	ribonuclease
rRNA	ribosomal RNA
RT	room temperature
s	second(s)
SDS	sodium dodecyl sulfate
SEM	standard error of the mean
SI	stomatal index
SLGC	stomatal lineage ground cell
T	thymine
T-DNA	transfer DNA
Taq	*Thermus aquaticus*
TBE	Tris/borate/EDTA
TBS	Tris-buffered saline
TE	Tris/EDTA
TEMED	tetramethylethylenediamine
Tris	tris(hydroxymethyl)aminomethane
Trp	tryptophan
UV	ultraviolet
v/v	volume per volume
VLFR	very low fluence response
w/v	weight per volume
Wc	continuous white light
YEB	yeast extract broth
YFP	yellow fluorescent protein

Nomenclature

Nomenclature of Arabidopsis genes and proteins

AXR3	Gene, locus, wild-type allele
axr3-1	Mutant allele
AXR3	Protein
axr3-1	Mutant protein

Exception: Nomenclature of photoreceptors

PHYB	Gene, locus, wild-type allele
phyB	Mutant allele
PHYB	Apoprotein
phyB	Holoprotein (with chromophore)

Abstract

Plants have evolved a complex regulatory network to perceive and transmit light signals. In Arabidopsis, the COP1/SPA complex acts as a central repressor within this network. It forms part of a ubiquitin ligase that targets activators of the light response for degradation and thereby regulates processes such as seedling development, stomata differentiation, vegetative plant growth and the induction of flowering. But while light signal transduction has been extensively studied over the past decades, light regulation of the COP1/SPA complex is still not fully understood and in some aspects of plant development, additional regulators of the light response are yet to be identified.

In the first part of this study, I investigated the role of the SPA proteins within the COP1/SPA complex and their regulation by light. Light controls COP1 nucleocytoplasmic partitioning, but monitoring COP1 subcellular localisation in a *spa* quadruple mutant showed that its nuclear accumulation in darkness is not changed by the absence of the SPA proteins. However, analysis of protein levels revealed that SPA1 and SPA2 are themselves regulated by rapid, light-induced proteasomal degradation, suggesting that light inactivates COP1/SPA complexes in part by reducing SPA protein levels. SPA2 is more strongly degraded than SPA1, which correlates with the fact that SPA2, but not SPA1, loses its repressor function when seedlings are exposed to light. However, degradation is not the sole reason for the lack of SPA2 function in light-grown seedlings, implying that an additional post-translational mechanism must inactivate the remaining SPA2 protein in the cell.

In the second part of this study, I characterised the Aux/IAA protein AXR3, a repressor of auxin signalling, as a novel regulator of light-dependent stomatal development. The *axr3-1* gain-of-function mutant displays enhanced stomata formation in darkness, which results from increased cell divisions in the stomatal lineage. Epistasis analysis demonstrated that AXR3 acts genetically upstream of the YDA MAP kinase cascade, but in parallel with COP1, TMM and members of the ER family to regulate stomatal development. Furthermore, this study showed that auxin is required for the suppression of stomata formation in darkness while light appears to counteract its effect. Taken together, these results imply that AXR3 regulates stomatal development in response to light and auxin signals although the mechanism of this regulation remains elusive.

Zusammenfassung

Pflanzen haben ein komplexes Regulationsnetzwerk für die Wahrnehmung von Lichtsignalen entwickelt. Der COP1/SPA-Komplex fungiert als zentraler Repressor innerhalb dieses Netzwerks in Arabidopsis. Er ist Teil einer Ubiquitinligase, welche die Degradation von positiven Faktoren der Lichtantwort induziert und damit Prozesse wie Keimlingsentwicklung, Stomatadifferenzierung, vegetatives Pflanzenwachstum und Blühinduktion reguliert. Obwohl die Lichtsignaltransduktion innerhalb der letzten Jahrzehnte umfassend untersucht worden ist, ist die Lichtregulation des COP1/SPA-Komplexes noch nicht vollständig geklärt. Darüber hinaus sind weitere Faktoren für eine normale Lichtantwort erforderlich, doch nicht in allen Bereichen der lichtgesteuerten Entwicklung sind diese Faktoren bereits identifiziert worden.

Im ersten Teil der vorliegenden Arbeit habe ich die Rolle der SPA-Proteine innerhalb des COP1/SPA-Komplexes und ihre Regulation durch Licht untersucht. Licht kontrolliert die Lokalisation von COP1 innerhalb der Zelle, allerdings zeigte die Beobachtung der subzellulären Lokalisation von COP1 in einer *spa* Quadrupelmutante, dass seine Akkumulation im Zellkern in Dunkelheit durch die Abwesenheit der SPA-Proteine nicht beeinflusst wird. Analyse der SPA-Proteinlevel zeigte jedoch, dass SPA1 und SPA2 selbst durch rasche, licht-induzierte Degradation im $26S$-Proteasom reguliert werden, was nahelegt, dass Licht den COP1/SPA-Komplex zumindest zum Teil durch Reduzierung der SPA-Proteinlevel inaktiviert. SPA2 wird stärker degradiert als SPA1, was mit der Tatsache korreliert, dass SPA2, aber nicht SPA1, seine Repressorfunktion verliert, wenn Keimlinge dem Licht ausgesetzt sind. Allerdings ist die Degradation nicht der einzige Grund für die Unterdrückung der SPA2-Repressorfunktion in im Licht gewachsenen Keimlingen, weshalb angenommen werden kann, dass ein weiterer post-translationaler Mechanismus das verbliebene SPA2-Protein in der Zelle inaktiviert.

Im zweiten Teil dieser Arbeit habe ich das Aux/IAA-Protein AXR3, einen Repressor der Auxin-Signaltransduktion, als einen neuen Regulator der lichtabhängigen Stomataentwicklung charakterisiert. Die „Gain-of-function"-Mutation *axr3-1* führt zu verstärkter Stomatabildung in Dunkelheit, welche aus erhöhter Zellteilung innerhalb der Stomata-Zelllinie resultiert. Epistasieanalyse offenbarte, dass AXR3 oberhalb der YDA MAP-Kinasekaskade, jedoch parallel mit COP1, TMM und Mitgliedern der ER-Familie wirkt.

Darüber hinaus konnte gezeigt werden, dass Auxin für die Unterdrückung der Stomataentwicklung im Dunkeln benötigt wird, wohingegen Licht diesem Effekt entgegenwirkt. Zusammengenommen weisen diese Ergebnisse darauf hin, dass AXR3 die Stomataentwicklung in Antwort auf Auxin- und Lichtsignale reguliert, auch wenn der Mechanismus dieser Regulation noch unklar ist.

1 Introduction

1.1 Light signal transduction

Plants have evolved a remarkable degree of plasticity to cope with changes in their environment, thereby ensuring their survival and reproductive success. To this end, they need to perceive environmental factors and adjust their growth and development accordingly. Light is among the most crucial environmental factors as it serves as the plant's primary source of energy. Hence, plants monitor its quality, intensity, direction and periodicity and use this information to modulate many processes throughout their development, including seed germination, seedling de-etiolation, stomata differentiation, phototropic growth, shade avoidance and the transition to flowering (Neff et al., 2000). At the molecular level, a complex regulatory network that includes photoreceptors, transcription factors and components of the protein degradation machinery acts to perceive, transmit and respond to light signals.

1.1.1 Light is perceived by several sets of photoreceptors

In the model plant *Arabidopsis thaliana* (Arabidopsis), five classes of photoreceptors have been described, which regulate many developmental processes in response to different light qualities (Figure 1.1). Among them, phytochromes are the most well characterised. They are dimeric receptors that absorb red (R) and far-red light (FR) through a covalently attached linear tetrapyrrole chromophore, phytochromobilin, and exist in two distinct conformations: they are synthesised in the biologically inactive Pr form, which upon R-absorption is converted to the biologically active Pfr form. Pfr can be reconverted to Pr by absorption of FR or more slowly by dark reversion (Rockwell et al., 2006). This photoconversion results in a dynamic photoequilibrium of Pr and Pfr that allows the plant to measure the ratio of R to FR (Franklin and Quail, 2010).

The Arabidopsis genome contains five phytochrome-encoding genes (*PHYA-E*), which belong to two different classes: *PHYA* encodes the only light-labile type I phytochrome,

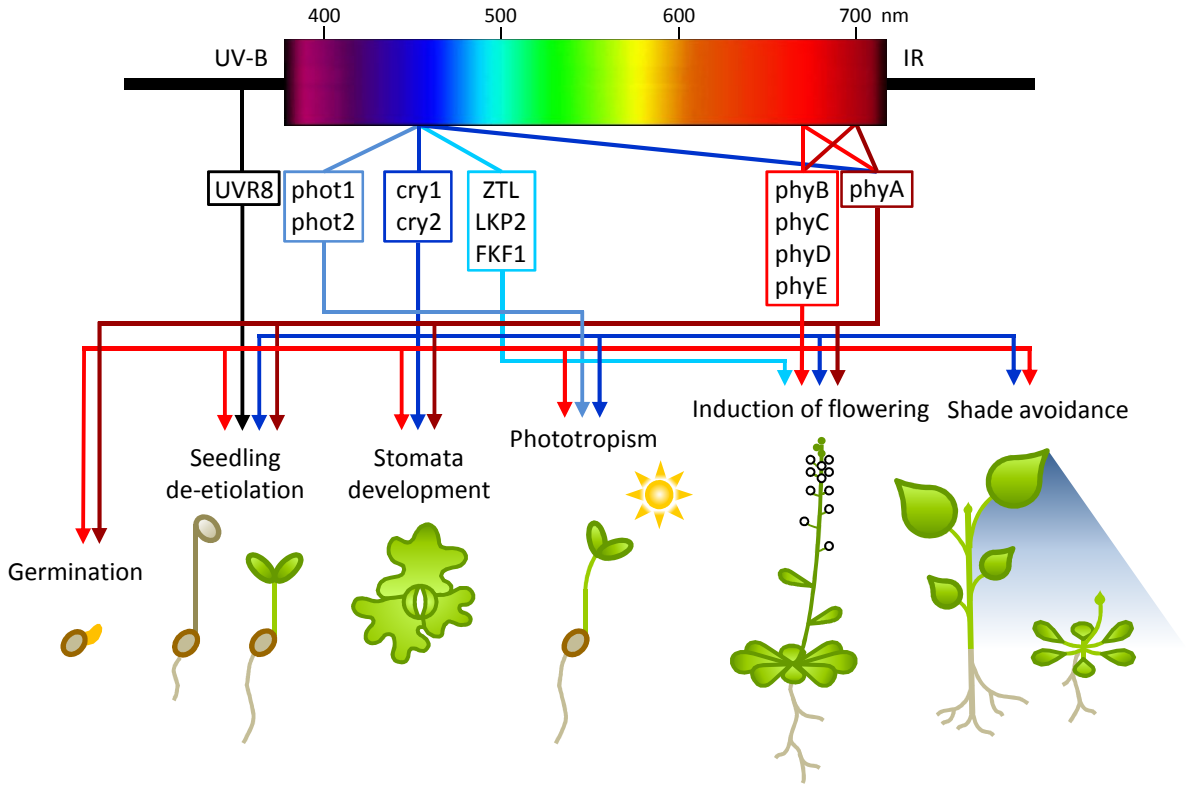

Figure 1.1: Light regulates plant development through distinct sets of photoreceptors.
Distinct classes of photoreceptors have evolved in Arabidopsis to perceive light of different wavelengths: the UVR8 protein mediates UV-B responses, while cryptochromes, phototropins and members of the ZTL family respond to B. Phytochromes absorb R and FR; phyB-E signal in response to R whereas phyA mainly signals in response to FR although it is involved in responses to B and R as well.
Arrows indicate the developmental processes regulated by the respective photoreceptors.

whereas *PHYB-E* encode light-stable type II phytochromes (Sharrock and Quail, 1989; Clack et al., 1994). In response to R, type II phytochromes translocate from the cytosol to the nucleus (Sakamoto and Nagatani, 1996; Kircher et al., 1999, 2002), where they mediate R/FR-photoreversible low fluence responses (LFRs) as well as non-photoreversible high-irradiance responses (HIRs) to continuous R (Rc) (Casal et al., 1998; Li et al., 2011). In contrast, phyA is involved in very low fluence responses (VLFRs) over a broad range of wavelengths and in HIRs to continuous FR (FRc), both of which are non-photoreversible (Casal et al., 1998; Li et al., 2011). phyA is imported into the nucleus upon interaction of its Pfr form with the nucleocytoplasmic shuttle proteins FAR-RED ELONGATED HYPOCOTYL 1 (FHY1) and FHY1-LIKE (FHL) (Hiltbrunner et al., 2006; Genoud et al., 2008), but its FRc-specific action peak arises at least in part from FR-induced dissociation from FHY1 and FHL in the nucleus (Rausenberger et al., 2011).

Cryptochromes are photolyase-like proteins that absorb blue (B) and UV-A light through their non-covalently bound flavin adenine dinucleotide (FAD) chromophores (Chaves et al.,

2011). Of the three cryptochrome-encoding genes (*CRY1-3*) of Arabidopsis, only *CRY1* and *CRY2* have so far been shown to encode functional photoreceptors (Yu et al., 2010). Light-stable cry1 mediates both low and high light responses while light-labile cry2 is mainly involved in responses to low B and has a major role in the perception of photoperiod (Ahmad and Cashmore, 1993; Guo et al., 1998; Lin et al., 1998; Mockler et al., 1999; Yu et al., 2007). Both receptors act primarily in the nucleus although cry1 may also function in the cytoplasm (Wu and Spalding, 2007; Yu et al., 2007).

Phytochromes and cryptochromes cooperatively regulate several aspects of plant development. Cryptochromes, phyB and phyA promote seedling de-etiolation and stomatal development in response to B, R and FR, respectively (Nagatani et al., 1991; Somers et al., 1991; Ahmad and Cashmore, 1993; Dehesh et al., 1993; Nagatani et al., 1993; Reed et al., 1993; Whitelam et al., 1993; Kang et al., 2009). Shade avoidance is normally triggered by a low R:FR ratio perceived by phyB (Nagatani et al., 1991; Somers et al., 1991), but recently a shade avoidance response caused by attenuated B has been assigned to cryptochrome function (Pierik et al., 2009; Keller et al., 2011). Antagonistic functions have been observed in the regulation of flowering time: the transition to flowering is promoted by cry1, cry2 and phyA but repressed by phyB (Guo et al., 1998; Mockler et al., 2003; Valverde et al., 2004). Finally, seed germination is exclusively mediated by phytochromes, primarily phyB (Botto et al., 1996; Shinomura et al., 1994). In contrast to phyA and phyB, phyC-E have comparatively minor roles in plant development and in many cases appear to act redundantly with phyB (Hennig et al., 2002; Franklin et al., 2003a,b).

Besides cryptochromes and phyA, two other photoreceptor families mediate B responses in Arabidopsis. The phototropins phot1 and phot2 absorb B through flavin mononucleotide (FMN) chromophores bound to their light oxygen voltage (LOV) domains (Christie, 2007). They regulate phototropic growth responses, cotyledon and leaf expansion as well as hypocotyl growth (Liscum and Briggs, 1995; Folta and Spalding, 2001; Sakai et al., 2001; Sakamoto and Briggs, 2002; Ohgishi et al., 2004), but also direct movements such as stomatal opening and chloroplast translocation (Kinoshita et al., 2001; Sakai et al., 2001). Members of the ZEITLUPE (ZTL) protein family, including ZTL, LOVE KELCH PROTEIN 2 (LKP2) and FLAVIN-BINDING KELCH F-BOX PROTEIN 1 (FKF1), also perceive B via LOV domains (Demarsy and Fankhauser, 2009; Ito et al., 2012). These proteins act as components of E3 ubiquitin ligases and regulate the circadian clock and photoperiodic flowering through light-dependent protein degradation (Más et al., 2003; Imaizumi et al., 2003, 2005; Kim et al., 2007; Sawa et al., 2007). Finally, UV-B RESISTANCE 8 (UVR8) has recently been identified as the UV-B photoreceptor (Rizzini et al.,

2011). It regulates UV-B-dependent seedling de-etiolation (Favory et al., 2009), but may also be involved in leaf expansion and stomatal development (Wargent et al., 2009).

1.1.2 Transcription factors and the COP1/SPA complex convey light signals downstream of photoreceptors

More than 20% of all expressed genes in Arabidopsis are regulated by light (Ma et al., 2001; Tepperman et al., 2001; Jiao et al., 2005); this regulation involves a large set of transcription factors, which affect expression of their target genes by binding to light-responsive elements (LREs) in the promoters of these genes (Jiao et al., 2007). Some of these transcription factors are directly controlled by photoreceptors, among them the PHYTOCHROME INTERACTING FACTORS (PIFs) of the basic helix-loop-helix (bHLH) superfamily. PIFs are constitutively localised in the nucleus (Castillon et al., 2007) and act as negative regulators of light responses as they repress seed germination but promote skotomorphogenesis as well as shade avoidance (Leivar and Quail, 2011). In the light, binding of the PIFs by phytochromes results in PIF phosphorylation, ubiquitination and subsequent degradation in the $26S$ proteasome (Bauer et al., 2004; Shen et al., 2005; Al-Sady et al., 2006; Shen et al., 2007, 2008). Conversely, cry2 positively regulates the function of the bHLH transcription factor CRY-INTERACTING BHLH 1 (CIB1) by B-dependent interaction to promote floral initiation (Liu et al., 2008a).

In addition to direct regulation of transcription factors, photoreceptors indirectly control gene expression via post-translational mechanisms. Genes of the *CONSTITUTIVELY PHOTOMORPHOGENIC/DE-ETIOLATED/FUSCA* (*COP/DET/FUS*) group are involved in this process; *cop/det/fus* mutants show a constitutively photomorphogenic phenotype, displaying short hypocotyls and open cotyledons in darkness (Figure 1.2) (Kwok et al., 1996), suggesting that they represent negative regulators of light signalling. Extensive research over the last 20 years has shown that COP/DET/FUS proteins act as parts of CULLIN 4 (CUL4)-DAMAGED DNA BINDING PROTEIN 1 (DDB1)-based E3 ubiquitin ligases, which control targeted protein degradation, and in the COP9 signalosome (CSN), which controls activity of these CUL4-DDB1 ligases (Lau and Deng, 2012; Stratmann and Gusmaroli, 2012).

COP1 is the most well characterised member of the *COP/DET/FUS* group: it is found in many higher eukaryotes including humans (Yi et al., 2002), where it has a role in tumourigenesis (Marine, 2012). In Arabidopsis, *COP1* is involved in many developmen-

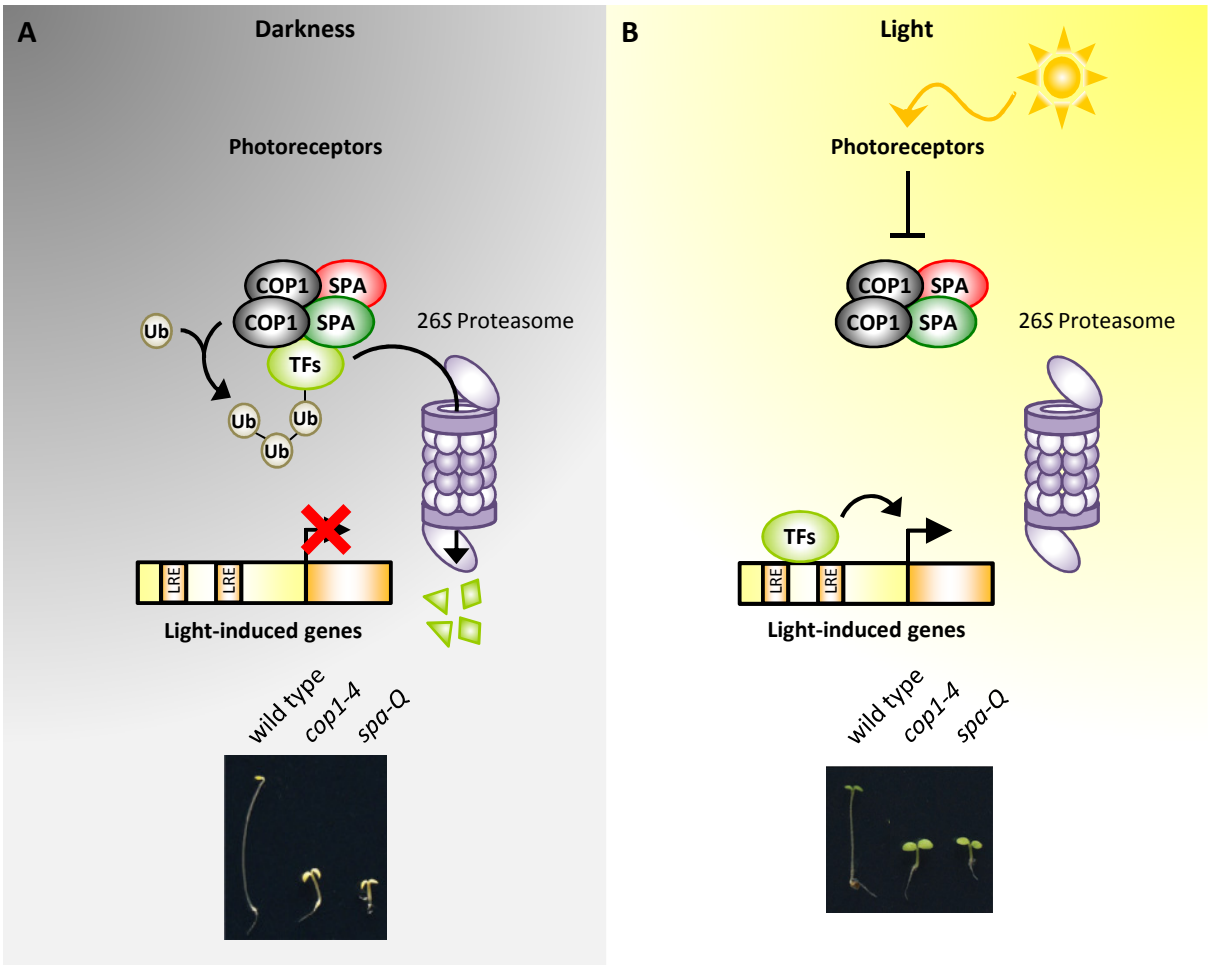

Figure 1.2: The COP1/SPA complex acts as a repressor of photomorphogenesis.
A: In darkness, the COP1/SPA complex suppresses photomorphogenesis by ubiquitination of photomorphogenesis-promoting transcription factors (TFs), thereby targeting them for degradation in the 26*S* proteasome. Therefore, dark-grown wild-type seedlings display a skotomorphogenic phenotype characterised by a long hypocotyl and closed cotyledons whereas *cop1* and *spa1 spa2 spa3 spa4* (*spa-Q*) mutants show constitutive photomorphogenesis. **B:** In the light, photoreceptors are active and repress the COP1/SPA complex. Therefore, photomorphogenesis-promoting TFs accumulate and promote the expression of light-induced genes by binding to light response elements (LREs) in their promoters. This leads to a photomorphogenic phenotype of wild-type seedlings, characterised by a short hypocotyl and open cotyledons. But even under these conditions the COP1/SPA complex retains residual activity as *cop1* and *spa-Q* mutants are overstimulated by light (Photographs modified from Hoecker, 2005).

tal processes, most of which are light-dependent: it represses seedling de-etiolation and stomatal development in darkness (Deng et al., 1991; Deng and Quail, 1992; Kang et al., 2009), controls root and vegetative plant growth (Deng and Quail, 1992; Sassi et al., 2012), promotes the shade avoidance response and prevents the induction of flowering under non-inductive short-day conditions (McNellis et al., 1994).

COP1 encodes a 76 kDa protein that contains an N-terminal RING-finger motif, a central coiled-coil domain and seven C-terminal WD40 repeats; in addition, it features both a

nuclear localisation sequence (NLS) and a cytoplasmic localisation sequence (CLS) (Deng and Quail, 1992; Torii et al., 1998; Stacey et al., 1999, 2000). A RING domain is found in many E3 ubiquitin ligases and is known to recruit E2 ubiquitin-conjugating enzymes (Deshaies and Joazeiro, 2009). COP1 was indeed shown to ubiquitinate positive regulators of the light response such as the basic leucine zipper (bZIP) transcription factor LONG HYPOCOTYL 5 (HY5), the bHLH transcription factor LONG HYPOCOTYL IN FAR-RED 1 (HFR1) and the MYB transcription factor LONG AFTER FAR-RED 1 (LAF1) *in vitro* and to be responsible for their proteasomal degradation in darkness *in vivo* (Ang et al., 1998; Osterlund et al., 2000; Seo et al., 2003; Jang et al., 2005; Yang et al., 2005).

The WD40 domain of COP1 is essential for interaction with HY5, HY5-HOMOLOGUE (HYH) and HFR1 (Torii et al., 1998; Holm et al., 2002; Jang et al., 2005). It also interacts with other COP1 targets including the floral promoter CONSTANS (CO) (Liu et al., 2008b; Jang et al., 2008), the photomorphogenesis-promoting B-box zinc finger protein BBX22 (SALT TOLERANCE HOMOLOG 3/STH3, LIGHT-REGULATED ZINC FINGER 1/LZF1) (Datta et al., 2008), the anthocyanin biosynthesis-controlling MYB transcription factors PAP1 and PAP2 (Maier et al., 2013) and the photoreceptors phyA, phyB and cry2 (Wang et al., 2001; Yang et al., 2001; Seo et al., 2004). Thus, the WD40 domain appears to be the primary substrate recognition site of COP1.

In contrast to the WD40 repeats, the coiled-coil domain of COP1 is necessary for self-dimerisation (Torii et al., 1998) as well as for interaction with its co-factors of the SUPPRESSOR OF PHYA-105 (SPA) family (Hoecker and Quail, 2001; Laubinger and Hoecker, 2003; Laubinger et al., 2004). Mutations in all four *SPA* genes of Arabidopsis result in a constitutively photomorphogenic phenotype similar to that of *cop/det/fus* mutants (Laubinger et al., 2004). Moreover, the SPA proteins show a high similarity to COP1 as they also contain a coiled-coil domain and C-terminal WD40 repeats, but their N-terminus features a domain with high similarity to serine/threonine kinases (Hoecker et al., 1999; Laubinger and Hoecker, 2003). All SPA proteins interact with COP1 and each other (Hoecker and Quail, 2001; Laubinger and Hoecker, 2003; Laubinger et al., 2004; Zhu et al., 2008) and appear to form tetrameric complexes consisting of two COP1 and two SPA proteins (Zhu et al., 2008), lending further support to the hypothesis that these proteins act in concert to repress light signalling. However, the exact role of the SPA proteins within COP1/SPA complexes is still unclear.

Although COP1 on its own has ubiquitin ligase activity *in vitro* (Osterlund et al., 2000; Seo et al., 2003; Yang et al., 2005), which can be either enhanced or reduced by the presence of recombinant SPA1 (Saijo et al., 2003; Seo et al., 2003), the COP1/SPA tetramer is now

thought to act in a multi-subunit ubiquitin ligase complex including CUL4, RING BOX 1 (RBX1) and DDB1 (Chen et al., 2010). CUL4 serves as scaffold that binds RBX1 and DDB1, RBX1 recruits E2 enzymes to the ligase and DDB1 acts as an adapter protein that binds WD40 proteins such as COP1 and SPAs (Biedermann and Hellmann, 2011), which serve as the substrate recognition unit of the complex (Chen et al., 2010).

Activity of the COP1/SPA complex is strongly regulated by light: in darkness, it targets positive regulators of the light response for degradation in the $26S$ proteasome (Figure 1.2) and thereby represses light signal transduction. In the light, it is thought to be repressed by cryptochromes, phyA and phyB although the mechanism is still under debate (Yi and Deng, 2005; Lau and Deng, 2012). COP1 accumulates in the nucleus in darkness, but is excluded from the nucleus in the light (von Arnim and Deng, 1994) and thereby separated from its target proteins. However, nuclear exclusion of COP1 upon light exposure is a relatively slow process that takes approximately 24 h (von Arnim et al., 1997) and therefore appears to be a long-term response that can neither account for rapid changes in the transcriptome induced by B, R and FR irradiation (Tepperman et al., 2001; Jiao et al., 2003; Tepperman et al., 2004) nor for rapid re-accumulation of the COP1 targets HY5 and HFR1 upon light exposure (Yang et al., 2005; Li et al., 2010). In the case of the cryptochromes, direct interaction with COP1 is required for fast inhibition of the complex, but their interaction with COP1 is light-independent (Wang et al., 2001; Yang et al., 2001). However, they interact with SPA1 in a B-dependent manner (Lian et al., 2011; Liu et al., 2011a; Zuo et al., 2011). Binding of cry1 to SPA1 disrupts COP1-SPA1 interaction and thereby presumably reduces activity of the complex (Lian et al., 2011; Liu et al., 2011a) while binding of cry2 to SPA1 does not impair COP1-SPA1 interaction but strengthens cry2-COP1 interaction and thereby may repress COP1 function (Zuo et al., 2011). Mechanisms for rapid inhibition of the COP1/SPA complex by the phytochromes have not yet been identified (Lau and Deng, 2012).

Notably, the COP1/SPA complex retains residual function also in the light as light-grown *cop1* and *spa1 spa2 spa3 spa4* quadruple (*spa-Q*) mutant seedlings exhibit increased light responses (Figure 1.2) (McNellis et al., 1994; Laubinger et al., 2004). In this regard, COP1-dependent degradation of phyA, phyB and cry2 in the light (Shalitin et al., 2002; Seo et al., 2004; Jang et al., 2010) may represent a negative feedback loop that fine-tunes light responses and prevents overstimulation by light.

1.1.3 The SPA proteins regulate different aspects of plant development

The *spa1* mutant was first identified as a suppressor mutation of a weak *phyA* allele (Hoecker et al., 1998) and identification of the corresponding gene led to discovery of the *SPA1-RELATED* genes *SPA2*, *SPA3* and *SPA4*. Based on sequence similarity, they can be divided into two subgroups: The first subgroup comprises *SPA1* and *SPA2*, which originate from a gene duplication during evolution (Simillion et al., 2002). The respective proteins contain an N-terminal extension as well as NLSs, which are not found in the members of the second subgroup, i.e. SPA3 and SPA4 (Laubinger and Hoecker, 2003; Laubinger et al., 2004).

Among the *spa* single mutants, *spa1* displays the strongest phenotypic differences compared to the wild type as it exhibits increased photomorphogenesis in B, R and FR (Hoecker et al., 1998, 1999; Baumgardt et al., 2002) and also flowers earlier in short days (Laubinger et al., 2006). A mutation in a single *SPA* gene does not change the skotomorphogenic growth habit of a dark-grown seedling, but *spa-Q* mutants show strong constitutive photomorphogenesis in darkness (Laubinger et al., 2004). These plants are also strongly impaired in vegetative growth and flower very early (Laubinger et al., 2004; Balcerowicz et al., 2011), suggesting that a high degree of redundancy exists among the *SPA* genes. However, analysis of *spa* double and triple mutants showed that the *SPA* genes have not only overlapping but also distinct functions during plant development (Figure 1.3). Both *SPA1* and *SPA2* are sufficient to suppress photomorphogenesis in dark-grown seedlings; in contrast, only *SPA1*, and to a minor extent *SPA3* and *SPA4*, prevent excessive light responses in light-grown seedlings whereas the function of *SPA2* at this stage is negligible (Laubinger et al., 2004; Fittinghoff et al., 2006; Balcerowicz et al., 2011). *SPA3* and *SPA4* appear to be the major regulators of vegetative plant growth (Laubinger et al., 2004) while *SPA1* and *SPA4* are the predominant players in the shade avoidance response (Rolauffs et al., 2012). Finally, *SPA1* represents the major regulator of flowering time among the *SPA* genes (Laubinger et al., 2006).

The different contributions of each *SPA* gene to distinct developmental processes are also reflected at the regulatory level. The transcript levels of *SPA1*, *SPA3* and *SPA4* rise upon light exposure while those of *SPA2* remain unchanged (Hoecker et al., 1999; Fittinghoff et al., 2006). Furthermore, the SPA proteins exhibit distinct light- and organ-specific

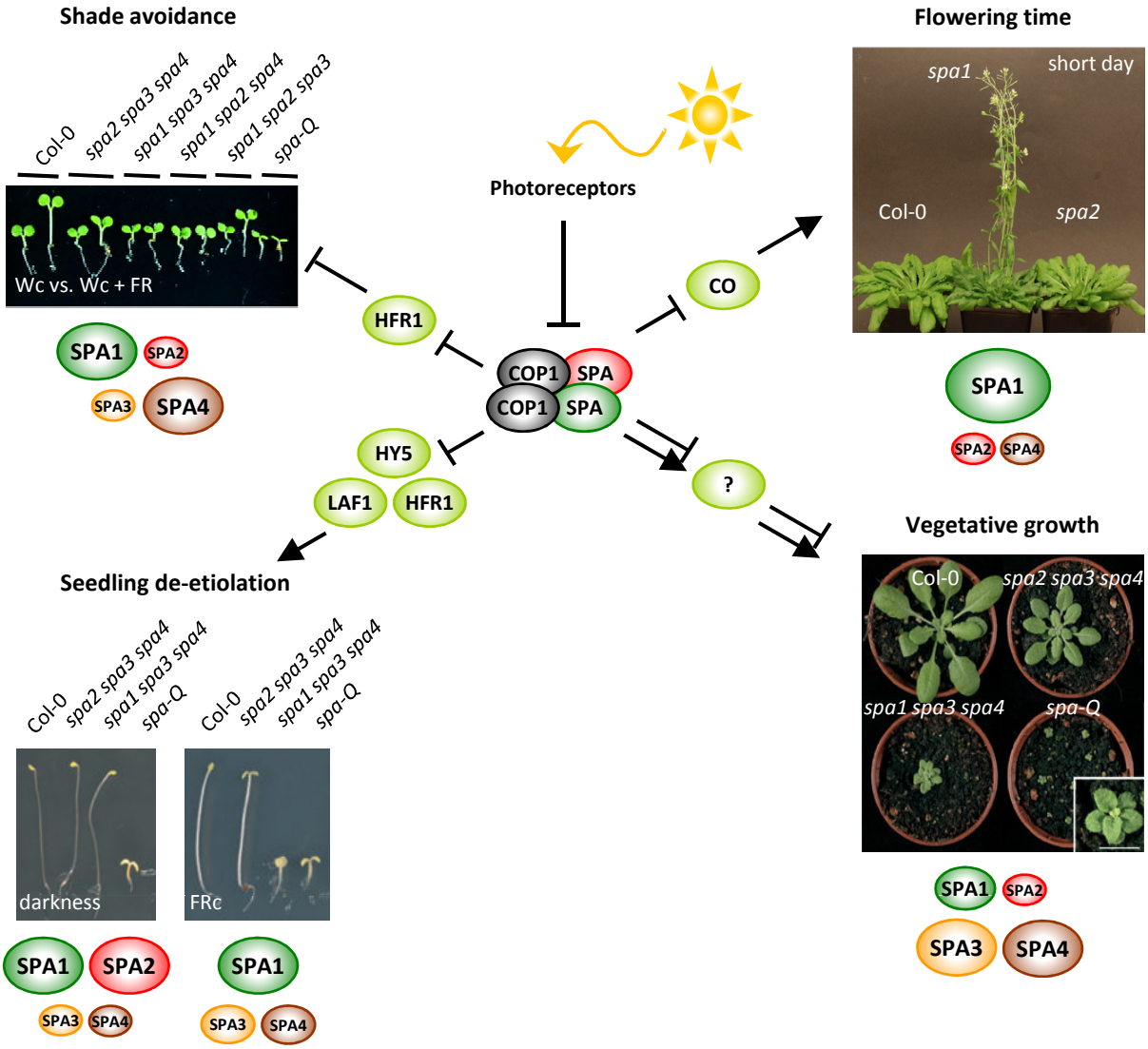

Figure 1.3: SPA proteins have overlapping but also distinct functions during plant development.
The COP1/SPA complex regulates many stages of plant development. It targets transcription factors such as HY5, HFR1 and LAF1 for degradation and thereby represses seedling de-etiolation and promotes hypocotyl elongation during shade avoidance. It is also involved in the suppression of flowering in short-day conditions by preventing CO protein accumulation and in vegetative growth regulation although in this case its targets are yet unknown. SPA proteins contribute differently to these processes. Both SPA1 and SPA2 are sufficient to suppress photomorphogenesis in dark-grown seedlings while SPA1, and to a lesser extent SPA3 and SPA4, prevent overstimulation of seedlings by light. SPA1 and SPA4 are main regulators of the shade avoidance response, SPA3 and SPA4 are the major regulators of vegetative plant growth and SPA1 is the predominant player in the suppression of flowering under short-day conditions. Arrows indicate positive regulation, perpendicular lines indicate negative regulation. Size of the SPA spheres corresponds to their importance at the respective developmental stage (Photographs modified from Laubinger et al., 2006; Balcerowicz et al., 2011; Rolauffs et al., 2012).

accumulation patterns (Zhu et al., 2008). Taken together, these observations suggest that spatiotemporal control of the SPA proteins may contribute to functional specificity of distinct COP1/SPA complexes.

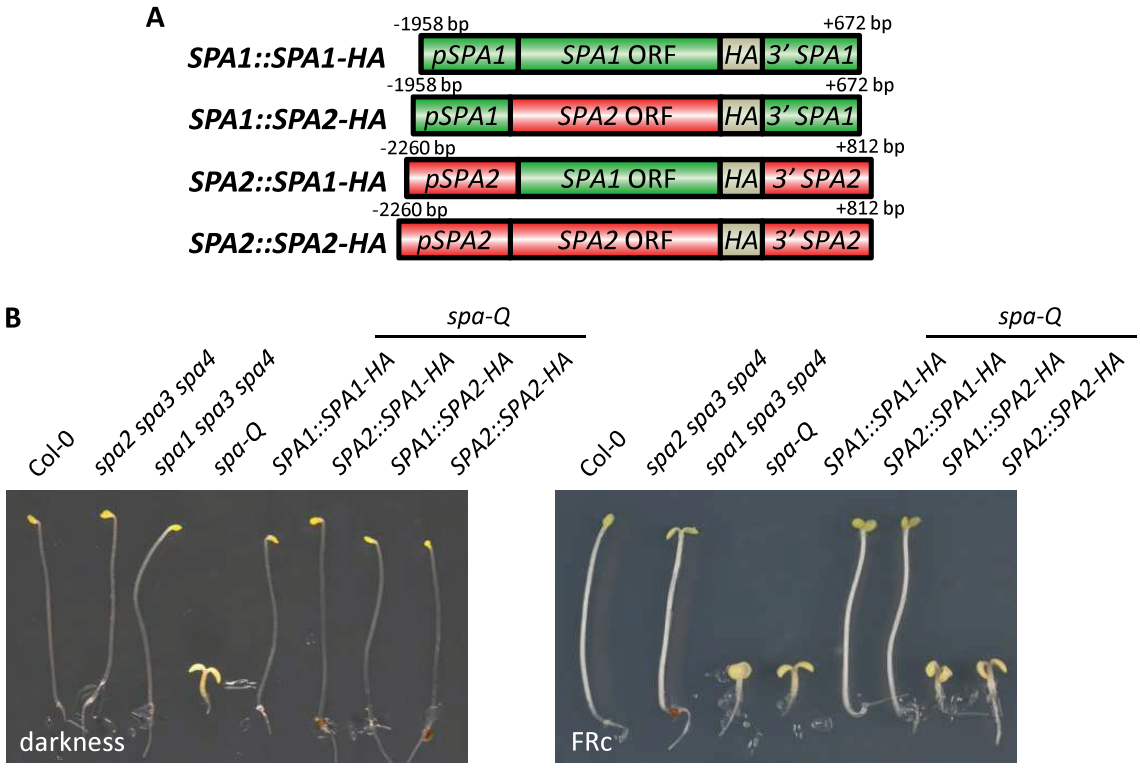

Figure 1.4: The SPA2 protein sequence accounts for the lack of *SPA2* function in light-grown seedlings.
A: Schematic representation of chimeric *SPA1*/*SPA2* constructs containing the *SPA1* or *SPA2* promoter (*pSPA1*, *pSPA2*), the *SPA1* or *SPA2* ORF, an HA tag and the 3' untranslated region of *SPA1* or *SPA2* (*3' SPA1*, *3' SPA2*). **B:** Visual phenotype of 4-d-old transgenic *spa-Q* seedlings expressing the chimeric *SPA1*/*SPA2* constructs shown in A. Seedlings were grown in darkness or FRc ($0.05\,\mu mol\,m^{-2}\,s^{-1}$). Col-0, *spa-Q* and *spa* triple mutant seedlings are shown as controls (modified from Balcerowicz et al., 2011).

The molecular basis for the different functions of SPA1 and SPA2 in light-grown seedlings was analysed in detail. To this end, chimeric constructs were generated that express the *SPA1* and *SPA2* open-reading frames (ORFs), fused to an HA tag, under control of the *SPA2* and *SPA1* 5' and 3' regulatory sequences, respectively. Constructs expressing the *SPA1* and *SPA2* ORFs from their own regulatory sequences served as controls (Balcerowicz et al., 2011; Figure 1.4 A). These constructs were introduced into a *spa1 spa2 spa3* and a *spa-Q* mutant background. Phenotypic analysis revealed that all four constructs suppress photomorphogenesis in dark-grown *spa1 spa2 spa3* and *spa-Q* mutant seedlings whereas only those containing the *SPA1* ORF prevent overstimulation of the seedlings by light (Balcerowicz et al., 2011; Figure 1.4 B). Therefore, only the protein sequence of the respective *SPA* gene appears to determine its functionality, or the lack thereof, in light-grown seedlings.

1.2 Auxin

The ability of plants to adjust their development to a multitude of environmental conditions requires a sophisticated regulatory network to coordinate the required developmental processes. The phytohormone auxin is considered to be a master regulator of plant development as it controls cell proliferation, cell elongation and cell differentiation at many developmental stages from embryogenesis to senescence (Teale et al., 2006; Vanneste and Friml, 2009; Perrot-Rechenmann, 2010). Hence, auxin function is tightly controlled via its metabolism, transport and perception.

1.2.1 Several metabolic pathways contribute to auxin homeostasis

Indole-3-acetic acid (IAA) appears to be the major naturally occurring auxin (Woodward and Bartel, 2005). In Arabidopsis, IAA is mainly synthesised from L-tryptophan (L-Trp) (Ljung, 2013) although a Trp-independent pathway has been suggested as well (Ouyang et al., 2000). The IAA-precursors indole-3-pyruvic acid (IPyA), indole-3-acetamide (IAM) and indole-3-acetaldoximine (IAOx) are characteristic compounds of three separate, Trp-dependent IAA-biosynthesis pathways (Mashiguchi et al., 2011; Stepanova et al., 2011), among which the IPyA pathway is the most well characterised. TRYPTOPHAN AMINOTRANSFERASE OF ARABIDOPSIS 1 (TAA1), which has also been described as WEAK ETHYLENE-INSENSITIVE 8 (WEI8) and SHADE AVOIDANCE 3 (SAV3), and its two homologues TAA1-RELATED 1 (TAR1) and TAR2 synthesise IPyA from L-Trp (Stepanova et al., 2008) while flavin monooxygenases of the YUCCA (YUC) family subsequently convert IPyA to IAA (Figure 1.5 A) (Mashiguchi et al., 2011; Stepanova et al., 2011).

Besides biosynthesis, conjugation and degradation also affect levels of free IAA. IAA can be conjugated to amino acids and sugars and amido synthases of the GH3 family appear to be involved in this process (Staswick et al., 2005). IAA can also be degraded to 2-oxoindole-3-acetic acid (oxIAA), but enzymes involved in this oxidation process have so far not been identified (Ljung, 2013).

1.2.2 Auxin is transported in a polar fashion

While all parts of a young plant have the capability to synthesise auxin, *de novo* biosynthesis is highest in dividing tissues of cotyledons and young leaves as well as in shoot and root meristems (Ljung et al., 2001). Since auxin distribution, manifested in local auxin maxima and minima as well as auxin gradients, is involved in the control of many devel-

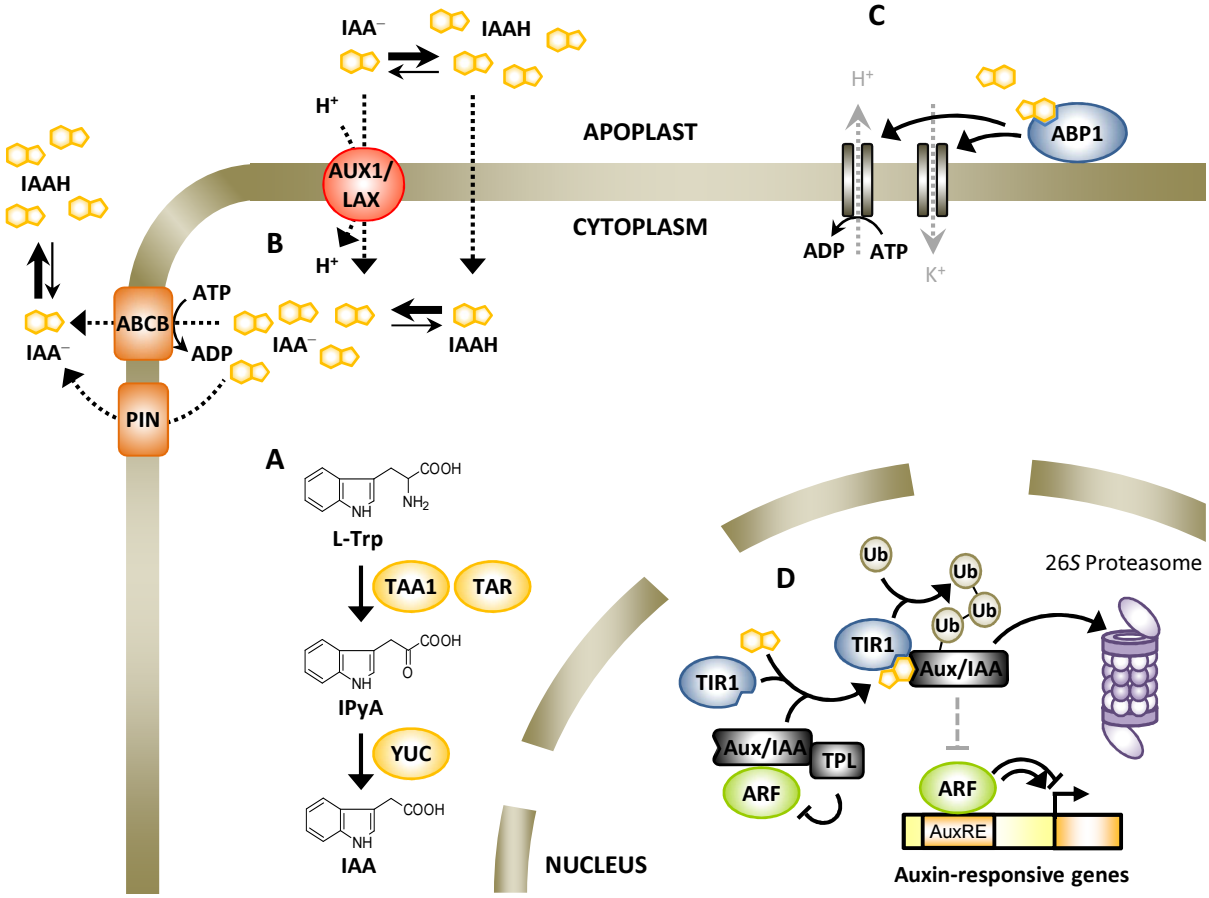

Figure 1.5: Overview of auxin biosynthesis, transport and signalling.
A: IAA is primarily synthesised from L-Trp by a pathway involving TAA1 and TAR tryptophan aminotransferases as well as flavin monooxygenases of the YUC family. **B:** Auxin is transported into the cell by a pH-driven ion-trap mechanism: uncharged IAA (IAAH) diffuses through the membrane and is converted to its anionic form (IAA) in the cytosol. In addition, auxin is imported via transporters of the AUX1/LAX family and exported via transporters of the PIN and ABCB families. **C, D:** Auxin signalling takes place at two different locations. At the plasma membrane, ABP1 mediates rapid auxin responses such as activation of ion channels and H^+-ATPases (C). In the nucleus, Aux/IAA proteins and their co-repressor TPL inhibit the activity of ARFs in the absence of auxin. Auxin allows TIR1 and Aux/IAA proteins to interact, whereupon the Aux/IAA proteins are ubiquitinated by the SCF^{TIR1} E3 ubiquitin ligase and subsequently degraded in the 26*S* proteasome (D). Therefore, the ARFs are de-repressed and regulate auxin-responsive genes by binding to auxin response elements (AuxREs) in their promoters.

opmental responses, auxin transport needs to be tightly regulated (Tanaka et al., 2006). Auxin can move long distances via mass flow in the phloem, but it is also distributed via cell-to-cell translocation in a mostly polar way (Figure 1.5 B) (Zazímalová et al., 2010).

A chemiosmotic model was proposed for polar auxin transport (Rubery and Sheldrake, 1974; Raven, 1975): protonated, lipophilic IAA molecules enter the cell via passive diffusion through the plasma membrane; due to the higher pH in the cytoplasm, IAA is deprotonated and the negatively charged IAA-anions are unable to diffuse back through the plasma membrane. Therefore, auxin can only leave the cell with the help of transporters and the location of these transporters can direct auxin efflux.

Several different classes of auxin transporters have been identified since postulation of the chemiosmotic model: while members of the AUXIN-RESISTANT 1 (AUX1)/LIKE-AUX1 (LAX) family contribute to auxin influx by IAA-proton-symport, auxin efflux is mediated by B-type ATP-binding cassette transporters (ABCBs) and carriers of the PIN-FORMED (PIN) family by ATP- and gradient-driven mechanisms, respectively (Petrásek and Friml, 2009; Zazímalová et al., 2010). All these transporters exhibit asymmetric distributions within different tissues (Swarup et al., 2001; Bandyopadhyay et al., 2007; Feraru and Friml, 2008), which is in agreement with the polarity of auxin transport. The PIN proteins seem to be particularly crucial for proper plant development because perturbations in their localisation or functionality result in severe defects in embryo development, root meristem patterning, lateral organ development, vascular tissue differentiation and tropic growth responses (Friml, 2010).

1.2.3 Two spatially separated signalling pathways transduce the auxin signal

At the cellular level, auxin is perceived by two different types of receptors. The glycoprotein AUXIN BINDING PROTEIN 1 (ABP1) is largely localised in the ER, but several lines of evidence suggest that a small portion of ABP1 is secreted from the cell and acts as an auxin receptor at the plasma membrane (Figure 1.5 C) (Jones and Venis, 1989; Jones and Herman, 1993; Henderson et al., 1997; Woo et al., 2002). ABP1 is thought to control rapid auxin responses such as turgor-induced cell elongation by regulation of ion fluxes and membrane potential (Sauer and Kleine-Vehn, 2011) and prevents endocytosis of PIN proteins, thereby increasing auxin efflux and desensitising the auxin response (Robert et al., 2010).

Auxin regulates the expression of hundreds of genes, but this effect is largely independent of ABP1 (Mockaitis and Estelle, 2008; Chapman and Estelle, 2009). In contrast, auxin receptors of the TRANSPORT INHIBITOR RESPONSE 1 (TIR)/AUXIN-BINDING F-BOX (AFB) family act in the nucleus to control auxin-dependent gene expression (Figure 1.5 D) (Kepinski and Leyser, 2005; Dharmasiri et al., 2005a,b). They form the substrate recognition unit of SCF (Skp1, CUL1, F-box) ubiquitin ligases that target repressors of the auxin response for degradation in an auxin-dependent manner (Gray et al., 2001).

At low auxin concentrations, AUXIN/INDOLE-3-ACETIC ACID (Aux/IAA) repressor proteins, together with their co-repressor TOPLESS (TPL), inhibit the transcriptional regulatory function of AUXIN RESPONSE FACTORS (ARFs) by heterodimerisation (Ulmasov et al., 1999; Tiwari et al., 2001; Szemenyei et al., 2008). Aux/IAAs interact with the C-terminal domain of ARFs via two conserved domains termed domain III and IV (Ulmasov et al., 1999) whereas domain I of the Aux/IAA proteins is an active repressor domain that is required for the recruitment of TPL (Szemenyei et al., 2008). Finally, domain II controls stability of the Aux/IAA repressors (Worley et al., 2000; Ouellet et al., 2001). Auxin promotes hydrophobic interaction of the TIR1/AFB receptors with this domain; this interaction leads to ubiquitination of Aux/IAA proteins by the $SCF^{TIR1/AFB}$ ubiquitin ligase and thereby to their subsequent degradation in the $26S$ proteasome (Gray et al., 2001; Kepinski and Leyser, 2005; Dharmasiri et al., 2005a,b; Tan et al., 2007). Thus, Aux/IAA proteins are degraded at high auxin concentrations, thereby ARFs are de-repressed and can regulate the expression of auxin-responsive genes through binding of auxin response elements (AuxREs) in their promoters (Ulmasov et al., 1997a,b; Tiwari et al., 2003). Many *Aux/IAA* genes are themselves positively regulated by auxin (Abel et al., 1995), providing another feedback mechanism that desensitises auxin signalling.

The Arabidopsis genome encodes 6 TIR1/AFB proteins (Dharmasiri et al., 2005b), 29 Aux/IAA proteins and 23 ARFs (Liscum and Reed, 2002). Specificity of auxin responses is determined by several factors that control the function of these signalling components, including their spatiotemporal regulation at the transcriptional and post-translational level, their stability and their affinities to each other (Hayashi, 2012).

1.2.4 Auxin and light signalling pathways interact

Light affects auxin levels, transport and responsiveness to manipulate plant growth and development (Halliday et al., 2009). Conflicting results have been obtained for the effect

of light on auxin biosynthesis. On the one hand, IAA levels are lower in dark-grown than in light-grown seedlings (Bhalerao et al., 2002) and low fluences of R induce Trp-independent auxin biosynthesis (Liu et al., 2011b); on the other hand, phyB negatively regulates auxin biosynthesis by decreasing transcript levels of *TAA1* (Tao et al., 2008) and increasing those of *SUPERROOT 2* (*SUR2*) (Hoecker et al., 2004), a suppressor of auxin biosynthesis (Delarue et al., 1998). In agreement with these findings, auxin is required for hypocotyl elongation under a low R:FR ratio (Tao et al., 2008) when phyB is mostly inactive.

Light also controls auxin transport and thereby the shoot:root auxin ratio. A high shoot:root ratio favours hypocotyl elongation whereas a low shoot:root ratio promotes cotyledon and root development (Halliday et al., 2009). To regulate auxin transport, light affects levels of auxin transporters such as PIN3 (Devlin et al., 2003) and PGP19 (Nagashima et al., 2008) as well as intracellular distribution of PIN proteins (Friml et al., 2002; Laxmi et al., 2008; Sassi et al., 2012).

Finally, components of the auxin signalling pathway are also light-regulated. Gain-of-function mutants of the *Aux/IAA* genes *SHORT HYPOCOTYL 2* (*SHY2*)/*IAA3*, *AUXIN-RESISTANT 2* (*AXR2*)/*IAA7* and *AXR3/IAA17* exhibit constitutively photomorphogenic phenotypes (Timpte et al., 1994; Leyser et al., 1996; Reed et al., 1998) due to a mutation in domain II that disrupts their auxin-dependent interaction with TIR1 (Gray et al., 2001). In addition, expression of *AXR2* and *SOLITARY ROOT* (*SLR*)/*IAA14* is positively regulated by HY5 and HYH (Cluis et al., 2004; Sibout et al., 2006). The photoreceptors themselves may also directly control auxin signalling; recombinant oat phyA was reported to bind and phosphorylate recombinant Arabidopsis IAA1, SHY2/IAA3, IAA9 and AXR3/IAA17 (Colón-Carmona et al., 2000) and interaction was also shown for Arabidopsis phyB with SHY2/IAA3 and AXR3/IAA17 (Tian et al., 2003). The biological relevance of these *in vitro* interactions, however, remains unclear since they appear to be light-insensitive.

1.3 Stomatal development and patterning

Stomata are epidermal pores that regulate gas exchange and transpiration. They are essential innovations of land plants because along with formation of a cuticle they allow CO_2 uptake while minimising transpiration (Peterson et al., 2010). Since CO_2 uptake and water loss strongly affect photosynthetic performance, not only stomatal opening but also stomatal development is strongly regulated by both intrinsic and environmental factors.

1.3.1 Stomatal development and the stomatal lineage

Stomatal development in Arabidopsis is a post-embryonic process that relies upon a set of cell divisions and cell state transitions within a specific epidermal cell lineage (Figure 1.6). Some protodermal cells do not undergo symmetric divisions to form pavement cells, but enter this stomatal lineage by becoming a meristemoid mother cell (MMC). The MMC divides asymmetrically, forming a larger daughter cell, the stomatal lineage ground cell (SLGC), and a smaller cell, the meristemoid, which retains self-renewing capability. This division is referred to as entry division and can be followed by up to two rounds of asymmetric amplifying divisions, by which the meristemoid surrounds itself with SLGCs, before it differentiates into a guard mother cell (GMC). This GMC then divides once symmetrically to generate two paired guard cells (GCs) that form the stoma (Nadeau and Sack, 2002b).

SLGCs may eventually become pavement cells, but they may divide asymmetrically as well, giving rise to satellite meristemoids. Such divisions are called spacing divisions because the satellite meristemoid is always oriented away from the existing stoma or stomatal precursor, thereby reinforcing the one-cell spacing rule, which states that two stomata are separated by at least one non-stomatal cell (Geisler et al., 2000).

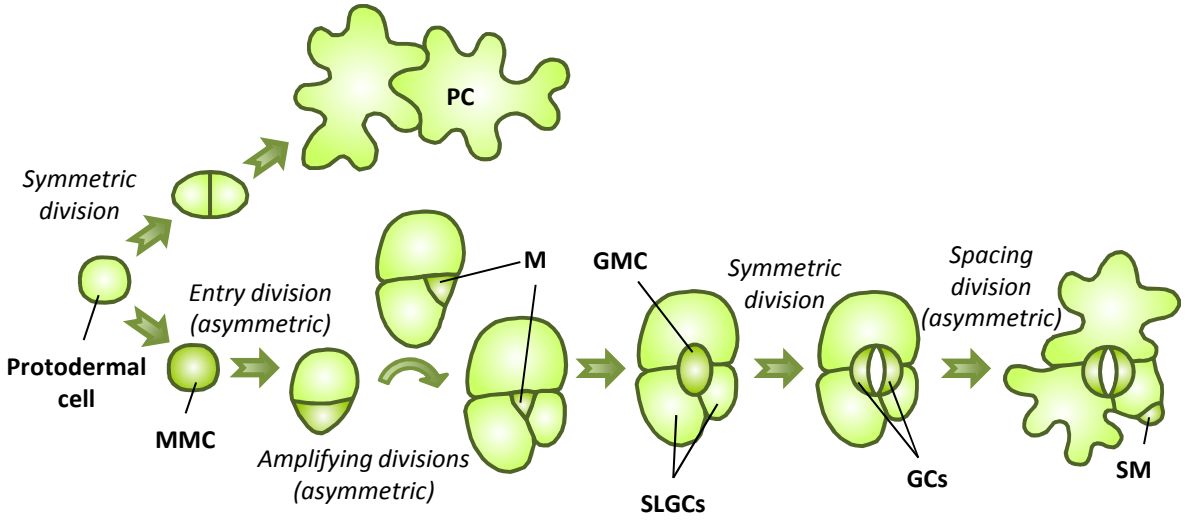

Figure 1.6: Schematic representation of stomatal development in Arabidopsis.
A protodermal cell can either divide symmetrically to form pavement cells (PCs) or it becomes a meristemoid mother cell (MMC) that divides asymmetrically to enter the stomatal lineage. This asymmetric division gives rise to a larger stomatal lineage ground cell (SLGC) and a smaller meristemoid (M), which retains self-renewing capability. The meristemoid can divide asymmetrically twice more, surrounding itself with SLGCs, before it differentiates into a guard mother cell (GMC). The GMC undergoes one symmetric division, producing two guard cells that form a stoma. The surrounding SLGCs can either differentiate into pavement cells or can undergo additional asymmetric divisions, giving rise to satellite meristemoids (SMs). In this case, the new meristemoid is always formed away from the existing stoma.

1.3.2 Stomatal development is regulated by intra- and intercellular signalling

The isolation of mutants with aberrant stomatal phenotypes has led to the identification of many key factors involved in stomatal development, which have been placed in a common regulatory pathway (Figure 1.7) (Serna, 2009; Lau and Bergmann, 2012; Pillitteri and Torii, 2012). The three bHLH transcription factors SPEECHLESS (SPCH), MUTE and FAMA are core components of this pathway and control consecutive steps of stomatal development. SPCH promotes entry and amplifying divisions in the stomatal lineage; correspondingly, it is expressed broadly in the protoderm in young tissues, but its expression is confined to MMCs and meristemoids later in development (MacAlister et al., 2007; Pillitteri et al., 2007). MUTE is required for the termination of amplifying divisions and the cell-state transition from the meristemoid to the GMC and is therefore exclusively expressed in late meristemoids (Pillitteri et al., 2007). Finally, FAMA restricts symmetric division of the GMC to one round and promotes the transition to GCs; hence, FAMA is expressed in GMCs and young GCs (Ohashi-Ito and Bergmann, 2006).

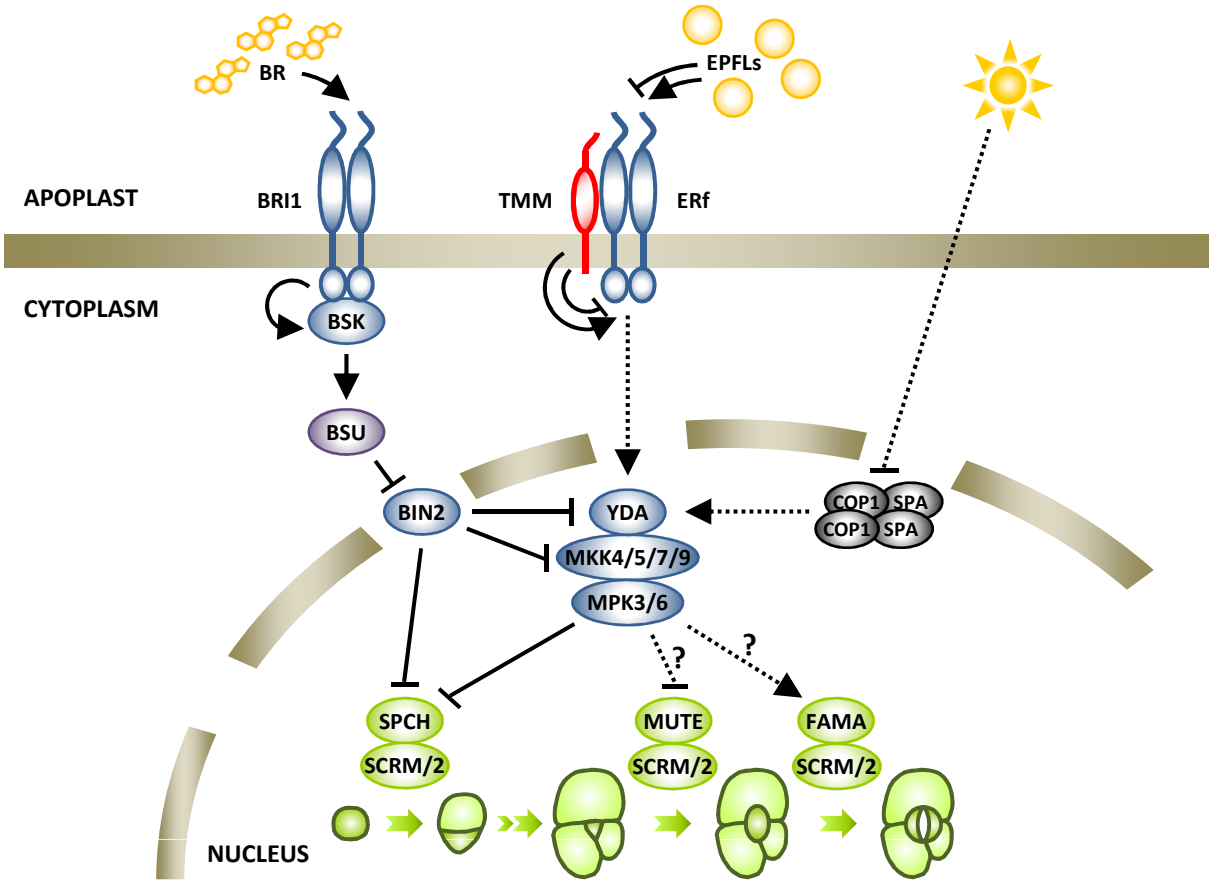

Figure 1.7: Stomatal development is regulated by a complex signalling pathway that integrates intrinsic and environmental signals.
SPCH, MUTE and FAMA, in concert with SCRM and SCRM2, regulate consecutive steps of stomatal development. Upstream of these bHLH transcription factors, a MAPK cascade consisting of the MKKK YDA, MKK4/5/7/9 and MPK3/6 suppresses stomatal development by phosphorylation of SPCH and possibly other factors involved in later developmental steps. The MAPK cascade is regulated by LRR receptor-like kinases of the ER family (ERf), whose activity is modulated by the LRR receptor-like protein TMM. The TMM-ERf module is in turn activated or inhibited by binding of EPFLs.
Brassinosteroids (BRs) regulate stomatal development by inhibition of BIN2, and the BR signalling components BRI1, BSK and BSU are required for this process. Active BIN2 phosphorylates and inactivates YDA, MKK4, MKK5 (thereby promoting stomata formation in cotyledons) and SPCH (thereby suppressing stomata formation in the hypocotyl). In contrast, light strongly promotes stomatal development through inhibition of the COP1/SPA complex, which acts genetically upstream of YDA.
Arrows indicate positive regulation, perpendicular lines indicate negative regulation. Solid lines represent confirmed biochemical interaction, dotted lines represent indirect or genetic interactions.

Two additional bHLH proteins, SCREAM (SCRM)/INDUCER OF CBF 1 (ICE1) and SCRM2, with largely redundant functions are expressed broadly throughout the stomatal lineage and promote all steps of stomatal development (Kanaoka et al., 2008). Both of them interact with SPCH, MUTE and FAMA and are required for their function (Kanaoka et al., 2008), suggesting that they act as heterodimers to regulate gene expression. Besides, two R2R3 MYB transcription factors, FOUR LIPS (FLP) and MYB88, control the

GMC to GC transition in parallel with FAMA, but no interaction with any of the other transcription factors has been observed (Lai et al., 2005).

Upstream of the aforementioned transcription factors, a mitogen-activated protein kinase (MAPK) cascade negatively regulates entry into and progression through the stomatal lineage although it appears to promote the transition from GMCs to GCs (Lampard et al., 2009). The MAPK module implicated in stomatal development comprises the MAPK kinase kinase (MKKK) YODA (YDA), the MAPK kinases (MKKs) MKK4, MKK5, MKK7 and MKK9 as well as the MAPKs MPK3 and MPK6 (Bergmann et al., 2004; Wang et al., 2007; Lampard et al., 2009). MPK3 and MPK6 directly phosphorylate SPCH *in vitro*, and this phosphorylation is required for the repression of SPCH activity *in vivo*, which likely involves phosphorylation-dependent degradation (Lampard et al., 2008). The MAPK target site of SPCH is not present in the other transcription factors that regulate stomatal development (Lampard et al., 2008), but *in vitro* phosphorylation of MUTE and MYB88 by MPK4 and MPK6, respectively (Popescu et al., 2009), raises the possibility that some of these factors may be controlled by MAPK cascades as well.

Additional negative regulators of stomatal development act upstream of the MAPK cascade. Leucin-rich repeat (LRR) receptor-like kinases of the ERECTA (ER) family (ERf), comprised of ER, ERECTA-LIKE 1 (ERL1) and ERL2, control stomatal patterning and differentiation by inhibiting discrete steps of stomatal development (Shpak et al., 2005). ER primarily restricts entry divisions whereas ERL1 mainly represses the transition of meristemoids to GMCs and orients spacing divisions; ERL2 acts redundantly with both ER and ERL1 in suppressing stomata formation (Shpak et al., 2005). In agreement with their partially distinct functions, ER is expressed in protodermal cells while ERL1 and ERL2 expression is restricted to meristemoids, GMCs, SLGCs and young GCs (Shpak et al., 2005). ER and ERL1 were also shown to homo- and heterodimerise *in vivo* (Lee et al., 2012), but whether this interaction is important for their function is yet unknown.

Activity of the ERf is modulated by the LRR receptor-like protein TOO MANY MOUTHS (TMM). TMM is widely expressed in the stomatal lineage (Nadeau and Sack, 2002a). In cotyledons and leaves, it restricts stomata differentiation and guides spacing divisions in concert with the ERf (Yang and Sack, 1995; Nadeau and Sack, 2002a; Shpak et al., 2005), but in hypocotyls and stems, it promotes stomatal development and thereby antagonises ERf function (Yang and Sack, 1995; Bhave et al., 2009). TMM lacks an intracellular effector domain (Nadeau and Sack, 2002a) and may therefore act as co-receptor of the ERf receptor-like kinases. Indeed, TMM heterodimerises with ER and ERL1 *in vivo* and thereby possibly affects their function (Lee et al., 2012).

Secreted, cysteine-rich peptides of the EPIDERMAL PATTERNING FACTOR-LIKE (EPFL) family represent ligands of the ERf receptors (Rychel et al., 2010; Lee et al., 2012). Two founding members of this family, EPIDERMAL PATTERNING FACTOR 1 (EPF1) and EPF2, act at specific stages of stomatal development corresponding to those of ERL1 and ER, respectively: EPF1 is expressed in late meristemoids and GMCs and reinforces the previously mentioned one-cell spacing rule (Hara et al., 2007) while EPF2 is expressed in MMCs as well as early meristemoids and SLGCs and restricts the number of cells that enter the stomatal lineage (Hara et al., 2009; Hunt and Gray, 2009). EPF1-ERL1 and EPF2-ER represent specific ligand-receptor pairs as EPF1 binds to ERL1 but not ER or TMM whereas EPF2 interacts with ER and TMM but not ERL1 *in vivo* (Lee et al., 2012). Both EPF1 and EPF2 promote phosphorylation of SPCH via MPK6 when expressed in tobacco leaves (Jewaria et al., 2013), supporting the idea that EPF-ERf ligand-receptor pairs control activity of the YDA MAPK cascade.

Additional EPFL peptides have been implicated in stomatal development: STOMAGEN/EPFL9 appears to be a mesophyll-derived signal that promotes stomata formation (Hunt et al., 2010; Sugano et al., 2010) whereas CHALLAH (CHAL)/EPFL6 as well as CHAL-LIKE 1 (CLL1)/EPFL5 and CLL2/EPFL4 can act as negative regulators of stomatal development, but their effect is attenuated by TMM (Abrash and Bergmann, 2010; Abrash et al., 2011).

1.3.3 Phytohormones control stomatal development

Several classes of phytohormones have been reported to affect stomatal development, and recently, a direct link between brassinosteroid (BR) signalling and stomatal development has been established (Figure 1.7). This link requires the BR signalling intermediate BR INSENSITIVE 2 (BIN2), a glycogen synthase kinase 3 (GSK3)-like kinase, but is independent of BR-regulated gene expression (Gudesblat et al., 2012; Kim et al., 2012). BIN2 phosphorylates YDA, MKK4, MKK5 and SPCH, thereby repressing the respective proteins (Gudesblat et al., 2012; Kim et al., 2012; Khan et al., 2013). BR signalling through the BR receptor BR INSENSITIVE 1 (BRI1), BR SIGNALING KINASE 3 (BSK3) and the phosphatase BRI1 SUPPRESSOR 1 (BSU1) inactivates BIN2, thus inhibiting stomata formation in cotyledons and leaves via de-repressing the YDA MAPK cascade (Kim et al., 2012) but promoting stomata formation in the hypocotyl via de-repressing SPCH (Gudesblat et al., 2012).

Other phytohormones may also influence stomatal development. Abscisic acid (ABA) negatively regulates stomata formation upstream of *SPCH* and *MUTE* (Franks and Farquhar, 2001; Tanaka et al., 2013) whereas ethylene was reported to induce stomata formation (Kieber et al., 1993; Serna and Fenoll, 1996). Furthermore, gibberellin (GA) treatment increases stomata formation in the hypocotyl, an effect that can be enhanced by additional application of ethylene or auxin (Saibo et al., 2003). However, no direct biochemical link to the stomatal development signalling pathway has yet been provided for any of these hormones.

1.3.4 Light promotes stomatal development

Environmental signals such as light, CO_2 concentration, temperature and humidity also control stomatal development (Casson and Gray, 2008; Casson and Hetherington, 2010), but the underlying mechanisms are largely unknown. *HIGH CARBON DIOXIDE* (*HIC*) is the only gene that has so far been shown to regulate stomata formation in response to CO_2 levels (Gray et al., 2000) while several components of the light signalling machinery have been reported to be involved in light-dependent stomata differentiation.

Light strongly promotes stomatal development; increased intensities of R correlate with an increased proportion of stomata in the leaf epidermis, an effect that depends on the repression of PIF4 by phyB (Boccalandro et al., 2009; Casson et al., 2009). Light also induces the formation of stomata at the seedling stage as stomata are found at very low numbers in the abaxial cotyledon epidermis of dark-grown seedlings (Kang et al., 2009). Cryptochromes, phyB and phyA promote the differentiation of stomata during de-etiolation of seedlings in response to B, R and FR, respectively, and this promotion requires repression of the COP1/SPA complex (Kang et al., 2009). The COP1/SPA complex acts genetically upstream of YDA, but in parallel with TMM, to regulate stomatal development (Figure 1.7) (Kang et al., 2009), but biochemical evidence that the COP1/SPA complex indeed affects activity of the YDA MAPK cascade has not yet been obtained.

1.4 Aims of this thesis

The COP1/SPA complex is a central regulator of light-dependent plant development and has been thoroughly investigated over the past 20 years, but the function of its components is still not fully understood. In addition, light also acts independently of the COP1/SPA complex to affect plant development. Hence, this thesis aimed both to further examine molecular and biochemical properties of the COP1/SPA complex and to characterise additional regulators of light-dependent plant development:

(1) Analysis of the effect of SPA proteins on COP1 subcellular localisation
The role of the SPA proteins within the COP1/SPA complex is still largely unknown. Since COP1 subcellular localisation, and thereby its function, is regulated by light, the first aim of this study was to investigate whether the SPA proteins are involved in the nuclear accumulation of COP1 in darkness.

(2) Dissection of the functional divergence of SPA1 and SPA2 in light-grown seedlings
SPA1 and SPA2 can both repress photomorphogenesis in dark-grown seedlings, but only SPA1 is active in light-grown seedlings; this effect is accounted for by the different sequences of the two proteins. Therefore, the second aim of this study was to analyse the differential regulation of SPA1 and SPA2 proteins by light and to identify the basis for their different functions in light-grown seedlings.

(3) Identification and characterisation of putative novel regulators of light-dependent stomatal development
Light promotes stomata formation by repression of the COP1/SPA complex, but a direct link between components of the light and stomatal development signalling pathways has not yet been identified. Auxin-insensitive *aux/iaa* mutants with a constitutively photomorphogenic phenotype similar to *cop1* and *spa* mutants also fail to suppress stomata formation in darkness. Hence, the third aim of this thesis was to further characterise stomatal development in these *aux/iaa* mutants and to establish a genetic network that links auxin and light signalling to the intrinsic pathway that controls stomatal development.

2 Results

2.1 SPA proteins do not affect COP1 subcellular localisation in darkness

Genetic interaction between *cop1* and *spa* mutants as well as direct physical interaction of all four SPA proteins with COP1 suggest that COP1 acts in concert with the SPA proteins in many aspects of plant development (Hoecker and Quail, 2001; Laubinger and Hoecker, 2003; Saijo et al., 2003; Laubinger et al., 2004). Furthermore, SPA1 was shown to modulate the ubiquitination activity of COP1 *in vitro* (Saijo et al., 2003; Seo et al., 2003). The exact mechanism, however, by which the SPA proteins affect COP1 function is yet unknown. Possible functions include recruitment of substrates, modification of the COP1 protein, stabilisation of the functional complex and regulation of COP1 nuclear accumulation (Yi and Deng, 2005).

In contrast to the constitutive nuclear localisation of SPA1 and SPA2 (Hoecker et al., 1999; Laubinger et al., 2004), COP1 subcellular localisation is dependent on light conditions: in darkness, COP1 resides in the nucleus, where it targets transcription factors for degradation, while in the light, it is excluded from the nucleus and therefore separated from its target proteins (von Arnim and Deng, 1994). Hence, promotion of COP1 nuclear accumulation could represent one mechanism by which the SPA proteins support COP1 function. To test this hypothesis, COP1 protein levels were examined in nuclei-depleted and nuclei-enriched protein fractions of dark-grown wild-type and *spa* quadruple null mutant (*spa-nQ*) seedlings. The COP1 protein was exclusively detected in the nuclei-enriched fractions of both genotypes (Figure 2.1 A), demonstrating that its nuclear accumulation in darkness is not changed by the absence of the SPA proteins.

In addition, COP1 subcellular localisation was monitored by fluorescence microscopy using a *35S::YFP-COP1* reporter line (Subramanian et al., 2006). In this line, YFP-COP1 accumulated in nuclear speckles as well as cytoplasmic inclusion bodies in darkness and hence, YFP-COP1 was detected both in nuclei-depleted and nuclei-enriched protein fractions of dark-grown *35S::YFP-COP1* seedlings (Figure 2.1 B, C, F, G; Supplemental

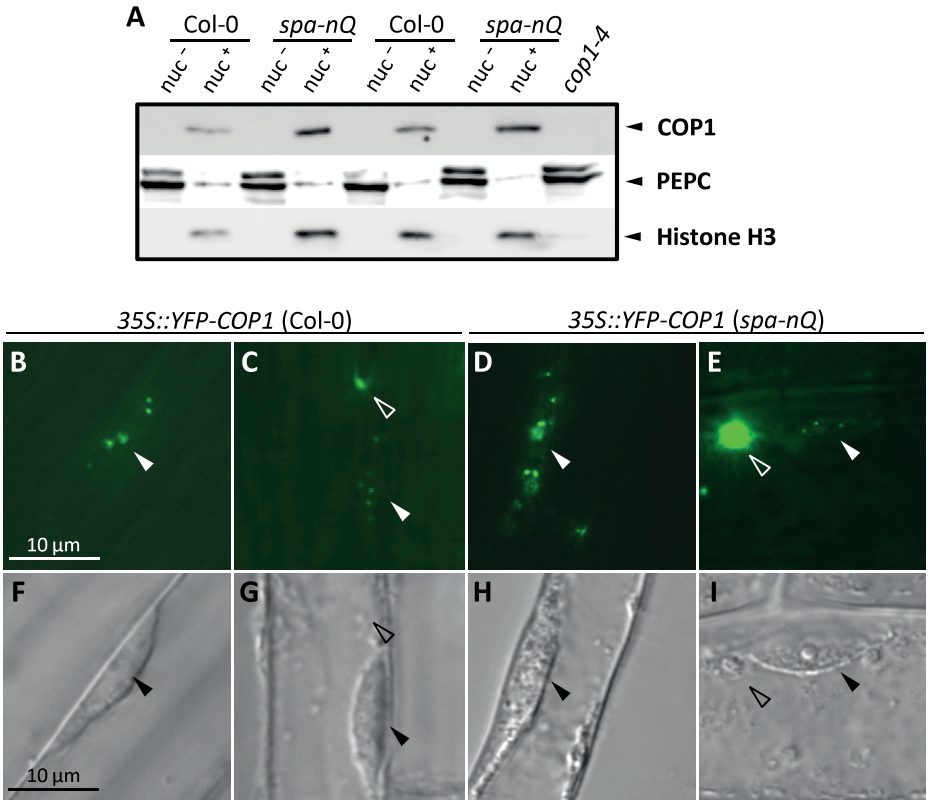

Figure 2.1: COP1 nuclear accumulation in darkness is not altered in the *spa-nQ* mutant. **A:** Immunodetection of COP1 protein in nuclei-depleted (nuc^-) and nuclei-enriched (nuc^+) protein fractions of 4-d-old dark-grown Col-0 and *spa-nQ* mutant seedlings. PEPC was used as a cytosolic marker, Histone H3 was used as a nuclear marker. Proteins were detected using anti-COP1, anti-PEPC and anti-Histone H3 antibodies, respectively. The nuclei-enriched fractions were 15 × concentrated compared to the nuclei-depleted fractions. Two independent biological replicates are shown. **B-I:** Representative nuclei in hypocotyls of 4-d-old dark-grown transgenic Col-0 (B, C, F, G) and *spa-nQ* (D, E, H, I) seedlings expressing a *35S::YFP-COP1* construct. The upper panel shows fluorescence microscopy images, the lower panel presents the corresponding brightfield images. Filled arrowheads denote nuclear speckles, unfilled arrowheads denote cytoplasmic inclusion bodies.

Figure S1). The *35S::YFP-COP1* line was crossed into the *spa-nQ* background, but no difference of YFP-COP1 accumulation was observed compared to the parental line (Figure 2.1 D, E, H, I). Thus, the similar localisation patterns of YFP-COP1 in the wild-type and *spa-nQ* backgrounds are in agreement with the subcellular localisation of native COP1 protein observed in the nuclear fractionation experiments. Taken together, these results strongly suggest that the SPA proteins are not required for COP1 nuclear accumulation in darkness.

2.2 SPA2 function in the light is repressed by rapid degradation as well as selective post-translational inactivation

The four *SPA* genes are differentially regulated by light at the transcriptional level (Fittinghoff et al., 2006) and the respective proteins exhibit distinct light- and tissue-specific accumulation patterns (Zhu et al., 2008). This differential regulation is accompanied by overlapping but also distinct functions of the *SPA* genes during plant development (Laubinger and Hoecker, 2003; Laubinger et al., 2004; Fittinghoff et al., 2006; Laubinger et al., 2006). In particular, *SPA1* and *SPA2* function equally well to suppress photomorphogenesis in dark-grown seedlings, whereas only *SPA1* is active in light-grown seedlings to prevent overstimulation by light (Laubinger et al., 2004; Fittinghoff et al., 2006; Balcerowicz et al., 2011).

2.2.1 SPA2-HA protein accumulates to lower levels than SPA1-HA protein in light-grown seedlings

Previous analysis of chimeric constructs harbouring different combinations of *SPA1* or *SPA2* ORFs with *SPA1* or *SPA2* regulatory sequences had shown that the protein sequence accounts for the lack of SPA2 repressor function in light-grown seedlings (Balcerowicz et al., 2011; Figure 1.4). To examine whether the functional differences conferred by the SPA protein sequences in seedlings are related to the levels of the respective proteins, their accumulation was analysed in transgenic seedlings grown in darkness and weak FRc, conditions in which the different phenotypes conferred by the *SPA1* and *SPA2* ORFs were apparent (Balcerowicz et al., 2011; Supplemental Figure S2 A, B). SPA1-HA and SPA2-HA were detected using an anti-HA antibody that allowed direct comparison of SPA1-HA and SPA2-HA protein levels. Several independent, homozygous transgenic lines were analysed per construct. Lines in the *spa1 spa2 spa3* rather than the *spa-Q* background were used in most cases since the former display a large and healthy adult plant phenotype due to the wild-type *SPA4* gene (Laubinger et al., 2004) and therefore produce larger amounts of seeds necessary for the experiments.

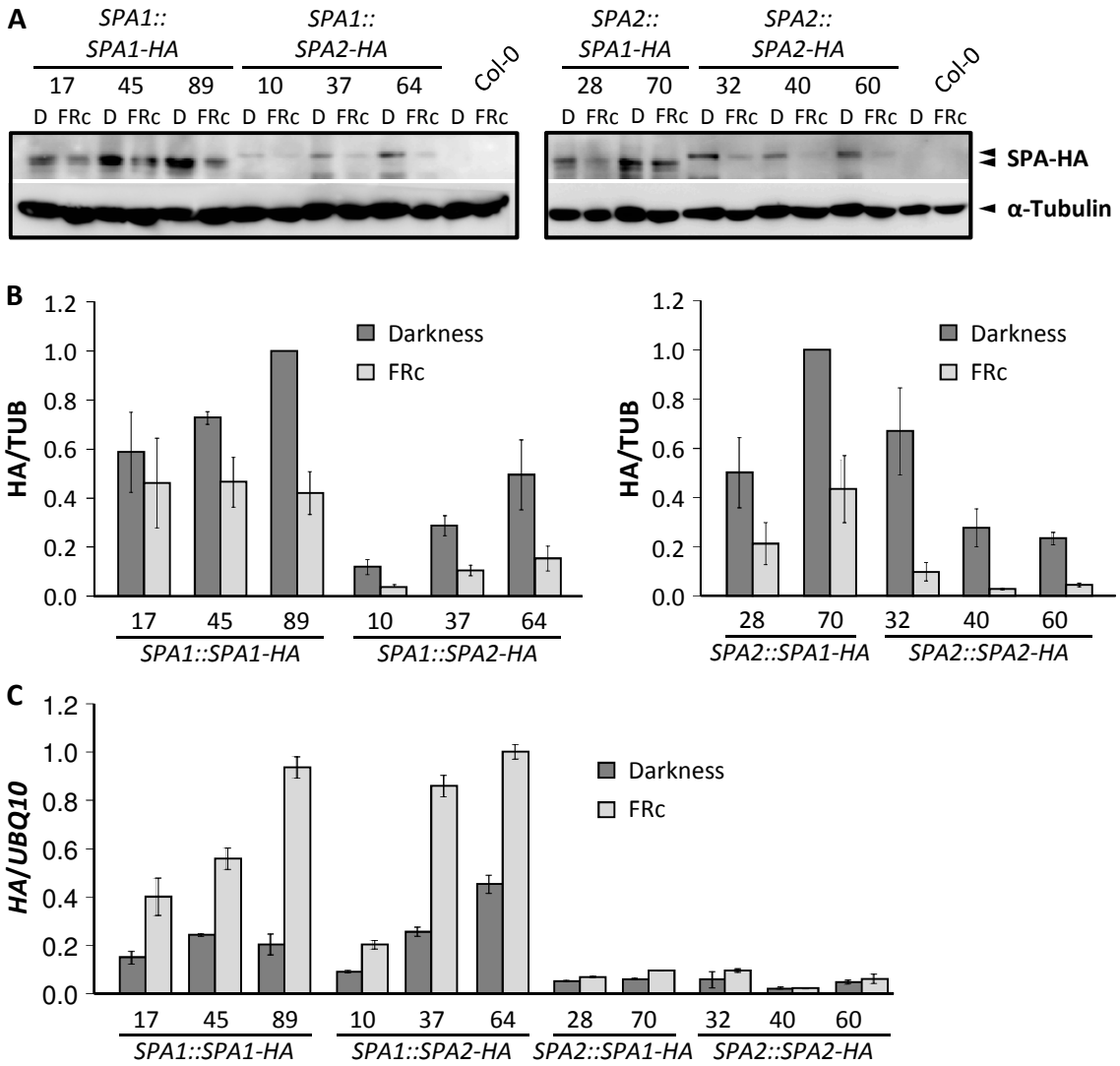

Figure 2.2: SPA2-HA protein accumulates to lower levels than SPA1-HA protein in the *spa1 spa2 spa3* mutant background.
A, B: Immunodetection (A) and quantification (B) of SPA1-HA and SPA2-HA protein levels in 4-d-old *spa1 spa2 spa3* mutant seedlings grown in darkness or FRc ($0.35\,\mu mol\,m^{-2}\,s^{-1}$). SPA1-HA and SPA2-HA were expressed from the *SPA1* promoter (left) and *SPA2* promoter (right), respectively, and detected using an anti-HA antibody. Numbers indicate independent transgenic lines. Tubulin levels are shown as loading control. Protein levels were normalised to tubulin levels and expressed relative to the respective highest-accumulating line. **C:** Transcript levels of *SPA1-HA* and *SPA2-HA* in darkness or FRc in the lines shown in A. Transcript levels were normalised to *UBQ10* and calibrated to the highest-expressing line.
Error bars represent the standard error of the mean (SEM) of two to three biological replicates.

Strikingly, SPA2-HA accumulated to lower levels than SPA1-HA when expressed from the same promoter (Figure 2.2 A, B). While most SPA1-HA lines also displayed higher SPA-HA levels than the SPA2-HA lines in darkness, the effect was even more pronounced in FRc-grown seedlings. When expressed from the *SPA1* promoter, SPA2-HA levels were 3- to 10-fold lower than SPA1-HA levels in FRc; similarly, levels of SPA2-HA expressed

from the *SPA2* promoter were 4- to 15-fold lower than those of SPA1-HA expressed from the same promoter (Figure 2.2 A, B). Comparable results were obtained for SPA-HA levels in transgenic *spa-Q* seedlings (Supplemental Figure S3 A, B) and in the leaves of adult *spa-Q* plants grown in short day conditions (Supplemental Figure S4 A), showing that the protein levels are similarly affected in young and adult tissue.

These differences in SPA1-HA and SPA2-HA protein levels were not reflected by the respective *SPA-HA* transcript levels. Lines expressing SPA-HA proteins from the *SPA1* promoter showed elevated transcript levels in FRc- compared to dark-grown seedlings while levels were similar in darkness and FRc when SPA-HA proteins were expressed from the *SPA2* promoter (Figure 2.2 C; Supplemental Figure S3 C). This confirms previously described characteristics of the two promoters (Fittinghoff et al., 2006). Moreover, levels of *SPA1-HA* and *SPA2-HA* transcripts were very similar when expressed from the same promoter (Figure 2.2 C; Supplemental Figure S3 C), demonstrating that differential expression is not the cause for the observed differences in protein levels.

2.2.2 Light exposure leads to rapid degradation of SPA1-HA and SPA2-HA in the 26*S* proteasome

Since SPA2-HA accumulates to lower levels than SPA1-HA in FRc-grown seedlings, their stability appears to be differentially regulated by light. To investigate whether this is a rapid response, transgenic seedlings expressing SPA1-HA and SPA2-HA from the light-insensitive *SPA2* promoter were grown in darkness and then exposed to FR for short periods of time. While COP1 levels were unchanged by exposure to FR, SPA1-HA and SPA2-HA levels were strongly reduced within 1 h of FR irradiation (Figure 2.3 A-C). Only a weak additional decrease was observed in the following 23 h, suggesting that this light-dependent reduction in SPA-HA protein levels is a relatively fast process. *SPA-HA* transcript levels remained unchanged throughout the experiment (Figure 2.3 D), suggesting that light downregulates SPA-HA protein levels in a post-transcriptional manner. Moreover, light exposure reduced SPA1-HA levels 3-fold at most, but reduced SPA2-HA levels up to 12-fold (Figure 2.3 A, B). Thus, light appears to destabilise SPA2-HA more strongly than SPA1-HA.

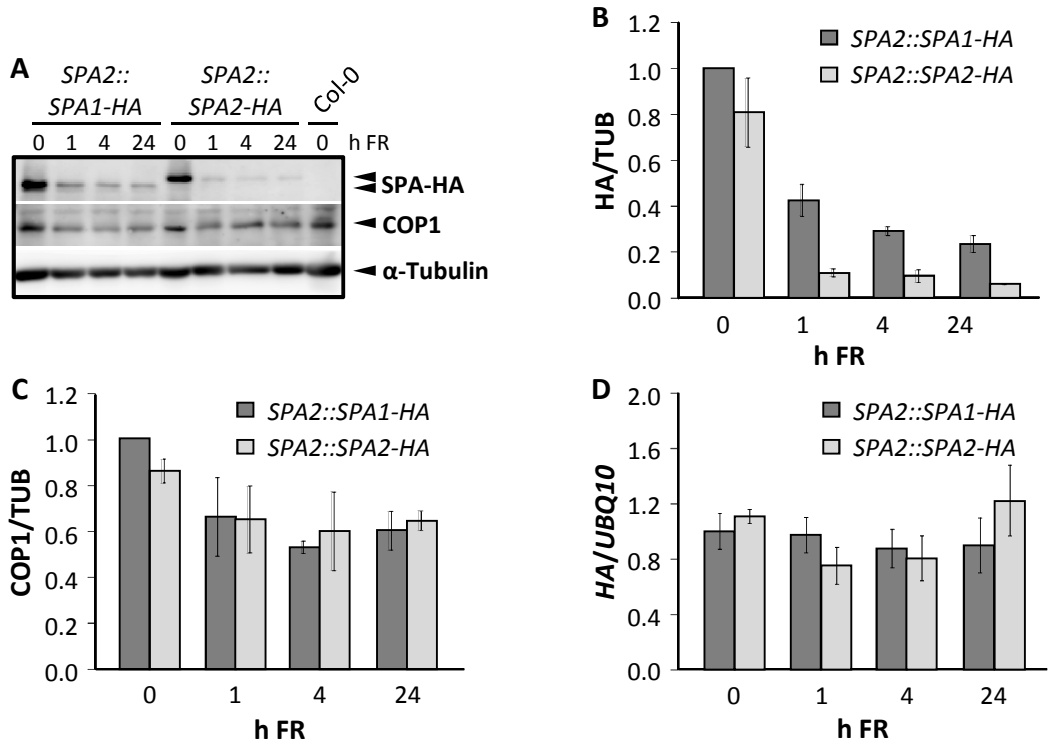

Figure 2.3: Light exposure leads to rapid destabilisation of SPA1-HA and SPA2-HA.
A-C: Immunodetection (A) and quantification of SPA1-HA, SPA2-HA (B) and COP1 (C) protein levels in 4-d-old *spa1 spa2 spa3* seedlings grown in darkness and then shifted to FR ($0.35\,\mu mol\,m^{-2}\,s^{-1}$) for the indicated periods of time. *SPA1::SPA1-HA* line 28 and *SPA2::SPA2-HA* line 32 were used for these experiments due to similar protein levels in darkness. SPA-HA protein levels were detected using an anti-HA antibody. Tubulin levels are shown as loading control. SPA-HA and COP1 protein levels were normalised to tubulin levels and expressed relative to SPA1-HA and COP1 levels in darkness, respectively.
D: Transcript levels of *SPA1-HA* and *SPA2-HA* in the lines shown in A. Transcript levels were normalised to *UBQ10* and calibrated to *SPA1-HA* levels in darkness. Error bars represent the SEM of two biological replicates.

Proteasomal degradation represents an important mechanism by which light controls the stability of proteins (Hoecker, 2005). To test whether SPA1-HA and SPA2-HA are degraded in the $26S$ proteasome, dark-grown seedlings were shifted to FR while being treated with the proteasome inhibitor MG132. MG132 treatment was able to eliminate light-induced destabilisation of both SPA1-HA and SPA2-HA proteins without affecting the respective transcript levels (Figure 2.4). Hence, light destabilises the two proteins by promoting their degradation in the $26S$ proteasome.

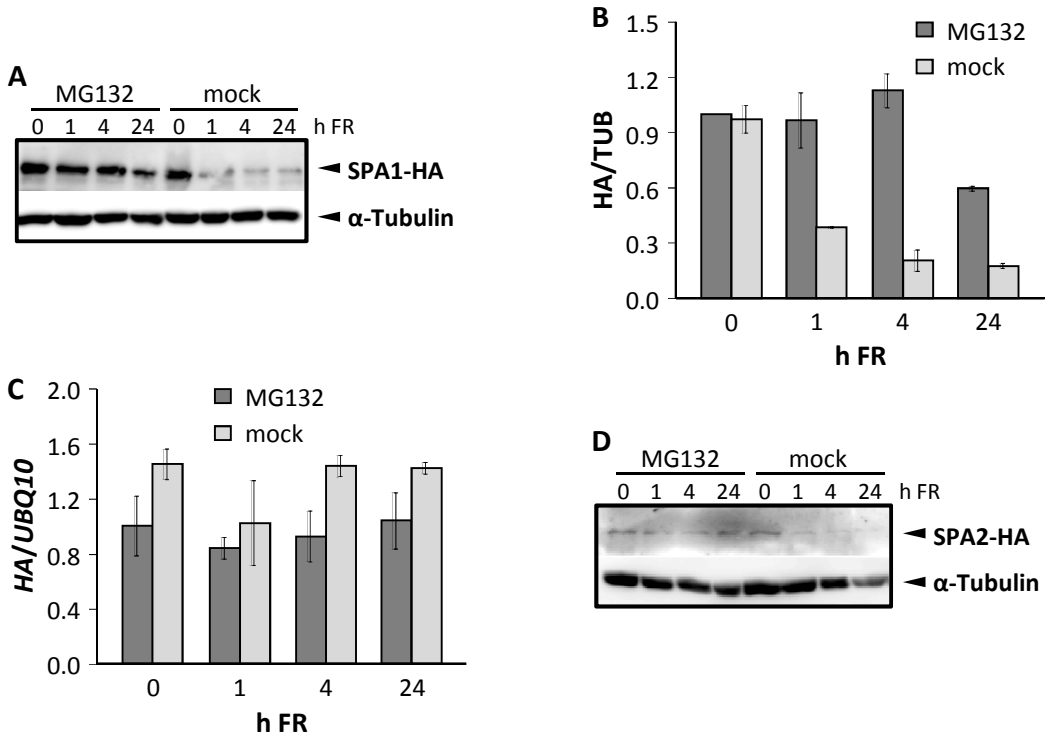

Figure 2.4: SPA1-HA and SPA2-HA are degraded via the 26*S* proteasome.
A, B: Immunodetection (A) and quantification (B) of SPA1-HA protein levels in 4-d-old *spa1 spa2 spa3* seedlings (line 28) grown in darkness and then shifted to FR (0.35 µmol m^{-2} s^{-1}) for the indicated periods of time while being treated with MG132 or mock-treated. SPA1-HA protein levels were detected using an anti-HA antibody. Tubulin levels are shown as loading control. SPA1-HA protein levels were normalised to tubulin levels and expressed relative to SPA1-HA in darkness before MG132 treatment. **C:** Transcript levels of *SPA1-HA* in the lines shown in A. Transcript levels were normalised to *UBQ10* and calibrated to *SPA1-HA* levels in dark-grown seedlings before MG132 treatment. **D:** Immunodetection of SPA2-HA protein levels in 4-d-old *spa1 spa2 spa3* seedlings (line 32) grown in darkness and then shifted to FR (0.35 µmol m^{-2} s^{-1}) for the indicated periods of time while being treated with MG132 or mock-treated. Protein levels were too low to be quantified.
Error bars represent the SEM of two biological replicates.

2.2.3 Lack of SPA2 protein function in light-grown seedlings is not solely due to SPA2 degradation

The differential destabilisation of SPA1 and SPA2 by light likely represents an important mechanism by which their functional diversity is obtained. To test whether the light-induced reduction in SPA2 protein level accounts for the observed lack of *SPA2* function in light-grown seedlings, transgenic lines are required that accumulate SPA1-HA and SPA2-HA at equal levels in FRc. To this end, 30 additional transgenic lines were screened that express SPA1-HA or SPA2-HA in the *spa1 spa2 spa3* mutant background. All lines

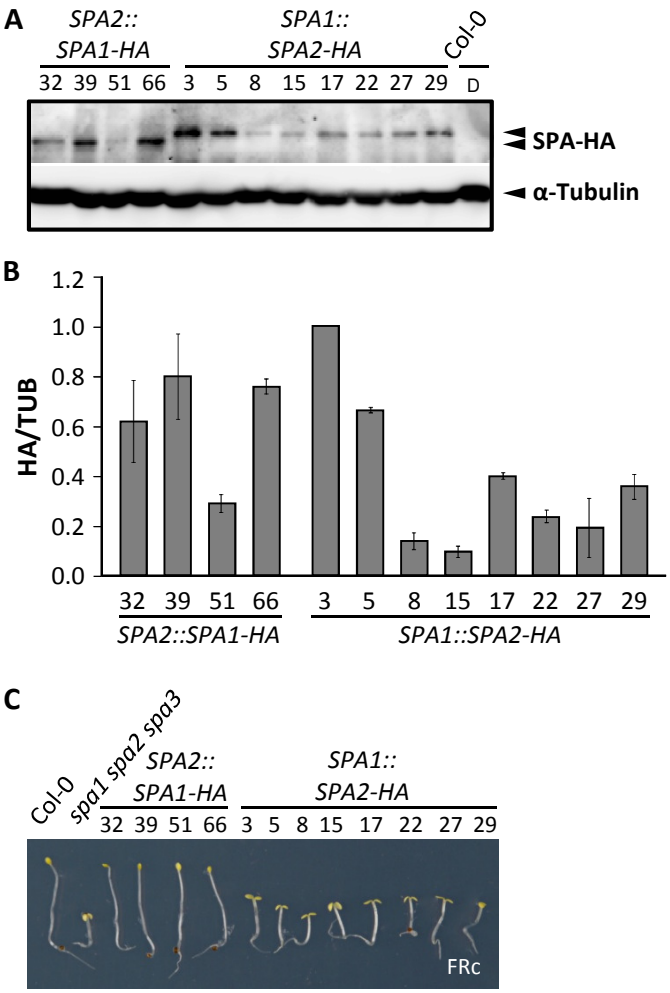

Figure 2.5: Accumulation of high SPA2 protein levels does not restore SPA2 repressor function in FRc.
A, B: Immunodetection (A) and quantification (B) of SPA1-HA and SPA2-HA protein levels in 4-d-old transgenic *spa1 spa2 spa3* mutant seedlings expressing the indicated *SPA promoter::ORF* constructs when grown in weak FRc ($0.05\,\mu mol\,m^{-2}\,s^{-1}$). SPA-HA protein levels were detected using an anti-HA antibody. Tubulin levels are shown as loading control. SPA-HA protein levels were normalised to tubulin levels and expressed relative to the highest-accumulating line. Error bars represent the SEM of two biological replicates. **C:** Visual phenotype of 4-d-old FRc-grown seedlings of the *SPA promoter::ORF* lines used for immunoblot analysis shown in A.
Numbers indicate independent transgenic lines that were selected from a set of 30 lines screened for similar SPA1-HA and SPA2-HA protein levels.

displayed lower levels of the respective SPA-HA protein in FRc-grown compared to dark-grown seedlings (Supplemental Figure S5). Most lines also showed lower levels of SPA2-HA than SPA1-HA, but two lines expressing SPA2-HA from the light-induced *SPA1* promoter (lines 3 and 5) accumulated levels of SPA2-HA in FRc that were as high or even higher than those of SPA1-HA in lines expressing SPA1-HA from the light-insensitive *SPA2* promoter (Figure 2.5 A, B).

Analysis of the seedling phenotype revealed that even the lines expressing high levels of SPA2-HA did not show any repression of photomorphogenesis in weak FRc while all lines expressing SPA1-HA did (Figure 2.5 C). Thus, increasing the level of SPA2 to that of SPA1 does not convert SPA2 into a functional repressor of light signalling in light-grown seedlings, implying that there must be an additional mechanism by which light selectively inactivates SPA2.

2.3 The repressor of auxin signalling AXR3 is involved in light regulation of stomatal development

Photomorphogenesis of Arabidopsis seedlings is not only characterised by the suppression of hypocotyl elongation and the opening and greening of cotyledons, but also by the formation of stomata (von Arnim and Deng, 1996). The abaxial cotyledon epidermis of dark-grown seedlings contains almost no mature stomata, whereas light-grown seedlings display a large number of fully developed stomata (Kang et al., 2009). Promotion of stomata formation by light requires repression of the COP1/SPA complex by phytochromes and cryptochromes, but the exact mechanism by which the COP1/SPA complex regulates stomatal development is yet unknown (Kang et al., 2009). The auxin-insensitive mutants *axr2-1*, *axr3-1* and *shy2-2* were previously reported to be defective in the suppression of stomata formation in darkness (Ranjan, 2010), suggesting that the respective genes may represent novel regulators of light-dependent stomatal development.

2.3.1 Gain-of-function *aux/iaa* mutants fail to suppress stomata differentiation in dark-grown seedlings

The gain-of-function *aux/iaa* mutants *axr2-1*, *axr3-1* and *shy2-2* display a constitutively photomorphogenic phenotype similar to, although less pronounced than, *cop1-4* and *spa1 spa2 spa3* mutants, with short hypocotyls and partially opened cotyledons when grown in darkness (Timpte et al., 1994; Leyser et al., 1996; Reed et al., 1998; Figure 2.6 A). Dark-grown *cop1-4* and *spa1 spa2 spa3* mutants show in addition an increased proportion of mature stomata among all epidermal cells, also referred to as the stomatal index (SI), in the abaxial cotyledon epidermis (Kang et al., 2009; Figure 2.6 B, C). I quantified the stomatal phenotype of the *aux/iaa* mutants to determine whether their reported defect in the suppression of stomatal development in darkness is reflected by an increased SI as well. Indeed, the SI of the three mutants was increased compared to the wild type, in which almost no mature stomata were found (Figure 2.6 B, C; Supplemental Figure S6). In contrast, the proportion of stomatal precursors, i.e. meristemoids and GMCs, was not changed or only mildly reduced in the three *aux/iaa* mutants, suggesting that these mutations not only promote the differentiation of stomatal precursors to mature stomata,

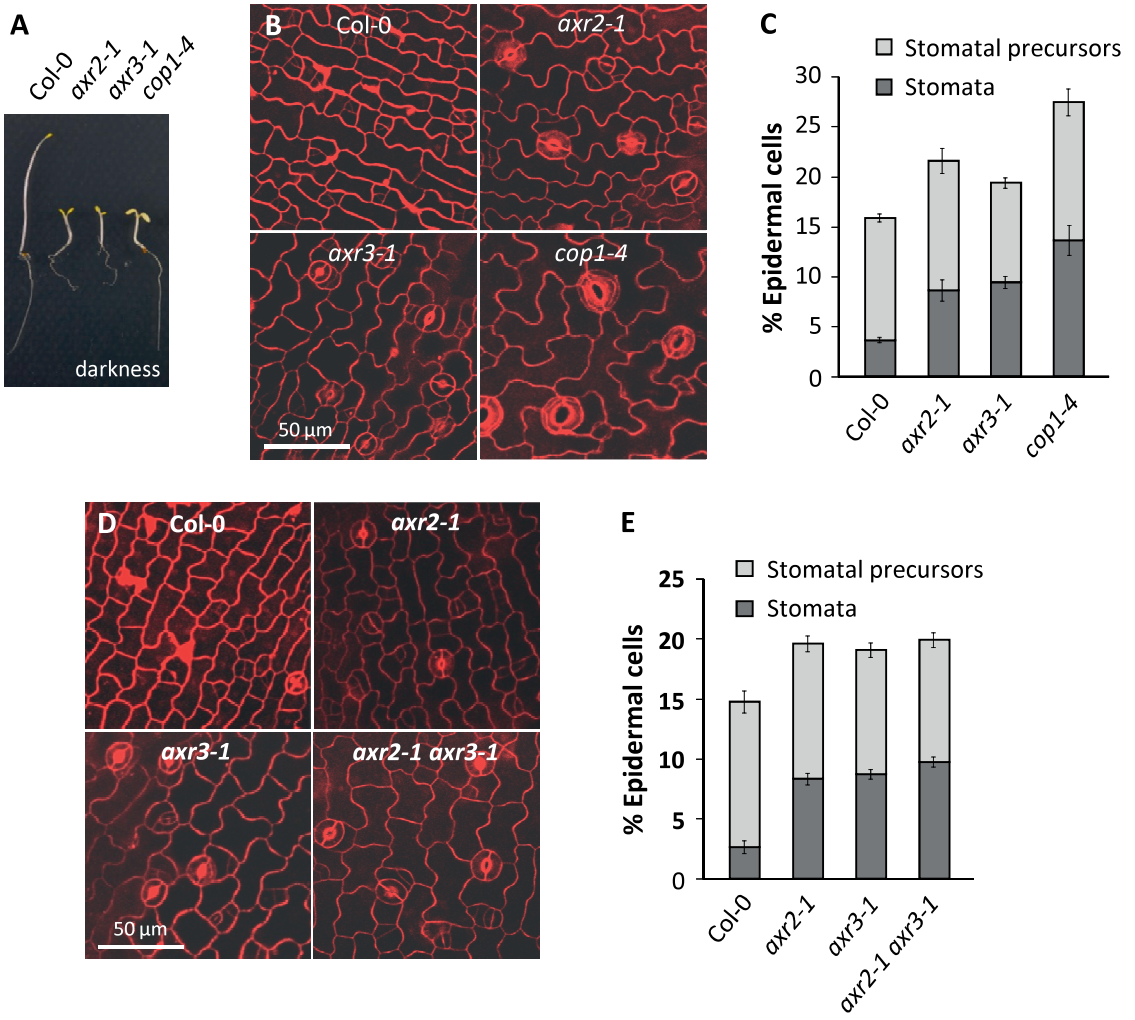

Figure 2.6: The constitutively photomorphogenic mutants *axr2-1* and *axr3-1* display increased stomata formation in darkness.
A: Visual phenotype of 4-d-old dark-grown seedlings of the indicated genotypes. **B, D:** Confocal images of the abaxial cotyledon epidermis of 10-d-old dark-grown seedlings of the indicated genotypes. Cell outlines were visualised by propidium iodide (PI) staining. **C, E:** Quantification of the stomatal phenotypes shown in B and D, respectively, expressed as the percentage of stomata and stomatal precursors among total epidermal cells. Error bars represent the SEM (n = 10).

but also enhance early steps of stomatal development. The *axr2-1 axr3-1* double mutant displayed no additional increase in stomata formation when compared to the single mutants (Figure 2.6 D, E), implying that the respective genes have largely redundant functions with regard to stomatal development.

The stomata-overproducing phenotype of the *aux/iaa* mutants appears to be darkness-specific; no strong changes in the percentage of stomata and stomatal precursors were observed in the abaxial cotyledon epidermis of seedlings grown in continuous white light (Wc) or in the abaxial epidermis of true leaves (Figure 2.7 A-D). A weak phenotype,

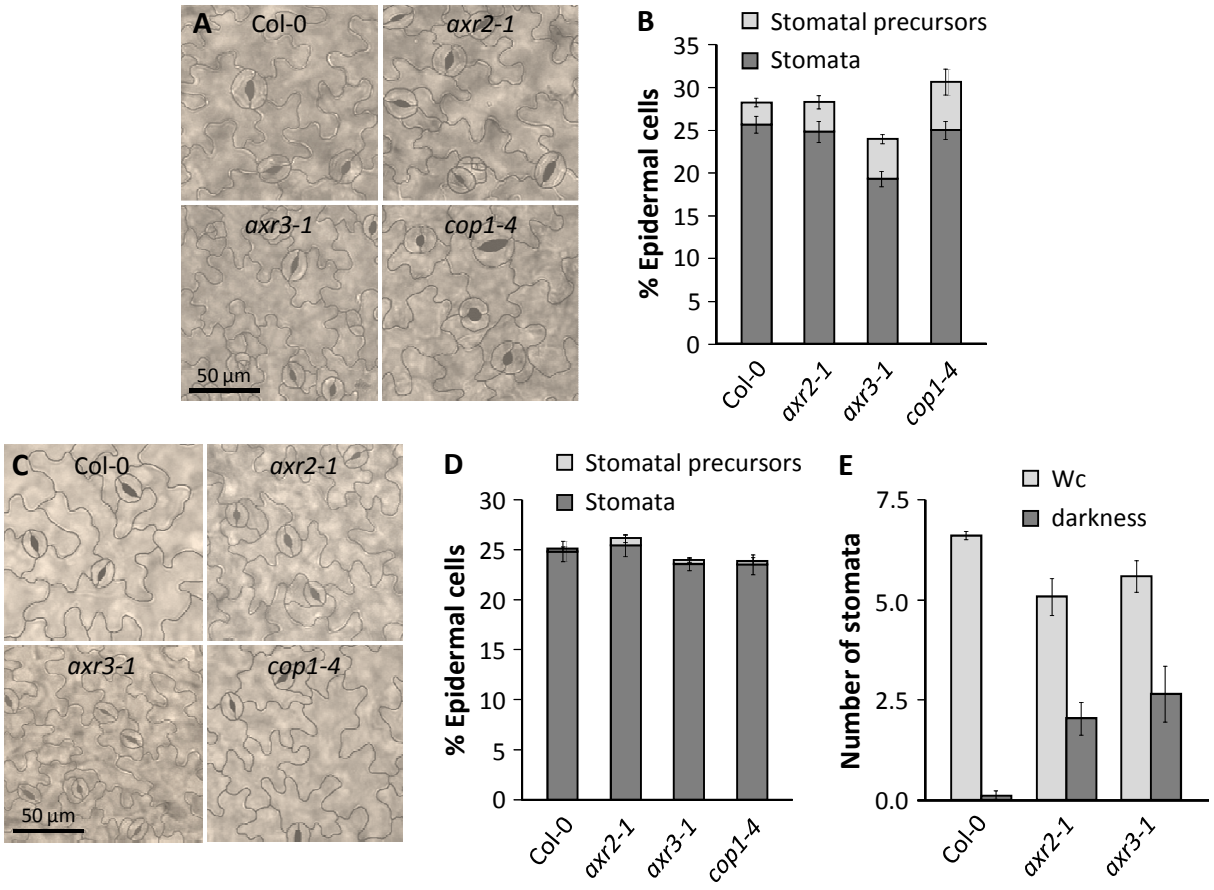

Figure 2.7: The stomatal phenotype of *axr2-1* and *axr3-1* is specific to dark-grown seedlings. **A, C:** Brightfield images of the abaxial cotyledon epidermis of 10-d-old seedlings grown in Wc ($25\,\mu mol\,m^{-2}\,s^{-1}$) (A) and of the abaxial epidermis of true leaves of 3-week-old long day-grown plants (C) of the indicated genotypes. Cell outlines were traced in dark grey. **B, D:** Quantification of the stomatal phenotypes shown in A and C, respectively. **E:** Quantification of stomata in hypocotyls of 10-d-old seedlings of the indicated genotypes grown in darkness or Wc ($25\,\mu mol\,m^{-2}\,s^{-1}$).
Error bars represent the SEM (n = 10).

however, was found in hypocotyls as those of dark-grown wild-type seedlings did not contain any stomata whereas two to three stomata were found in the hypocotyls of dark-grown *axr2-1* and *axr3-1* mutant seedlings (Figure 2.7 E). Furthermore, only *axr2-1*, but not *axr3-1*, displayed a weak increase in the SI of the adaxial cotyledon epidermis in darkness (Supplemental Figure S7), indicating that the defect in the suppression of stomata differentiation primarily affects the abaxial epidermis.

To investigate whether the enhanced stomata formation in dark-grown *aux/iaa* mutants is a post-embryonic defect, the abaxial cotyledon epidermis of dark-grown seedlings was examined over a time course from 2 to 10 days post germination (dpg). Virtually no mature stomata were observed in the cotyledon epidermis of 2-d-old wild-type, *axr2-1* and *axr3-1* mutant seedlings; the first stomata appeared between 3 and 4 dpg and excessive

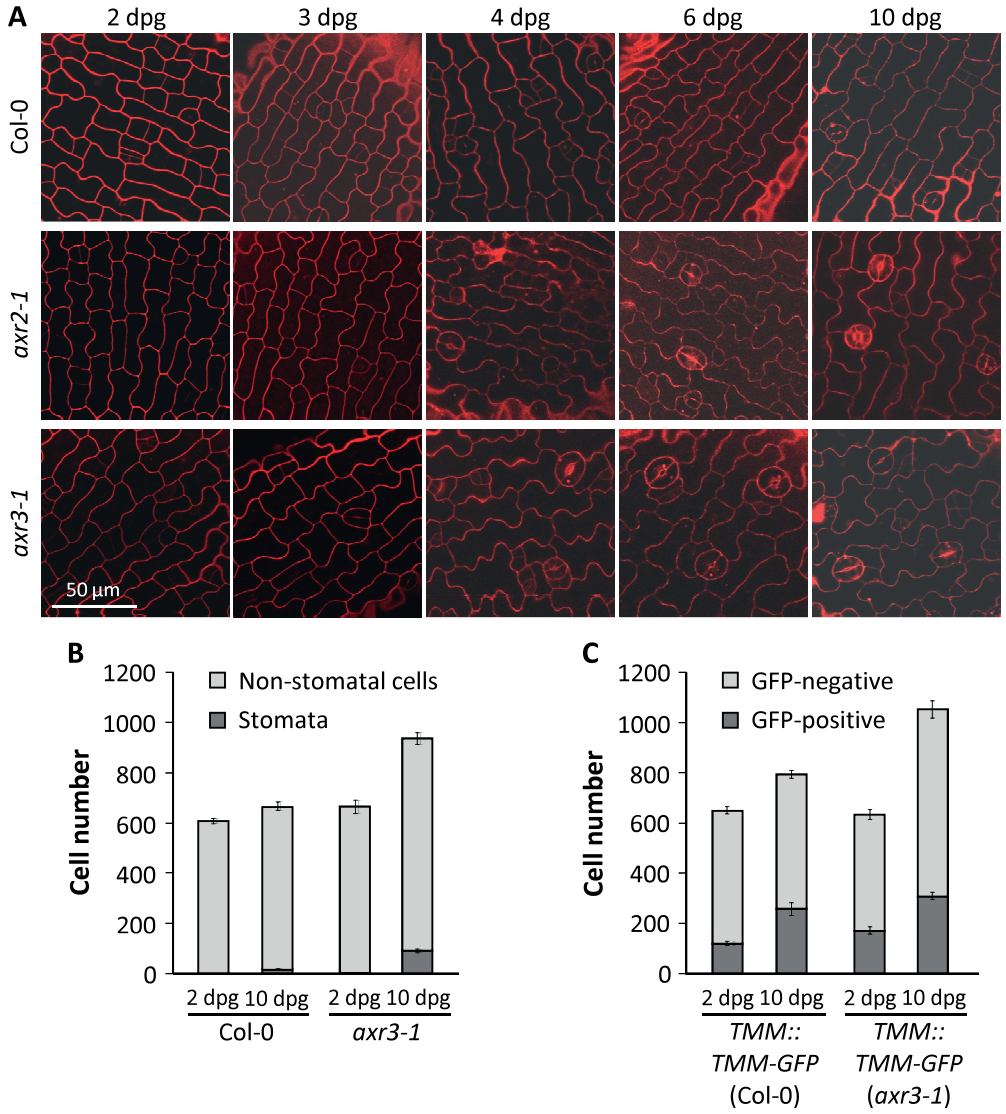

Figure 2.8: The *axr3-1* mutant shows a post-embryonic increase in epidermal cell division. **A:** Confocal images of the abaxial cotyledon epidermis of dark-grown Col-0, *axr2-1* and *axr3-1* seedlings between 2 and 10 days post germination (dpg). Cell outlines were visualised by PI staining. **B:** Quantification of stomata and non-stomatal cells in the abaxial cotyledon epidermis of 2- and 10-d-old dark-grown Col-0 and *axr3-1* seedlings. **C:** Quantification of GFP-positive and GFP-negative cells in the abaxial cotyledon epidermis of 2- and 10-d-old dark-grown Col-0 and *axr3-1* seedlings expressing a *TMM::TMM-GFP* construct. Error bars represent the SEM (n = 10).

stomata developed in *axr2-1* and *axr3-1* in the following days (Figure 2.8 A). In 10-d-old seedlings, the number of stomata in *axr3-1* was approximately five times higher than in the wild type (Figure 2.8 B). Notably, not only the number of stomata but also the number of non-stomatal cells increased strongly between 2 and 10 dpg in the *axr3-1* mutant, but not in the wild type (Figure 2.8 B).

Similar results were obtained from the analysis of 2- and 10-d-old dark-grown wild-type and *axr3-1* seedlings harbouring a *TMM::TMM-GFP* construct, which has previously

been reported to be expressed in meristemoids, GMCs and SLGCs (Nadeau and Sack, 2002a) and could thus be used as a marker for not completely differentiated stomatal lineage cells. In the wild-type background, only the number of GFP-positive cells increased from 2 to 10 dpg whereas the number of both GFP-positive and GFP-negative cells increased in the *axr3-1* background during this period (Figure 2.8 C). These results further support the hypothesis that the stomatal lineage contains the only epidermal cells dividing in cotyledons of dark-grown seedlings and that *axr3-1* increases epidermal cell number likely by enhancing both entry into and progression through the stomatal lineage.

2.3.2 The stomata-overproducing phenotype of *axr3-1* depends on functional *SPCH*, *MUTE* and *FAMA*

The genes *SPCH*, *MUTE* and *FAMA* encode bHLH transcription factors that are master regulators of consecutive steps in stomatal development. Loss of function of any of these genes results in the arrest of stomatal development at the step controlled by the respective gene: *spch* mutants display an epidermis completely devoid of stomata (MacAlister et al., 2007; Pillitteri et al., 2007) whereas *mute* and *fama* mutants have arrested meristemoids and GMC clusters ("*fama* tumours"), respectively, in place of mature stomata (Ohashi-Ito and Bergmann, 2006; Pillitteri et al., 2007). To investigate genetic interactions of the *Aux/IAA* genes with *SPCH*, *MUTE* and *FAMA*, *axr3-1 spch-3*, *axr3-1 mute-1* and *axr3-1 fama-1* double mutants were generated. The abaxial cotyledon epidermis of dark-grown *axr3-1 spch-3*, similar to that of the *spch-3* single mutant, consisted exclusively of pavement cells (Figure 2.9 A). Phenotypes of the *axr3-1 mute-1* and *axr3-1 fama-1* double mutants also resembled those of the *mute-1* and *fama-1* single mutants, respectively, although the numbers of meristemoids and "*fama* tumours" were increased by the additional *axr3-1* mutation (Figure 2.9 A-C), indicating that the *mute-1* and *fama-1* mutations are not completely epistatic to *axr3-1*. Taken together, these observations suggest that *AXR3* acts genetically upstream of the three bHLH factor genes and requires their functionality to enhance stomata differentiation.

Strikingly, cell division was severely impaired in the *spch-3* background: no difference in cell numbers was observed in the abaxial cotyledon epidermis of 2- and 10-d-old *spch-3* mutant seedlings (Figure 2.9 D), confirming that stomatal lineage cells are the only epidermal cells undergoing division in dark-grown cotyledons. The epidermis of *axr3-1 spch-3* contained slightly more cells than that of the *spch-3* single mutant, but again no changes in cell number were detected between 2- and 10-d-old seedlings (Figure 2.9 D). This indi-

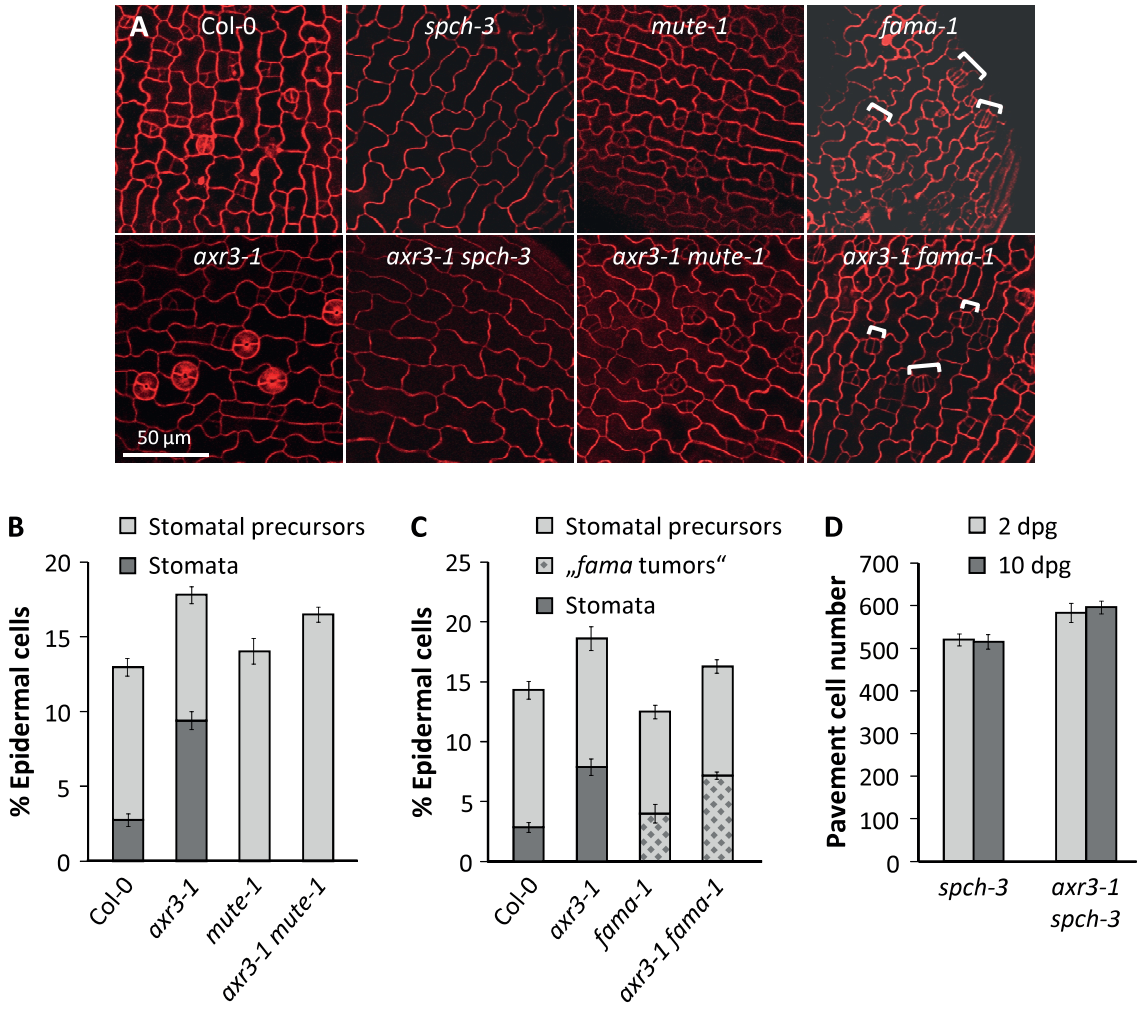

Figure 2.9: The *axr3-1* mutation requires functional *SPCH*, *MUTE* and *FAMA* to promote stomatal development.
A: Confocal images of the abaxial cotyledon epidermis of 10-d-old dark-grown seedlings of the indicated genotypes. Cell outlines were visualised by PI staining. Brackets highlight "*fama* tumours". **B, C:** Quantification of stomata, stomatal precursors and "*fama* tumours" in the abaxial cotyledon epidermis of 10-d-old dark-grown seedlings of the indicated genotypes. **D:** Quantification of pavement cells in the abaxial cotyledon epidermis of 2- and 10-d-old dark-grown *spch-3* and *axr3-1 spch-3* seedlings.
Error bars represent the SEM (n = 10).

cates that the effect of the *axr3-1* mutation on cell division is dependent on the presence of the stomatal lineage.

Despite the observed dependence of the *axr3-1* phenotype on the presence of the three bHLH factors, their transcripts were only slightly elevated in dark-grown *axr2-1* and *axr3-1* mutants compared to the wild type (Supplemental Figure S8) whereas *SPCH* and *FAMA* transcript levels are clearly increased in dark-grown *cop1-4* mutants (Kang et al., 2009; Supplemental Figure S8). Furthermore, no visible change in localisation or signal strength was observed for the GFP signal of the transcriptional reporters *SPCH::nucGFP*

and *MUTE::GFP* (MacAlister et al., 2007) as well as for the translational reporters *MUTE::MUTE-GFP* and *FAMA::FAMA-GFP* (Pillitteri et al., 2007) when introduced into the *axr3-1* background (Supplemental Figure S9). Thus, any major effect *axr3-1* may have on the three bHLH transcription factors appears to be post-translational.

2.3.3 A constitutively active YDA MAPK cascade completely suppresses stomata formation in *axr3-1*

The YDA MAPK cascade acts upstream of SPCH, and probably also MUTE and FAMA, to suppress stomatal development (Ohashi-Ito and Bergmann, 2006; MacAlister et al., 2007; Lampard et al., 2008). It integrates signals from the light and BR signalling pathways (Kang et al., 2009; Kim et al., 2012; Khan et al., 2013), raising the possibility that it is also a downstream factor in AXR3 signalling.

Loss-of-function *yda* and *mpk3 mpk6* mutants as well as *MKK4-MKK5RNAi* plants have an epidermis consisting almost exclusively of stomata (Bergmann et al., 2004; Wang et al., 2007); therefore, additive effects of the *axr3-1* mutation would be difficult to detect in these backgrounds. In contrast, expression of constitutively active versions of YDA, MKK4 and MKK5 results in an epidermis completely devoid of stomata (Bergmann et al., 2004; Wang et al., 2007), but many lines expressing these constructs show strong silencing effects (Wang et al., 2007) and were thus not suitable for crossing and subsequent epistasis analysis. Instead, *axr3-1* was crossed to *GVG*-Nt-*MEK2*^{DD} plants, which harbour a dexamethasone (DEX)-inducible construct of a constitutively active version of tobacco MEK2, which is functionally interchangeable with Arabidopsis MKK4 and MKK5 (Ren et al., 2002). This transgenic line was reported to be very stable in Arabidopsis (Wang et al., 2007). Both in the wild-type and the *axr3-1* background, induction of Nt-*MEK2*^{DD} expression resulted in the complete absence of stomata (Figure 2.10), in-

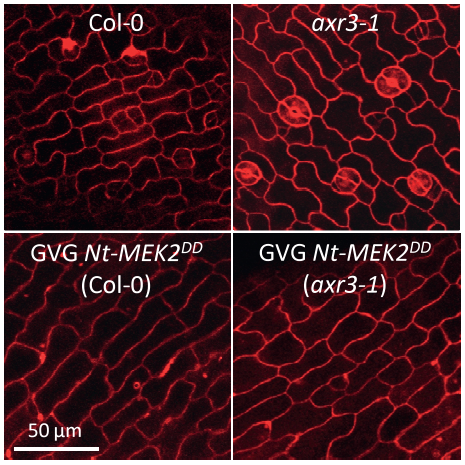

Figure 2.10: A constitutively active MKK suppresses stomata formation also in the *axr3-1* background.
Confocal images of the abaxial cotyledon epidermis of 10-d-old dark-grown seedlings of Col-0, *axr3-1* as well as transgenic Col-0 and *axr3-1* seedlings expressing the DEX-inducible *GVG*-Nt-*MEK2*^{DD} construct. Seedlings were grown on medium supplemented with 0.02 µM DEX. Cell outlines were visualised by PI staining.

dicating that the positive effect of the *axr3-1* mutation on stomatal development cannot overcome the effect of a constitutively active YDA MAPK cascade. Therefore, *AXR3* seems to act genetically upstream of *MPK3*, *MPK6*, *MKK4* and *MKK5*.

2.3.4 AXR3 acts in parallel with TMM and members of the ER family to regulate stomatal development

Upstream of the YDA MAPK cascade, the LRR receptor-like protein TMM and LRR receptor-like kinases of the ERf act cooperatively to restrict stomatal development in cotyledons of light-grown seedlings and in true leaves (Bergmann et al., 2004; Shpak et al., 2005; Lee et al., 2012; Jewaria et al., 2013). To test whether AXR3 acts through these proteins to affect stomatal development, genetic interactions between *axr3-1*, *tmm-1* and various *er*(*l*) mutants were tested.

The *tmm-1* mutant exhibits a strong stomata-overproducing and clustering phenotype in leaves and cotyledons when grown in the light (Yang and Sack, 1995; Supplemental Figure S10 A, B). In darkness, however, *tmm-1* hardly forms any mature stomata at all, but shows an increased number of meristemoids compared to the wild type (Kang et al., 2009; Figure 2.11 A, B). This phenotype was dramatically altered by an additional *axr3-1* mutation; the *axr3-1 tmm-1* double mutant not only displayed a higher proportion of stomata than the *axr3-1* single mutant, but also developed stomatal clusters in darkness (Figure 2.11 A, B). In contrast, its stomatal phenotype was similar to the *tmm-1* single mutant in the light (Supplemental Figure S10 A, B). Thus, the two mutations have synergistic effects and *axr3-1* seems to provide a sensitised background in which lack of *TMM* causes the formation of stomatal clusters also in darkness.

The *TMM::TMM-GFP* translational reporter was also used to investigate any effects of *axr3-1* on *TMM*: the GFP signal was detected in meristemoids, GMCs and adjacent cells in both the wild type and *axr3-1*. In addition, the subcellular localisation of TMM-GFP appeared to be unaffected by the *axr3-1* mutation as the GFP signal was observed at the plasma membrane and in intracellular structures in both cases (Supplemental Figure S10 C). This is in agreement with the lack of epistasis between the *axr3-1* and *tmm-1* mutations and further supports the hypothesis that *TMM* and *AXR3* act in parallel to regulate stomatal development.

Members of the *ERf* act in concert with *TMM* (Shpak et al., 2005; Lee et al., 2012), but

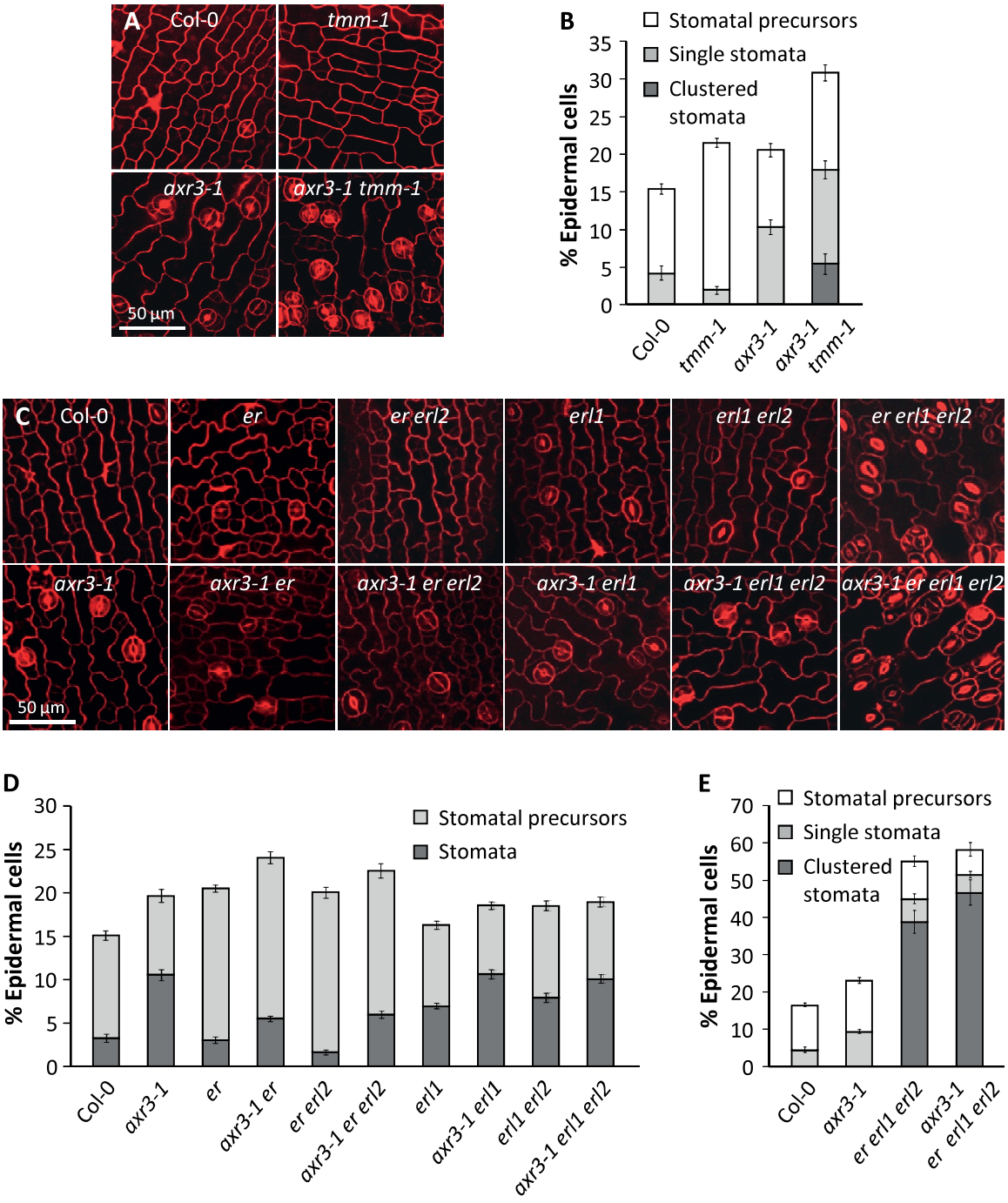

Figure 2.11: The *axr3-1* mutation shows additive and synergistic effects with loss-of-function mutations in *TMM* and *ERf* genes.
A, C: Confocal images of the abaxial cotyledon epidermis of 10-d-old dark-grown seedlings of the indicated genotypes. Cell outlines were visualised by PI staining. **B, D, E:** Quantification of the stomatal phenotypes shown in B and D, respectively. Error bars represent the SEM (n = 10).

different *ERf* genes affect different steps of stomatal development: in the light, *ER* primarily prevents entry divisions into the stomatal lineage whereas *ERL1* predominantly inhibits subsequent development of stomatal precursors; *ERL2* has minor functions in both processes. A knock-out of all three *ERf* genes results in a stomata clustering phenotype that is even stronger than that of a *tmm* mutant (Shpak et al., 2005).

Functional divergence of *ERf* members was also seen in dark-grown seedlings: *er* and *er erl2* mutants showed an increased proportion of stomatal precursors whereas *erl1* and *erl1 erl2* mutants formed more mature stomata than the wild type (Figure 2.11 C, D). An additional *axr3-1* mutation increased the proportion of stomata in each of these mutants although the increase caused by *axr3-1* was less pronounced than in the wild-type background (Figure 2.11 C, D). Furthermore, *axr3-1* also slightly increased the number of clustered stomata in the *er erl1 erl2* triple mutant (Figure 2.11 C, E). Taken together, these results suggest that, although an additional effect through receptors of the ERf is possible, AXR3 is able to act independently of these proteins to regulate stomatal development.

2.3.5 Light affects stomatal development separately through COP1 and AXR3

To date, the only established signalling pathway that links light signalling to the stomatal development signalling pathway involves inhibition of the COP1/SPA complex by phytochromes and cryptochromes and acts genetically upstream of *YDA*, but in parallel with *TMM* (Kang et al., 2009). *AXR3* exhibits similar genetic interactions with components of the stomatal development signalling pathway. To determine whether *COP1* and *AXR3* act in a common pathway, epistasis between *axr3-1* and the weak *cop1-4* mutation was tested. In contrast to the seedling-lethal *cop1-5* allele, which forms an epidermis consisting almost entirely of stomata regardless of light conditions, *cop1-4* has a relatively mild, darkness-specific stomata-overproducing phenotype (Kang et al., 2009) and was therefore suitable to test for additive effects with *axr3-1*. The *axr3-1 cop1-4* double mutant indeed produced a larger fraction of stomata than either single mutant (Figure 2.12 A, B), suggesting that both genes act in independent pathways. This is further corroborated by the fact that neither COP1 levels nor its subcellular localisation were changed in dark-grown *axr2-1* and *axr3-1* mutants (Figure 2.12 C, D) and that the transcript levels of *AXR2*, *AXR3* and *SHY2* in dark-grown *cop1-4* mutants were not significantly different from those detected in the wild type (Figure 2.12 E).

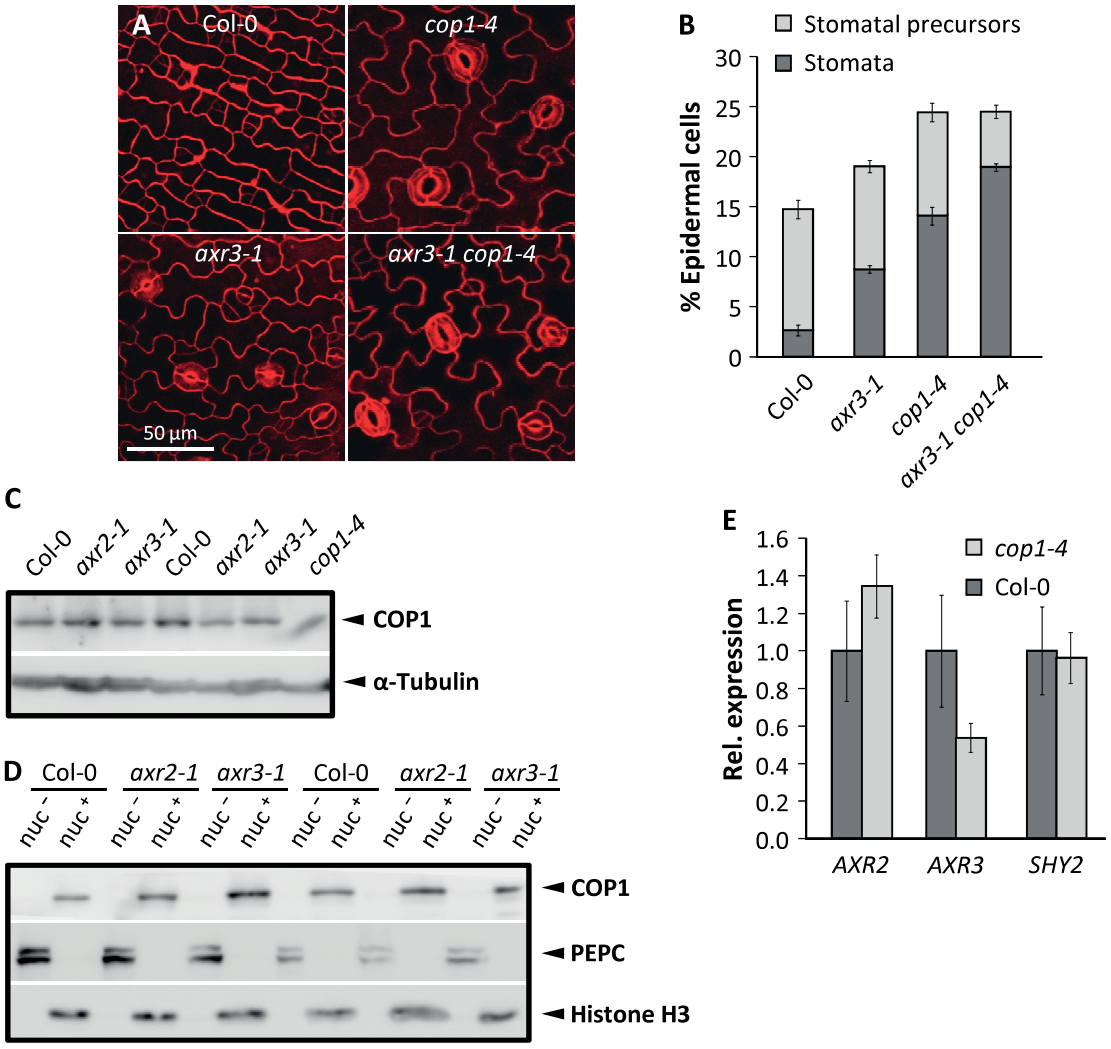

Figure 2.12: *AXR3* and *COP1* act independently in light-dependent stomatal development. **A:** Confocal images of the abaxial cotyledon epidermis of 10-d-old dark-grown seedlings of the indicated genotypes. Cell outlines were visualised by PI staining. **B:** Quantification of the stomatal phenotypes shown in A. Error bars represent the SEM (n = 10). **C, D:** Immunodetection of COP1 protein in total protein extracts (C) as well as nuclei-depleted (nuc^-) and nuclei-enriched (nuc^+) protein fractions (D) of 5-d-old dark-grown Col-0, *axr2-1* and *axr3-1* seedlings. Tubulin levels are shown as loading control for total protein extracts, PEPC is shown as a cytosolic marker and Histone H3 is shown as a nuclear marker. Proteins were detected using anti-COP1, anti-α-Tubulin, anti-PEPC and anti-Histone H3 antibodies, respectively. The nuclei-enriched fractions were 15 × concentrated compared to the nuclei-depleted fractions. Two independent biological replicates are shown. **E:** Transcript levels of *AXR2*, *AXR3* and *SHY2* in 5-d-old dark-grown Col-0 and *cop1-4* seedlings. Transcript levels were normalised to *UBQ10* and calibrated to the levels of dark-grown Col-0 seedlings. Error bars represent the SEM of three biological replicates.

2.3.6 Auxin can suppress stomata formation

The stomata-overproducing phenotype of the auxin-insensitive mutants *axr2-1*, *axr3-1* and *shy2-2* implies that auxin might be involved in the regulation of stomatal development. To test this hypothesis, the stomatal phenotypes of *axr2-1*, *axr3-1* and wild type were analysed in seedlings grown on media containing different concentrations of the synthetic auxin 1-naphtaleneacetic acid (NAA). In light-grown wild-type seedlings, NAA concentrations of 10 µM or higher strongly reduced the SI in the abaxial cotyledon epidermis, an effect that was much weaker in *axr2-1* and *axr3-1* (Figure 2.13 A; Supplemental Figure S11 A). In dark-grown seedlings, the low proportion of stomata in the wild type was further reduced when grown at 1 µM NAA, but was increased when grown at higher NAA concentrations (Figure 2.13 B; Supplemental Figure S11 B). This was not observed for *axr2-1* and *axr3-1*, which showed a slight reduction in their SI at NAA concentrations of 100 µM only (Figure 2.13 B; Supplemental Figure S11 B). Taken together, these results suggest that auxin inhibits stomatal development in a dosage-dependent manner and that the sensitivity to the auxin signal differs between dark- and light-grown seedlings.

Many auxin-regulated processes require the establishment of auxin gradients via polar auxin transport (Tanaka et al., 2006). Therefore, the stomatal phenotype of wild-type seedlings grown on medium supplemented with the polar auxin transport inhibitor 1-N-naphthylphthalamic acid (NPA) was analysed as well. Seedlings treated with NPA showed an increased SI in darkness compared to the mock-treated control whereas no differences were observed in Wc-grown seedlings (Figure 2.13 C). This indicates that proper distribution of auxin via polar auxin transport is required for the suppression of stomatal development in darkness, but that it is not necessary for the promotion of stomata differentiation by light.

To further test the hypothesis of auxin as a negative regulator of stomatal development, stomatal phenotypes of additional mutants exhibiting perturbed auxin biosynthesis or signalling were examined. The single mutants *wei8-1* (Stepanova et al., 2008) and *tir1-1* (Kepinski and Leyser, 2005), which show defects in auxin biosynthesis and perception, respectively, displayed no visible differences to wild-type stomatal patterning (Supplemental Figure S12 A, B). Higher order biosynthesis and signalling mutants, in contrast, showed clear defects with regard to their stomatal development. The *wei8 tar2* auxin biosynthesis mutant (Stepanova et al., 2008) exhibited enhanced stomata formation in

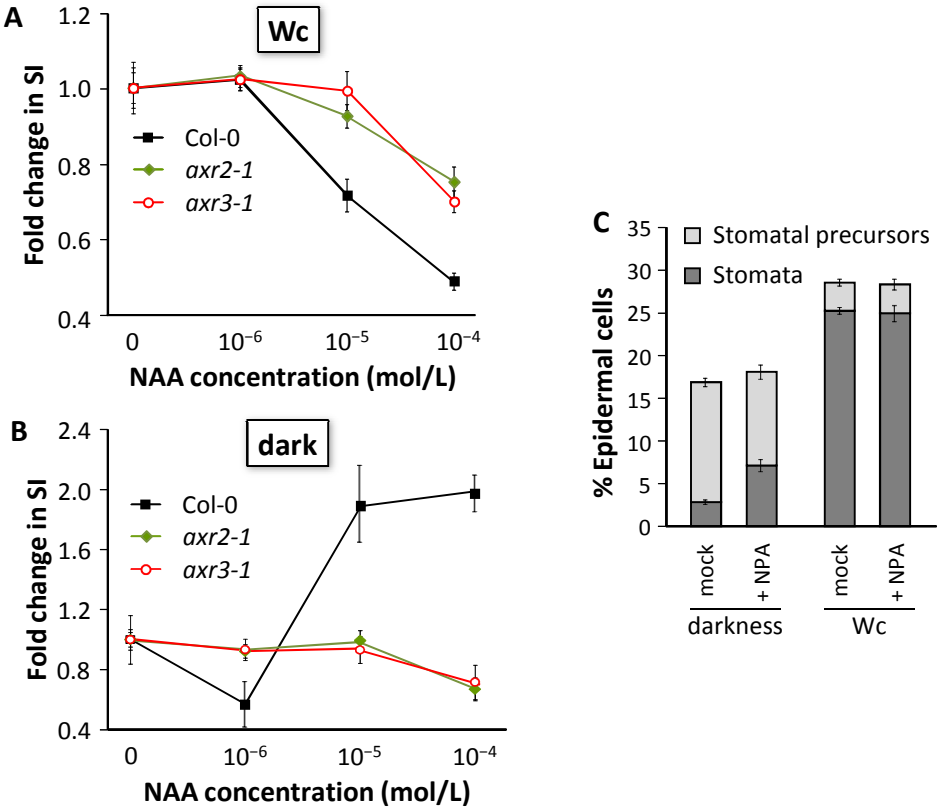

Figure 2.13: NAA and NPA treatments affect stomatal development.
A, B: Fold change in the SI of the abaxial cotyledon epidermis of 10-d-old Col-0, *axr2-1* and *axr3-1* seedlings grown in Wc (25 µmol m^{-2} s^{-1}) (A) or darkness (B) and treated with different concentrations of NAA. **C:** Quantification of stomata and stomatal precursors in the abaxial cotyledon epidermis of 10-d-old Col-0 seedlings grown in darkness or Wc (25 µmol m^{-2} s^{-1}) and treated with 10 µM NPA or mock-treated.
Error bars represent the SEM (n = 10).

darkness similar to *axr3-1* (Figure 2.14 A; Supplemental Figure S12 A). In *tir1 afb2 afb3* auxin receptor mutants, different classes of growth phenotypes have been described: class A seedlings are similar to the wild type, but have an agravitropic root and lack an apical hook in darkness; class B seedlings lack a root, form a rudimentary hypocotyl and often have a single cotyledon; class C seeds do not germinate (Dharmasiri et al., 2005b; Parry et al., 2009; Figure 2.14 B). Seedlings of classes A and B also differed in their stomatal phenotypes; class A seedlings formed more stomata in darkness while class B seedlings showed not only an even larger proportion of stomata in dark-grown seedlings, but also developed clusters of two to three stomata in darkness and Wc (Figure 2.14 A; Supplemental Figure S12 B). In summary, reduction of auxin biosynthesis or auxin perception caused enhanced stomata formation; this observation is consistent with a negative role of auxin in the regulation of stomatal development.

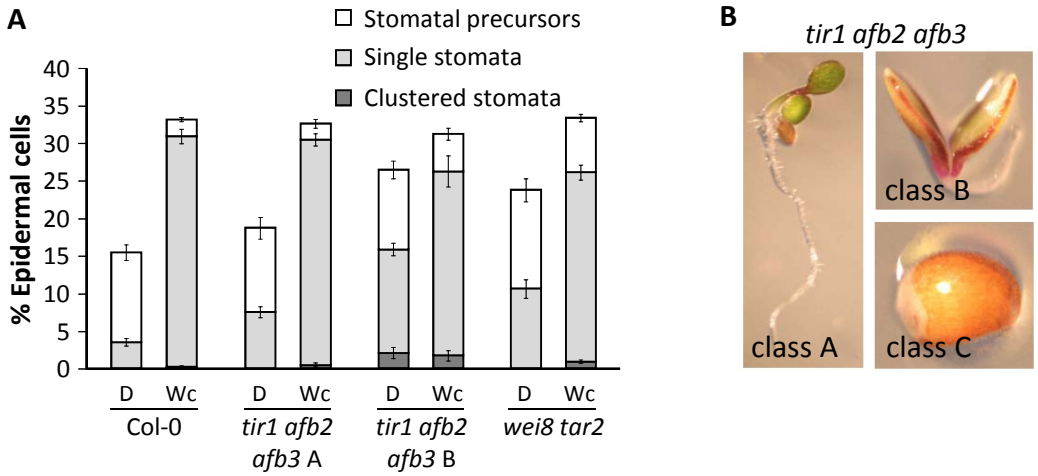

Figure 2.14: Mutants with impaired auxin biosynthesis or auxin signalling show altered stomatal phenotypes.
A: Quantification of stomata and stomatal precursors in the abaxial cotyledon epidermis of 10-d-old seedlings of the indicated genotypes grown in darkness or Wc ($25\,\mu mol\,m^{-2}\,s^{-1}$). Error bars represent the SEM (n = 10). **B:** Classification of *tir1 afb2 afb3* seedling phenotypes: class A seedlings are similar to wild type but show an agravitropic root, while class B seedlings are rootless and class C seeds do not germinate (Photographs modified from Parry et al., 2009).

2.3.7 YDA and members of the ER family are important for the regulation of stomatal development by auxin and light

Auxin appears to have an inhibitory effect on stomatal development whereas light clearly promotes stomata formation. To determine which components of the stomatal development signalling pathway are essential for the effect of auxin and light on stomata formation, stomatal phenotypes of a set of stomata-overproducing mutants were examined in response to these factors. The set comprised loss-of-function mutants of the MKKK YDA, of the TMM and ERf receptors and of the ERf ligands EPF1 and EPF2.

To test for the effect of auxin on the stomatal phenotypes of these mutants, seedlings were grown in Wc on plates containing 10 µM NAA. The proportion of stomata was clearly reduced in the cotyledon epidermis of NAA-treated *epf1 epf2* and *tmm-1* mutants in comparison to the untreated controls whereas it remained almost unchanged in *er erl1 erl2* and *yda-10* mutants (Figure 2.15 A). Therefore, the inhibitory effect of NAA on stomata formation seems to depend on *YDA* and members of the *ERf*.

The effect of light on the stomatal phenotypes of the stomata-overproducing mutants

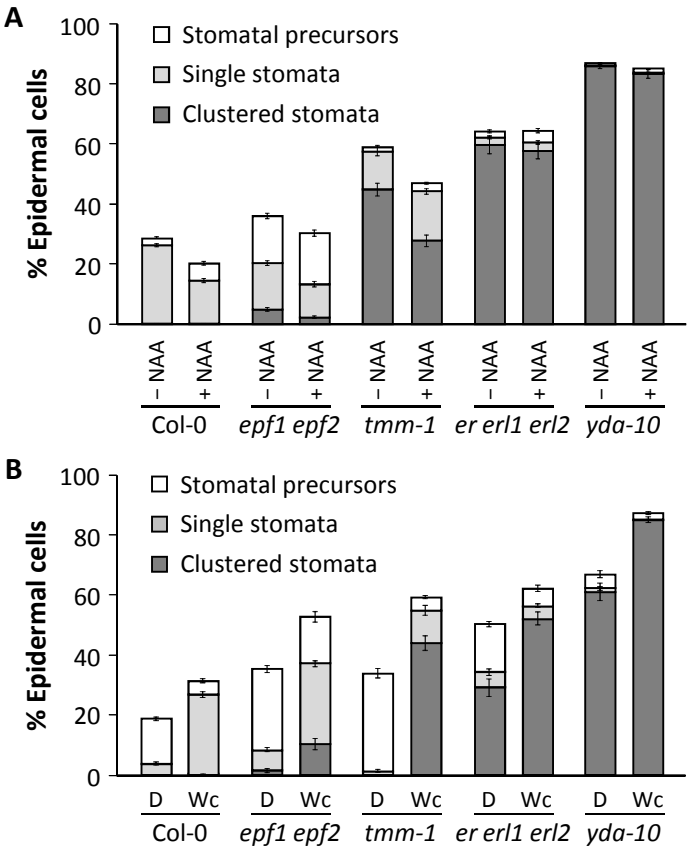

Figure 2.15: Effects of auxin and light on stomatal development are strongly attenuated in *yda* and *er erl1 erl2* mutants.
A: Quantification of stomata and stomatal precursors in the abaxial cotyledon epidermis of 10-d-old seedlings of the wild type and the indicated stomata-overproducing mutants grown in Wc ($25\,\mu mol\,m^{-2}\,s^{-1}$) and treated with 10 µM NAA or mock-treated. **B:** Quantification of stomata and stomatal precursors in the abaxial cotyledon epidermis of 10-d-old seedlings of the same genotypes as in A grown in darkness or Wc ($25\,\mu mol\,m^{-2}\,s^{-1}$).
Error bars represent the SEM (n = 10).

was tested as well. The SI of *yda-10* and *er erl1 erl2* was only slightly lower in dark-grown than in light-grown seedlings whereas the stomata-overproducing phenotypes of *tmm-1* and *epf1 epf2* were strongly attenuated and completely abolished, respectively, when grown in darkness (Figure 2.15 B). Therefore, *YDA*, but possibly also members of the *ERf*, represent components of the stomatal development signalling pathway that seem to be essential for the integration of not only auxin but also light signals. In contrast, *EPF1*, *EPF2* and *TMM* seem to be dispensable for the repression of stomata maturation in darkness. However, the lower proportion of mature stomata in dark-grown *epf1 epf2* and *tmm-1* mutants correlated with a larger proportion of stomatal precursors (Figure 2.15 B), suggesting that while the respective genes are not essential to prevent the formation of mature stomata in darkness, they may still be required for the suppression of early steps in stomatal development.

2.3.8 Auxin and brassinosteroids have additive effects on stomatal development

To date, BRs are the only phytohormones for which a direct link to the stomatal development signalling pathway has been described (Gudesblat et al., 2012; Kim et al., 2012). Moreover, BRs were reported to act interdependently with auxin to regulate many aspects of plant development (Nemhauser et al., 2004). To test whether this is also the case for their action in stomatal development, I analysed the effect of NAA in combination with bikinin, an inhibitor of GSK3-like kinases (De Rybel et al., 2009) that suppresses stomatal development in cotyledons by inhibition of BIN2 in the BR signalling pathway (Kim et al., 2012). Bikinin treatment reduced the SI of the wild type to the same level as NAA and had an even greater impact in the *tmm-1* mutant (Figure 2.16 A, B). In both genotypes, combined treatment with both NAA and bikinin caused a stronger reduction in the SI than treatment with either chemical alone. In the *axr3-1* mutant, responsiveness to NAA was decreased, but bikinin still suppressed stomata formation to the same level as in the wild type (Figure 2.16 C), confirming that its action does not require an intact auxin signalling pathway. In contrast, not only bikinin but also NAA was effective in the BR biosynthesis mutant *det2-1* (Li et al., 1996) as both chemicals reduced its SI approximately by half (Figure 2.16 D), suggesting that auxin does not act via BR biosynthesis to regulate stomatal development. Taken together, NAA and bikinin exhibited additive effects on all genotypes except the auxin-resistant *axr3-1* mutant. Therefore, auxin and brassinosteroids are likely to act independently in the regulation of stomatal development.

2.3.9 Expression of axr3-1-YFP in the epidermis can partially mimic the *axr3-1* mutant phenotype

The *axr3-1* mutation requires the presence of the stomatal lineage to promote stomata differentiation; however, it is unclear whether the axr3-1 protein itself acts in stomatal lineage cells to cause this effect or whether it acts non-cell-autonomously. To address this, an axr3-1 mutant protein fused to YFP was expressed under different tissue- or cell type-specific promoters in the wild-type background. The set of promoters used comprises the *35S* and *AXR3* promoters as positive controls, the *MERISTEM LAYER 1* (*ML1*) pro-

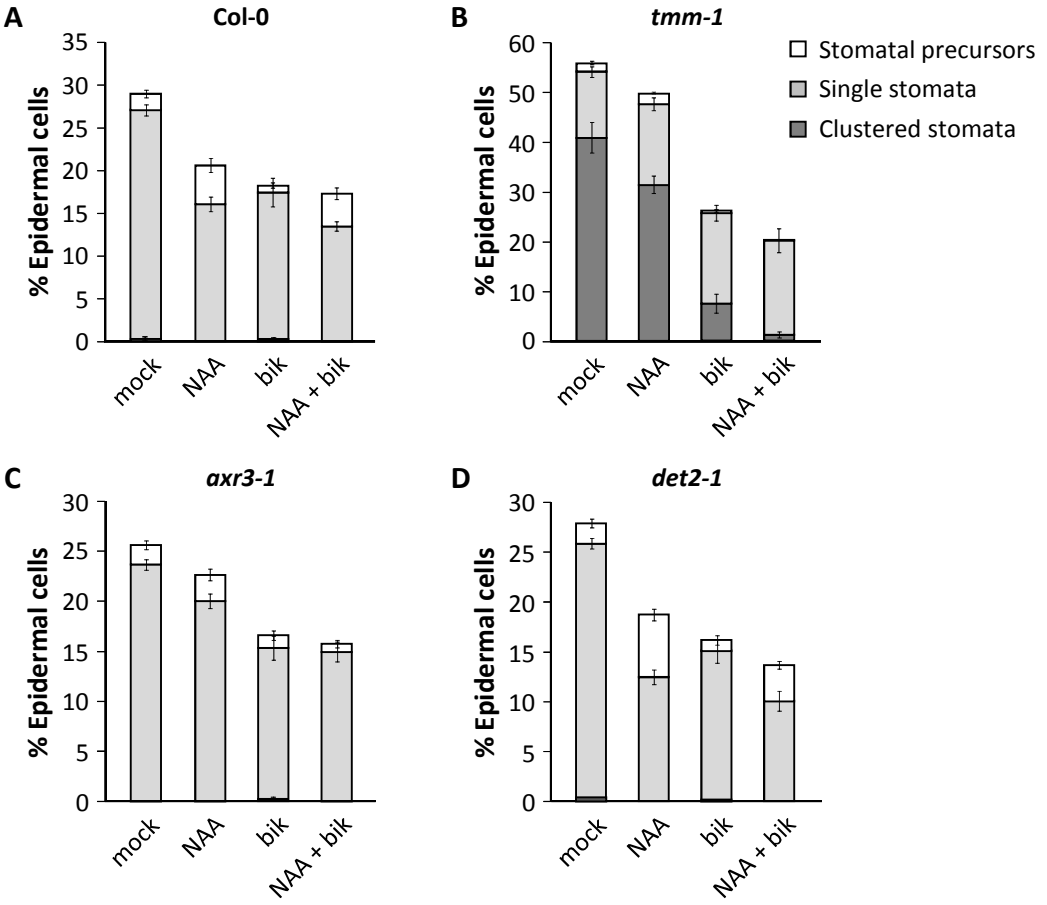

Figure 2.16: NAA and bikinin have additive effects on stomata formation.
Quantification of stomata and stomatal precursors in the abaxial cotyledon epidermis of 10-d-old Col-0 (A), *tmm-1* (B), *axr3-1* (C) and *det2-1* (D) seedlings grown in Wc ($25\,\mu mol\,m^{-2}\,s^{-1}$) and treated with 10 µM NAA, 30 µM bikinin, a combination of both or mock-treated. Error bars represent the SEM (n = 10).

moter for epidermal specificity (Sessions et al., 1999), the *CHLOROPHYLL A/B BINDING PROTEIN 3* (*CAB3*) promoter for mesophyll specificity (Susek et al., 1993) as well as the *SPCH* and *ICE1* promoters for specificity to the stomatal lineage. *SPCH* is expressed broadly in the protoderm in leaf primordia, but its expression is restricted to MMCs and young meristemoids later in development (MacAlister et al., 2007) while the *SCRM/ICE1* expression domain encompasses meristemoids, GMCs, young guard cells and SLGCs (Kanaoka et al., 2008).

In the T1 generation, 30-40 independent transgenic lines were obtained from BASTA selection. Four to five representative lines showing a 3:1 segregation of the resistance gene and correct tissue- or cell line-specific accumulation of the axr3-1-YFP fusion protein in the T2 generation were propagated further to obtain homozygous transgenic lines, which were then analysed in the T3 generation. However, no transgenic plants with visible axr3-1-

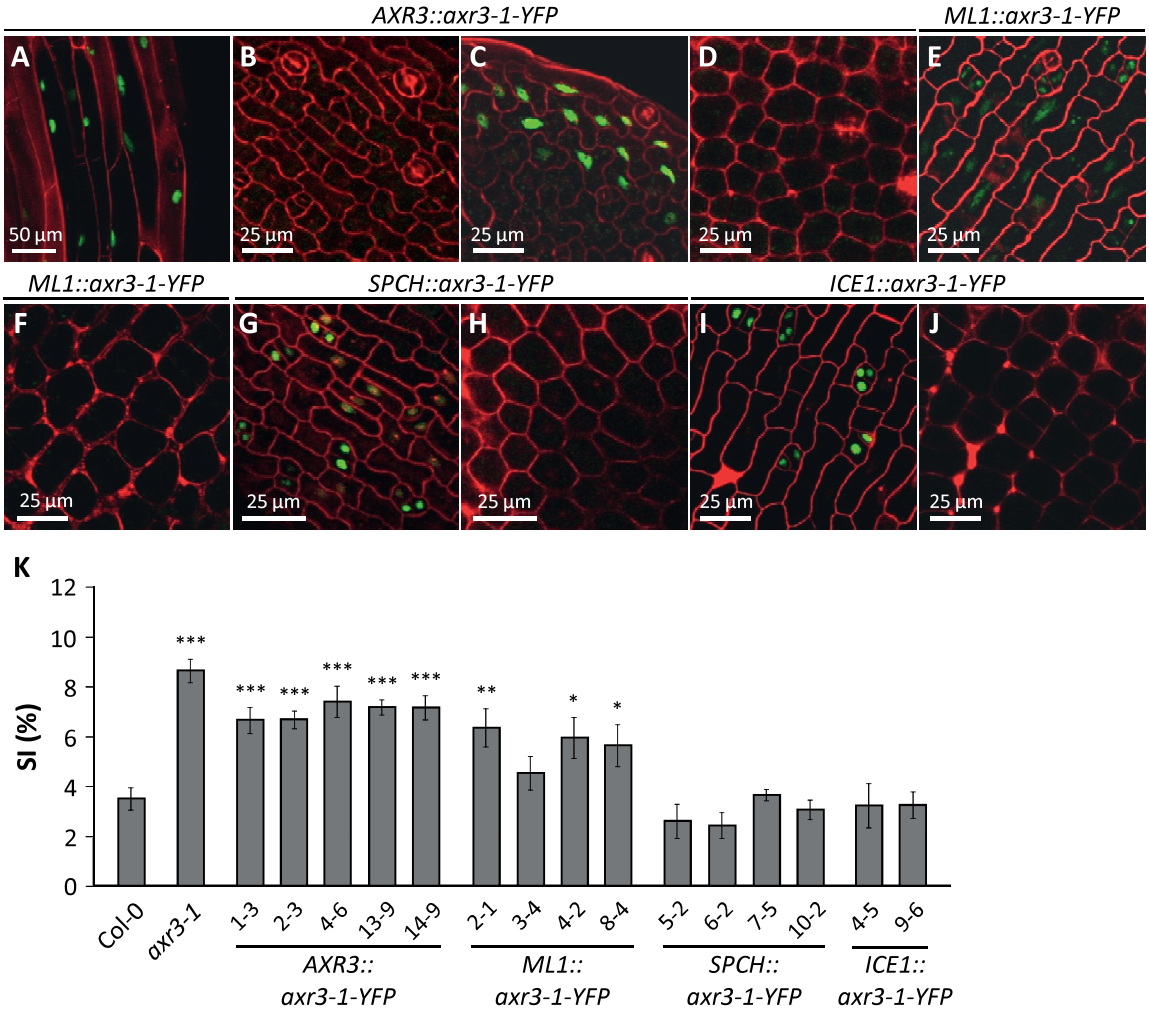

Figure 2.17: Expression of axr3-1-YFP exclusively in the epidermis increases the SI.
A-J: Accumulation of axr3-1-YFP protein in transgenic seedlings expressing the fusion protein from different promoters. **A-D:** Confocal images of the hypocotyl (A), the abaxial cotyledon epidermis (B, C) and the cotyledon mesophyll (D) in 5-d-old dark-grown *AXR3::axr3-1-YFP* seedlings (line 2-3). **E, F:** Confocal images of the abaxial cotyledon epidermis (E) and the cotyledon mesophyll (F) of 5-d-old dark-grown *ML1::axr3-1-YFP* seedlings (line 8-4). **G, H:** Confocal images of the abaxial cotyledon epidermis (G) and the cotyledon mesophyll (H) of 3-d-old dark-grown *SPCH::axr3-1-YFP* seedlings (line 10-2); **I, J:** Confocal images of the abaxial cotyledon epidermis (I) and the cotyledon mesophyll (J) of 5-d-old dark-grown *ICE1::axr3-1-YFP* seedlings (line 9-6). Cell outlines were visualised by PI staining. **K:** SI of the abaxial cotyledon epidermis of 10-d-old dark-grown seedlings of the indicated *promoter::axr3-1-YFP* lines. Numbers denote independent transgenic lines. Error bars represent the SEM (n = 10). Asterisks indicate significant differences to the wild type (Welch-corrected t-test: *** $P < 0.001$, ** $P < 0.01$, * $P < 0.05$).

YFP accumulation were found among those transformed with the *35S* promoter, implying that ubiquitous expression of the axr3-1 mutant protein might be lethal. Furthermore, most T1 plants expressing axr3-1-YFP from the *CAB3* or *ICE1* promoter did not set seed; therefore, none of the *CAB3::axr3-1-YFP* and only two of the *ICE1::axr3-1-YFP* lines could be propagated and analysed.

All propagated lines still showed axr3-1-YFP accumulation in the T3 generation (Figure 2.17 A-J; Supplemental Figure S13). In dark-grown *AXR3::axr3-1-YFP* seedlings, a YFP signal was detected in epidermal and cortical cells of the hypocotyl, in the upper part of the root and, in some lines, also in pavement cells close to the margin of the cotyledons (Figure 2.17 A, C; Supplemental Figure S13, upper panel). No YFP signal was detected in stomatal lineage cells of the abaxial cotyledon epidermis or in the mesophyll in any of those lines (Figure 2.17 B, D). Exclusive accumulation of axr3-1-YFP in the epidermis was found in dark-grown *ML1::axr3-1-YFP* seedlings, and the YFP signal in these lines was generally weaker than in lines expressing from any other promoter (Figure 2.17 E; Supplemental Figure S13, middle panel). The *SPCH::axr3-1-YFP* lines accumulated axr3-1-YFP in many epidermal cells with the strongest signals seen in small cells that lacked any sign of differentiation and often occurred in pairs (Figure 2.17 G; Supplemental Figure S13, lower panel). Finally, the YFP signal in the epidermis of *ICE1::axr3-1-YFP* lines was restricted to meristemoids, GMCs and cells adjacent to those (Figure 2.17 I; Supplemental Figure S13, lower panel). No YFP signal was detected in the mesophyll in any line expressing axr3-1-YFP from the *ML1*, *SPCH* or *ICE1* promoter (Figure 2.17 F, H, J).

The *promoter::axr3-1-YFP* lines were analysed for whether they mimic the *axr3-1* stomatal phenotype in dark-grown seedlings. The *AXR3::axr3-1-YFP* lines showed a significantly higher SI in the abaxial cotyledon epidermis than the wild type although it was slightly lower than the SI of the *axr3-1* mutant (Figure 2.17 K). A significant increase in the SI was also observed for all *ML1::axr3-1-YFP* lines except line 3-4 whereas the SI of seedlings expressing axr3-1-YFP from the *SPCH* and *ICE1* promoters exhibited an SI similar to the wild type (Figure 2.17 K). Therefore, it seems that expression of axr3-1 in the stomatal lineage is not sufficient to promote stomata formation, implying that axr3-1 rather acts non-cell-autonomously. However, it remains unclear whether it acts in the pavement cells of the cotyledon epidermis to affect stomatal lineage cells or whether it signals more distantly from the epidermis of the hypocotyl since both the *AXR3* and the *ML1* promoter expressed in both organs.

The phenotype of the *axr3-1* mutant is highly pleiotropic. It displays not only an increased SI and reduced hypocotyl length in darkness compared to the wild type, but also features shorter, agravitropic roots, increased adventitious rooting, hyponastic leaves of decreased size and increased apical dominance in the inflorescence (Leyser et al., 1996). Hypocotyl and vegetative plant phenotypes were also assessed in the *promoter::axr3-1-YFP* lines. The short hypocotyl phenotype of a dark-grown *axr3-1* mutant was mimicked by all *AXR3::axr3-1-YFP* lines (Figure 2.18 A, B). Expression of axr3-1-YFP from the *ML1* and *ICE1* promoters, but not from the *SPCH* promoter, caused a reduction in

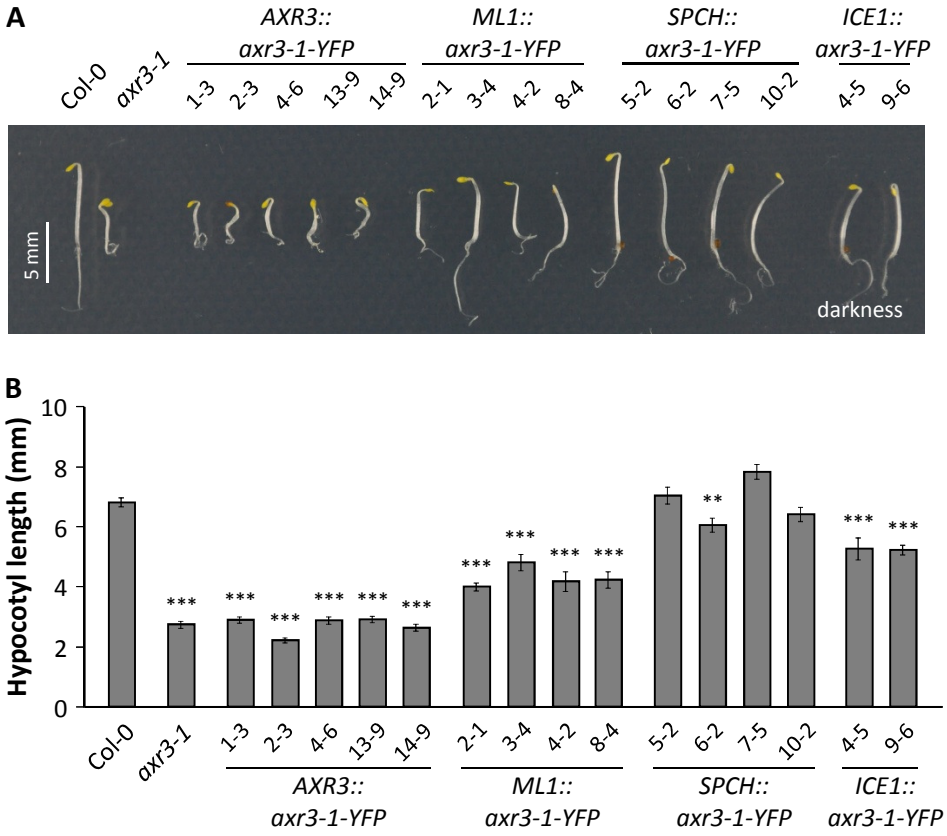

Figure 2.18: Plants expressing axr3-1-YFP in the epidermis partially mimic the phenotype of dark-grown *axr3-1* seedlings.
A: Visual phenotype of 4-d-old dark-grown seedlings of the indicated *promoter::axr3-1-YFP* lines. Numbers denote independent transgenic lines. Dark-grown Col-0 and *axr3-1* seedlings are shown as controls. **B:** Quantification of hypocotyl length of the lines shown in A. Error bars represent the SEM (n = 25). Asterisks indicate significant reduction in hypocotyl length compared to the wild type (Welch-corrected t-test: *** $P < 0.001$, ** $P < 0.01$, * $P < 0.05$).

hypocotyl length as well, but to a lesser extent (Figure 2.18 A, B). On the contrary, the vegetative growth phenotype of the *axr3-1* mutant, characterised by dwarfism and leaf hyponasty, was not mimicked entirely by any transgenic line. Four *AXR3::axr3-1-YFP* lines, however, showed some degree of dwarfism compared to the wild type and also displayed hyponastic leaves (Figure 2.19). Having slightly epinastic leaves, adult *ICE1::axr3-1-YFP* plants differed only mildly from the wild type whereas lines expressing axr3-1-YFP from the *SPCH* and *ML1* promoters had strongly epinastic, lanceolate leaves, and the *SPCH::axr3-1-YFP* plants were also smaller than the wild type (Figure 2.19). Hence, the pleiotropic phenotype of the *axr3-1* mutant may result from action of the mutant axr3-1 protein in different tissues and may also require additional *cis*-regulatory elements not present in the *AXR3::axr3-1-YFP* constructs.

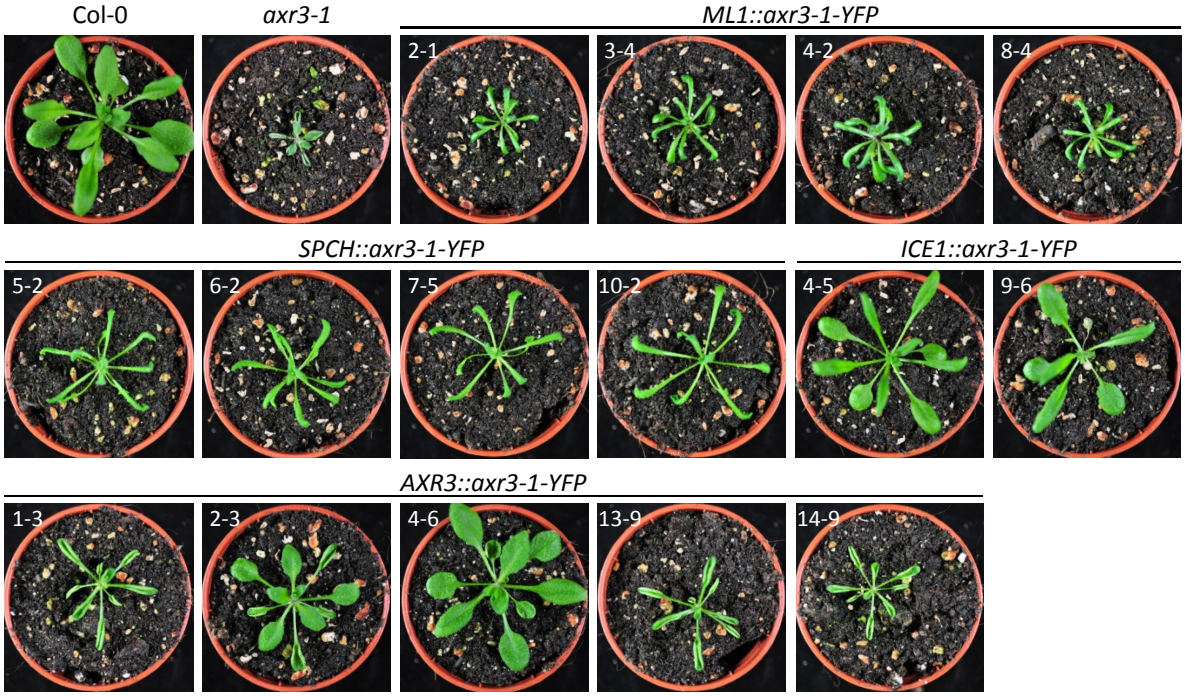

Figure 2.19: The *axr3-1* adult plant phenotype is not completely mimicked by any *promoter::axr3-1-YFP* line.
Visual phenotype of 24-d-old adult plants of the indicated *promoter::axr3-1-YFP* lines grown in long day conditions. Col-0 and *axr3-1* plants are shown as controls.

3 Discussion

3.1 SPA proteins are not required for COP1 nuclear accumulation in darkness

COP1 represents a central switch in light signal transduction, which suppresses light responses in darkness but is largely inactivated in the light. While rapid light responses are likely to be mediated by direct interaction of COP1 with photoreceptors (Yi and Deng, 2005; Lau and Deng, 2012), COP1 is also regulated by nuclear exclusion in response to extended light conditions (von Arnim and Deng, 1994; von Arnim et al., 1997). Nuclear localisation of COP1 is essential for its function in the proteasomal degradation of photomorphogenesis-promoting transcription factors (Stacey et al., 2000; Subramanian et al., 2004). Within the nucleus, COP1 is targeted to discrete domains, referred to as speckles or "photobodies", where it colocalises with other factors of the light signalling pathway, including SPA1 (Seo et al., 2003), the photoreceptors cry1, cry2 and phyA (Seo et al., 2004; Gu et al., 2012) as well as the COP1 substrates HY5, LAF1 and HFR1 (Ang et al., 1998; Seo et al., 2003; Jang et al., 2005).

In contrast to COP1, SPA1 and SPA2 are constitutively nuclear-localised (Hoecker et al., 1999; Laubinger et al., 2004) and may therefore trap COP1 in the nucleus by a light-reversible mechanism. However, this study shows that neither the level of nuclear COP1 nor its targeting to nuclear speckles in darkness is affected by a knock-out of all four *SPA* genes. Thus, SPA proteins seem to be dispensable for retention of COP1 in the nucleus under these conditions. It is however possible that SPA proteins regulate COP1 nucleo-cytoplasmic partitioning in response to other light conditions. Nuclear accumulation of COP1 and SPA1 was recently reported to be enhanced under FR in a phyB-dependent manner and COP1 nuclear accumulation was reduced in a *spa1* mutant under these conditions (Zheng et al., 2013). Nevertheless, SPA proteins promote COP1 function also in darkness (Saijo et al., 2003; Laubinger et al., 2004; Zhu et al., 2008) and hence, they must have additional functions within the COP1/SPA complex, which are yet unknown.

The mechanism by which COP1 is excluded from the nucleus in a light-dependent man-

ner also remains elusive. Both the NLS and the CLS of COP1 are essential for proper COP1 localisation (Stacey et al., 1999, 2000). Therefore, function of one or both of these targeting sequences must be regulated by light, e.g. through being masked by other proteins. The constitutively nuclear-localised CSN seems to be essential for COP1 nuclear accumulation. Nuclear accumulation of a GUS-COP1 fusion protein in darkness is lost in several *csn* mutants (Chamovitz et al., 1996). Furthermore, CSN1 interacts with the coiled-coil domain of COP1 and thereby promotes nuclear localisation of GUS-COP1 in onion epidermal cells, an effect that requires an intact COP1 NLS (Wang et al., 2009). Thus, interaction with the CSN may retain COP1 in the nucleus in darkness, e.g. by masking its CLS, which partially overlaps with the coiled-coil domain (Stacey et al., 1999). This model, however, does not explain by which mechanism light overcomes the CSN-dependent retention of COP1 in the nucleus.

Nuclear exclusion of COP1 is mediated by *cry1*, *phyB* and *phyA* in response to B, R and FR, respectively (Osterlund and Deng, 1998). They all interact with COP1 (Wang et al., 2001; Yang et al., 2001; Seo et al., 2004; Jang et al., 2010) and may thereby disrupt the interaction between COP1 and the CSN. Alternatively, the photoreceptors may themselves mask the COP1 NLS while the CLS is constitutive and causes nuclear export, or they may induce conformational changes in the COP1 protein that expose the CLS. Structural studies on the COP1 protein and its interactions with photoreceptors and cofactors may help to define the roles of COP1 subcellular targeting sequences and to understand their regulation by light.

3.2 Light differentially regulates *SPA1* and *SPA2*

Since the SPA proteins have partially distinct roles in plant development, they may confer specificity towards different COP1/SPA complexes. In particular, SPA1, but not SPA2, represents a potent repressor of light responses in light-grown seedlings while they function equally well to suppress photomorphogenesis in darkness (Laubinger et al., 2004; Fittinghoff et al., 2006; Balcerowicz et al., 2011). The protein sequences of SPA1 and SPA2 account for their different function in light-grown seedlings (Balcerowicz et al., 2011); therefore, I characterised the differential regulation of SPA1 and SPA2 proteins by light.

3.2.1 SPA2 is inherently incapable to suppress photomorphogenesis in light-grown seedlings

Two not mutually exclusive hypotheses regarding the lack of SPA2 function in the light were tested in this study: first, lower levels of SPA2 protein may prevent it from being a potent repressor in the light; second, the inability to suppress overstimulation of the seedling by light may be a feature of SPA2 repressor activity. SPA2-HA indeed accumulates to lower levels than SPA1-HA under weak FRc, which is in agreement with previous findings that levels of native SPA2, but not of SPA1, are lower in light-grown than in dark-grown seedlings (Zhu et al., 2008; Balcerowicz et al., 2011). Furthermore, exposure of dark-grown seedlings to weak FR causes preferential degradation of SPA2-HA in the $26S$ proteasome when compared to SPA1-HA. However, SPA2-HA still lacked repressor function in light-grown seedlings that accumulated SPA2-HA levels similar to those of SPA1-HA. Thus, the lack of SPA2 repressor function in the light is not solely due to protein abundance, but appears to be an intrinsic property of the SPA2 protein.

While reduction in protein levels in the light is not the sole cause for the lack of SPA2 repressor activity under these conditions, regulation of SPA2 abundance is still an important mechanism to define its function during plant development. High SPA2-HA levels due to expression from the *SPA1* promoter can partially complement leaf size, shade avoidance and flowering time phenotypes of the *spa-Q* mutant (Balcerowicz et al., 2011; Rolauffs et al., 2012), which is consistent with the fact that *SPA2* has a function in vegetative

growth, shade avoidance and photoperiodic flowering (Laubinger et al., 2004; Balcerowicz et al., 2011; Rolauffs et al., 2012). Therefore, SPA protein abundance, regulated via gene expression and protein stability, is important to control SPA function during plant development.

3.2.2 Light regulates COP1/SPA complexes at different levels

Light does not affect *COP1* transcript or COP1 protein levels (Deng and Quail, 1992; Zhu et al., 2008), but at least long-term, it regulates COP1 function by nucleocytoplasmic partitioning (von Arnim and Deng, 1994; von Arnim et al., 1997; Stacey et al., 2000; Subramanian et al., 2004). In contrast, SPA1 and SPA2 are not regulated through their subcellular localisation (Hoecker et al., 1999; Laubinger et al., 2004) and the present study shows that they are not required for COP1 nuclear accumulation in darkness. Instead, SPA1 and SPA2 seem to be involved in rapid responses to light; *SPA* genes are required for changes in gene expression that occur within 4 h of light exposure (Falke, 2009). Furthermore, the transcript levels of *SPA1*, but not of *SPA2*, are increased 1 h after exposure to R or FR (Hoecker et al., 1999; Fittinghoff et al., 2006) whereas both SPA1 and SPA2 are rapidly destabilised within 1 h of FR irradiation.

Light-dependent destabilisation of SPA1 and SPA2 requires their degradation in the 26*S* proteasome. The fact that higher SPA2 levels accumulate in light-grown *cop1* mutants than in the wild type suggests that COP1 contributes to destabilisation of SPA2 (Maier, 2011; Chen and Hoecker, unpublished results). Moreover, COP1 auto-ubiquitinates *in vitro* (Saijo et al., 2003; Seo et al., 2003), suggesting that proteasomal degradation of SPA1 and SPA2 results from auto-ubiquitination activity of the CUL4-DDB1$^{\text{COP1-SPA}}$ ubiquitin ligase. However, the molecular basis for the preferential degradation of SPA2 is still unclear. A deletion of the SPA1 N-terminus results in strong stabilisation of the protein (Yang and Wang, 2006), and this stabilising effect is light-dependent (Fackendahl, 2011). These observations indicate that the N-terminus of SPA proteins might be a regulatory domain targeted by light-dependent post-translational modification, which results in increased degradation of the protein. SPA1 and SPA2 proteins exhibit highest differences in their N-terminal sequences, which may represent the basis for differential regulation of SPA1 and SPA2 protein stability. Analysis of SPA2 deletion constructs as well as domain swap constructs between SPA1 and SPA2 may elucidate the role of the N-terminus in the control of SPA protein stability.

The fact that low levels of SPA2 do not solely account for its negligible function in light-grown seedlings implies that a post-translational mechanism selectively inactivates SPA2 in the light. However, the nature of this mechanism remains highly speculative. SPA interactions with target proteins or other components of the E3 ubiquitin ligase, e.g. COP1 or DDB1, might be affected by light. COP1 interacts with all SPA proteins regardless of light conditions, but the strength of these interactions may be reduced in the light (Saijo et al., 2003; Zhu et al., 2008; Lian et al., 2011; Liu et al., 2011a).

The effect of light on SPA repressor function is likely mediated by photoreceptors. Cryptochromes were shown to bind SPA1 in a B-dependent manner; cry1 is thought to inactivate COP1/SPA1 complexes by disruption of the COP1-SPA1 interaction in B (Lian et al., 2011; Liu et al., 2011a) whereas B-dependent binding of cry2 to SPA1 increases COP1-cry2 interaction strength and thereby possibly reduces COP1 activity (Zuo et al., 2011). COP1/SPA1 and COP1/SPA2 complexes might be differentially affected by photoreceptors because they exhibit different affinities for SPA1 and SPA2. Hence, photoreceptor binding might disrupt interactions of SPA2 with COP1 or target proteins more efficiently than those of SPA1 or it might differentially regulate activity of the respective E3 ubiquitin ligases. Since cry2, phyA and phyB are themselves targets of the COP1/SPA complex (Shalitin et al., 2002; Seo et al., 2004; Jang et al., 2010), it is also possible that COP1/SPA1 complexes promote degradation of these photoreceptors more efficiently than COP1/SPA2 complexes and hence more efficiently desensitise light signalling. Investigating the interactions and activities of COP1/SPA1 and COP1/SPA2 complexes in the presence of cofactors or photoreceptors may help to elucidate the distinct functions of SPA1 and SPA2 and their differential regulation by light.

Taken together, light differentially regulates SPA1 and SPA2 function at three different levels (Figure 3.1). First, the expression of *SPA1*, but not *SPA2*, is induced upon light exposure (Hoecker et al., 1999; Fittinghoff et al., 2006) and leads to an increase in SPA1 protein levels in the light (Fittinghoff et al., 2006; Zhu et al., 2008). Second, light destabilises SPA2 more strongly than SPA1, and this effect depends on proteasomal degradation of both proteins. Third, light selectively inhibits SPA2 repressor activity in light-grown seedlings by a yet unknown post-translational mechanism.

The question arises why such complexity in the light-dependent regulation of *SPA1* and *SPA2* is necessary. It likely represents a fine-tuning mechanism to tightly adjust physiological and developmental responses to changes in the light environment. Light inactivates COP1/SPA1 and COP1/SPA2 complexes partially via destabilisation of the SPA proteins; this process was recently shown to occur within 10 min after light exposure (Chen

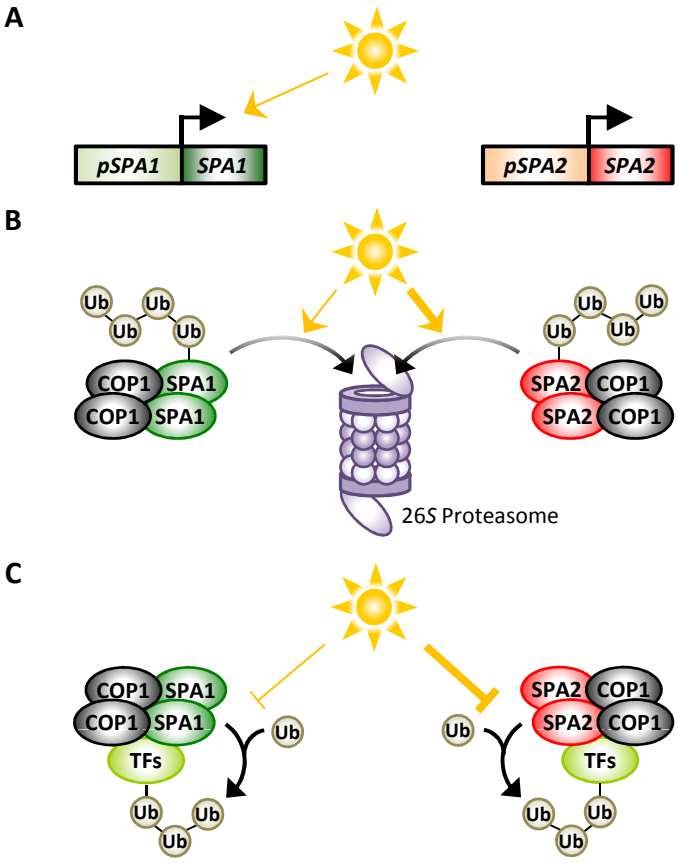

Figure 3.1: Light differentially regulates SPA1 and SPA2 at several levels.
Light modulates the function of COP1/SPA1 and COP1/SPA2 complexes at three different levels. First, it increases expression of *SPA1*, but not *SPA2* (A); second, it enhances proteasomal degradation of SPA2 more strongly than that of SPA1 (B); third, it selectively represses SPA2 activity (C). This differential regulation results in complete suppression of COP1/SPA2, but not COP1/SPA1, complexes in light-grown seedlings.
Arrows indicate positive regulation, perpendicular lines indicate negative regulation. Line width represents strength of light-dependent effects.

and Hoecker, unpublished results) and therefore helps to rapidly induce de-etiolation responses. Subsequently, the increase in *SPA1* transcript (and hence protein) level after 1 h (Hoecker et al., 1999; Fittinghoff et al., 2006) desensitises light signalling to prevent overstimulation of the seedling by light.

3.3 The Aux/IAA protein AXR3 represents a novel regulator of light-dependent stomatal development

Light promotes stomatal development in seedlings as part of the de-etiolation response (von Arnim and Deng, 1996) and repression of the COP1/SPA complex is required for this process (Kang et al., 2009). In the present study, I characterised a novel regulator of stomatal development, the Aux/IAA protein AXR3, and established its role within a genetic network that regulates stomatal development in response to intrinsic and external signals.

3.3.1 Auxin and light regulate stomatal development via AXR3

The *aux/iaa* gain of function mutants *shy2-2*, *axr2-1* and *axr3-1* display an increased SI in cotyledons of dark-grown seedlings compared to the wild type. This increase could arise from a larger number of stomata, or it could originate from a reduction in pavement cell number. Quantification of total epidermal cell numbers revealed that the numbers of both stomata and non-stomatal cells are increased in *axr3-1* compared to the wild-type. In dark-grown wild-type seedlings, almost no cell division occurs in the cotyledon epidermis between 2 and 10 dpg and most stomatal precursors do not pass the meristemoid stage. In contrast, *axr3-1* shows both increased entry into the stomatal lineage as well as enhanced maturation of stomatal precursors, resulting in a larger number of mature stomata while keeping the portion of precursors constant.

No increase in cell division caused by the *axr3-1* mutation was observed in a *spch* background, which lacks entry divisions into the stomatal lineage and therefore features an epidermis entirely composed of pavement cells. This demonstrates that the presence of the stomatal lineage is absolutely required for the effect of *axr3-1* on cell division. However, the fact that expression of an axr3-1-YFP fusion protein from stomatal lineage-specific promoters did not mimic the stomatal phenotype of the *axr3-1* mutant shows that action of the axr3-1 protein in stomatal lineage cells is not sufficient to increase stomata formation. Instead, it suggests that axr3-1 acts outside of the stomatal lineage to promote divisions within, implying that cell-cell communication is involved in this process. Further

investigation is required to define the domain in which axr3-1 acts to promote stomata formation and how its effect is transmitted from there to the stomatal lineage.

Upstream of the Aux/IAA proteins SHY2, AXR2 and AXR3, auxin induces their degradation by the SCF^{TIR1} ubiquitin ligase (Gray et al., 2001). The *aux/iaa* gain-of-function mutants *axr2-1*, *axr3-1* and *shy2-2* express stabilised versions of the respective Aux/IAA repressors that are less efficiently degraded by SCF^{TIR1} (Gray et al., 2001; Ouellet et al., 2001; Reed, 2001; Tian et al., 2003) and thus attenuate auxin responses. Hence, increased stomata production of the *aux/iaa* gain-of-function mutants likely results from their resistance to auxin, implying that auxin negatively regulates stomata formation in the wild type. In agreement with this hypothesis, perturbations in auxin levels, auxin distribution and auxin sensing influence stomatal development. Higher order auxin biosynthesis and signalling mutants display increased stomata formation, which was also seen for dark-grown wild-type seedlings treated with the polar auxin transport inhibitor NPA. Additionally, exogenous application of the synthetic auxin NAA reduces the SI of light-grown wild-type seedlings. In conclusion, these results strongly suggest that auxin represents a negative regulator of stomatal development.

IAA was found to promote stomata formation in the hypocotyl when applied together with GA (Saibo et al., 2003), but no auxin effect has yet been described on stomatal development in cotyledons. Auxin is, however, involved in many other aspects of cotyledon development. Local auxin maxima in the globular embryo stimulate cotyledon outgrowth while low auxin concentrations in between are required for cotyledon separation (Benková et al., 2003; Reinhardt et al., 2003). Auxin accumulation is also thought to be an early event in vascular differentiation in cotyledons and leaves (Sachs, 1991; Mattsson et al., 1999; Sieburth, 1999; Deyholos et al., 2000). Moreover, auxin establishes dorsoventral polarity in cotyledons and leaves; polar auxin transport generates a dorsoventral auxin gradient with highest auxin concentrations at the abaxial side, where the ARFs ETTIN (ETT)/ARF3 and ARF4 promote abaxial cell fate (Pekker et al., 2005; Hay et al., 2006). Intriguingly, higher auxin levels at the abaxial side correlate with the suppression of stomata differentiation specifically in the abaxial cotyledon epidermis of dark-grown seedlings observed in this study.

Auxin gradients not only establish polarity across tissues and organs, but also within cells and thereby guide asymmetric cell divisions. Auxin controls the orientation of apical division planes in the early embryo by inducing the degradation of BODENLOS (BDL)/IAA12, which in turn leads to increased MONOPTEROS (MP)/ARF5 activity (Berleth and Jurgens, 1993; Hamann et al., 1999, 2002). Furthermore, auxin promotes

CYCLIN D 6;1 (*CYCD6;1*) transcription to trigger asymmetric divisions in root cortex/endodermis initials (Cruz-Ramírez et al., 2012). Asymmetric divisions are essential processes also during stomatal development. In this context, the division plane is determined by localisation of the plant-specific proteins BREAKING OF ASYMMETRY IN THE STOMATAL LINEAGE (BASL) and POLAR LOCALIZATION DURING ASYMMETRIC DIVISION AND REDISTRIBUTION (POLAR) (Dong et al., 2009; Pillitteri et al., 2011), but auxin might be a possible upstream regulator of this process. However, defects in orientation of asymmetric divisions were detected only in the strongly distorted class B *tir1 afb2 afb3* seedlings, which exhibit mild stomatal clustering. This clustering might be a hint that auxin affects orientation of spacing divisions, but it might also be a secondary effect of a severely compromised seedling establishment.

Apart from the phenotype observed in light-grown class B *tir1 afb2 afb3* seedlings, all auxin-dependent defects in stomatal development were observed exclusively in dark-grown seedlings. Hence, light appears to restrict the auxin effect on stomata formation. It seems unlikely that light prevents auxin-dependent suppression of stomatal development by reducing overall auxin levels because these are lower in dark-grown than in light-grown seedlings (Bhalerao et al., 2002). However, in light-grown seedlings auxin might be redistributed from cotyledons to the hypocotyl and the root as polar auxin transport in the hypocotyl is induced upon light exposure (Liu et al., 2011b) and is required for hypocotyl elongation in the light, but not in darkness (Jensen et al., 1998). NPA treatment increased the SI in the cotyledon epidermis of dark-grown seedlings, indicating that proper auxin distribution is also required to suppress stomatal development in darkness. However, NPA had no effect on the SI of light-grown seedlings, implying that light does not counteract the inhibitory effect of auxin on stomatal development exclusively by polar auxin transport-dependent depletion of auxin in the epidermis. Employing reporters of auxin signalling such as *DR5rev::GFP* (Friml et al., 2003) or DII-VENUS (Brunoud et al., 2012) might reveal whether stomatal lineage cells show altered auxin responses compared to pavement cells in cotyledons of dark-grown seedlings and would thereby give a hint about auxin distribution in the epidermis.

Several lines of evidence suggest that light attenuates auxin signalling by positive regulation of Aux/IAA proteins. The constitutively photomorphogenic phenotype of the *aux/iaa* domain II mutants *shy2-2*, *axr2-1* and *axr3-1* implies that the wild-type proteins might be degraded in darkness, but stabilised by light (Reed, 2001). Light might stabilise Aux/IAA proteins by regulating the activity of the SCF^{TIR1} ubiquitin ligase; the CSN, a repressor of light signalling, interacts with SCF^{TIR1} and knock-down of *CSN5* results in decreased SCF^{TIR1}-mediated degradation of PsIAA16 (Schwechheimer et al.,

2001). Alternatively, binding of phytochromes might be involved in Aux/IAA stabilisation because oat phyA and Arabidopsis phyB interact with several Arabidopsis Aux/IAA proteins *in vitro* (Colón-Carmona et al., 2000; Tian et al., 2003). These *in vitro* interactions are light-independent, but since phytochromes translocate into the nucleus in a light-dependent manner, the interaction with nuclear-localised Aux/IAA proteins might occur only in the light *in vivo* (Reed, 2001). Light affects not only Aux/IAA protein stability, but also *Aux/IAA* gene expression. The photomorphogenesis-promoting transcription factors HY5 and HYH promote expression of *AXR2* and *SLR* (Cluis et al., 2004; Sibout et al., 2006), and nine *Aux/IAA* genes, including *SHY2* and *AXR3*, feature HY5 binding sites in their promoters (Lee et al., 2007). Since HY5 and HYH are well described COP1 targets (Ang et al., 1998; Osterlund et al., 2000; Holm et al., 2002), COP1 might regulate the expression of *Aux/IAA* genes through these transcription factors; however, transcript levels of *SHY2*, *AXR2* and *AXR3* are similar in dark-grown wild-type and *cop1-4* mutant seedlings, suggesting that COP1 is not required for the repression of their expression in darkness.

3.3.2 A genetic network for the control of stomatal development that integrates intrinsic and external signals

In this study, genetic interactions between *axr3-1* and various mutations in stomatal development genes were tested. The *axr3-1*-induced increase in SI depends on functional *SPCH*, *MUTE* and *FAMA* and a knock-out of these genes causes an arrest of stomatal development at the stage controlled by the respective gene even in the *axr3-1* mutant. However, the *axr3-1* mutation increases the number of meristemoids and "*fama*-tumours" in the *mute-1* and *fama-1* backgrounds, respectively. This demonstrates that the mutations are not completely epistatic and that if progression through the stomatal lineage is arrested, *axr3-1* still increases entry divisions into the stomatal lineage. The effect of *axr3-1* also requires a functional YDA MAPK cascade as the effect was abolished by a constitutively active MKK. In contrast, *axr3-1* exhibits additive and synergistic effects with *tmm* and *er*(*l*) mutations, suggesting that the respective genes act in independent pathways. Taken together, this epistasis analysis revealed that *AXR3* acts genetically upstream of the differentiation genes *SPCH*, *MUTE* and *FAMA* and genes encoding components of the YDA MAPK cascade, but functions in parallel with *TMM* and *ERf* patterning genes (Figure 3.2). However, auxin-induced reduction in stomata formation was abolished not only in *yda* but also in *er erl erl2* mutants, suggesting that the *ERf* genes might be important for the effect of auxin on stomatal development. Since the effect of

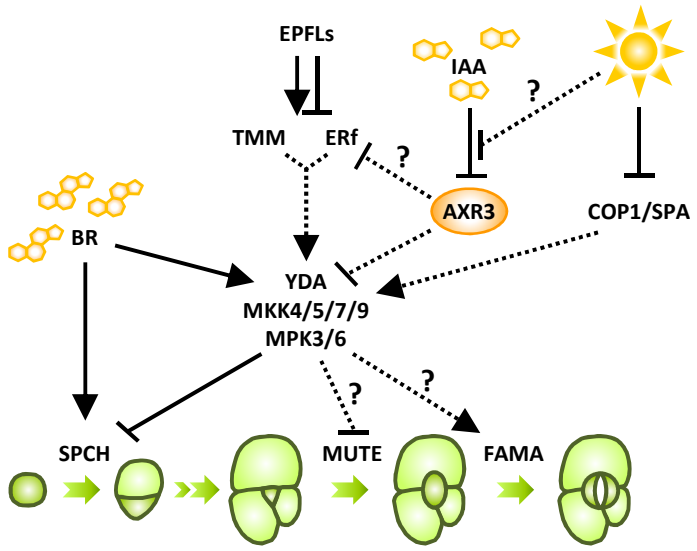

Figure 3.2: *AXR3* is part of a genetic network that controls stomatal development.
Auxin and light control the activity of the Aux/IAA protein AXR3, which promotes multiple steps in stomatal development. It appears to act upstream of the YDA MAPK cascade, but in parallel with TMM, the COP1/SPA pathway and the BR pathway. Hence, the YDA MAPK cascade represents a central integrator in the signalling pathway that regulates stomatal development.
Arrows indicate positive regulation, perpendicular lines indicate negative regulation. Solid lines represent confirmed biochemical interaction, dotted lines represent indirect or genetic interactions.

the *axr3-1* mutation in several *er*(*l*) mutants was not as strong as in the wild type background, it seems possible that *AXR3* affects stomata formation by both *ERf*-dependent and *ERf*-independent mechanisms.

So far, the YDA MAPK cascade appears to be a likely target of AXR3 in the regulation of stomatal development although its effect on the MAPK cascade might be indirect. Interestingly, auxin treatment increases MAPK activity in wild-type roots whereas MAPK activity is reduced in the auxin-insensitive mutant *axr4* (Mockaitis and Howell, 2000). Moreover, the MKKK NICOTIANA PROTEIN KINASE 1 (NPK1) represses early auxin responses in tobacco (Kovtun et al., 1998), suggesting that MAPK cascades might be involved in auxin signalling. Activity of the YDA MAPK cascade depends on the phosphorylation state of its components, and this is directly regulated by the GSK3-like kinase BIN2 (Kim et al., 2012; Khan et al., 2013) and the phosphatase AP2C3 (Umbrasaite et al., 2010). Since the TIR1/AFB-Aux/IAA signalling pathway predominantly regulates gene expression (Chapman and Estelle, 2009), a possible scenario is that auxin affects MAPK activity by transcriptional regulation of a kinase or a phosphatase. Several kinases and phosphatases are deregulated in the transcriptome of the *axr3-1* mutant (Overvoorde et al., 2005) and may therefore represent candidates for links between auxin and MAPK signalling. However, it needs to be tested whether AXR3 and auxin indeed affect phosphorylation and activity of components in the YDA MAPK cascade.

Besides its putative regulation via auxin, the YDA MAPK cascade integrates signals from the EPFL-ERf pathway (Lee et al., 2012; Jewaria et al., 2013), the BR signalling cascade (Kim et al., 2012; Khan et al., 2013) and the light signalling pathway (Kang et al., 2009). Thus, the YDA MAPK cascade appears to be a central switch in the decision of whether or not to form a stoma. This switch is regulated by both intrinsic and environmental signals and controls stomatal development at multiple stages.

Possible interconnections between *AXR3* and the light signalling pathway in the regulation of stomatal development were analysed in this study. *AXR3* regulates stomatal development in a light-dependent manner, but genetic interactions between *axr3-1* and *cop1-4* were additive, suggesting that *AXR3* acts independently of *COP1*. It cannot be excluded that COP1 has an effect on AXR3 and the other Aux/IAA proteins, but it seems unlikely that this is the only mechanism by which COP1 affects stomata formation. While even an *axr2-1 axr3-1* double mutant shows only moderate stomata overproduction in darkness, the seedling-lethal *cop1-5* allele displays much stronger stomata overproliferation regardless of light conditions (Kang et al., 2009). Thus, light regulates stomatal development via two at least partially distinct routes.

Interdependency between auxin and BRs in the regulation of stomatal development was also investigated in this study. The two phytohormones cooperatively promote lateral root development and hypocotyl elongation (Bao et al., 2004; Nemhauser et al., 2004) and some auxin responses are mediated by upregulation of BR biosynthesis (Chung et al., 2011). Auxin also affects the expression of the BR receptor genes *BRI1* and *BRI1-LIKE 3* (*BRL3*) while BRs control the expression of several *Aux/IAA* and *ARF* genes (Nemhauser et al., 2004). However, the present study shows that NAA and bikinin treatments, which induce auxin and BR signalling, respectively, decrease the SI in the cotyledons of light-grown seedlings in an additive manner, and that the inhibitory effect of NAA does not require BR biosynthesis. Thus, while crosstalk between the two signalling pathways exists, auxin and BRs seem to act independently to regulate stomatal development.

In summary, *AXR3* appears to be a novel regulator of stomatal development, which promotes stomata differentiation in response to light, an effect that is repressed by auxin in darkness. *AXR3* has been placed in a genetic network that controls stomatal development, yet the mechanism by which it promotes stomata formation remains elusive. Identification of downstream factors in the *AXR3* signalling pathway would greatly enhance understanding of the mechanisms underlying the coordination of auxin and light signalling in stomatal development.

4 Materials and Methods

4.1 Materials

4.1.1 Chemicals

Chemicals in research/pro analysis grade were obtained from AppliChem GmbH (Darmstadt, Germany), BD Biosciences (Heidelberg, Germany), Bio-Rad Laboratories GmbH (Munich, Germany), Carl Roth GmbH (Karlsruhe, Germany), Colgate-Palmolive GmbH (Hamburg, Germany), Duchefa Biochemie B.V. (Haarlem, Netherlands), Honeywell Riedel-de-Haen Specialty Chemicals Seelze GmbH (Seelze, Germany), Life Technologies GmbH (Karlsruhe, Germany), Merck KGaA (Darmstadt, Germany), Roche Diagnostics GmbH (Mannheim, Germany), SERVA Electrophoresis GmbH (Heidelberg, Germany), Sigma-Aldrich Chemie GmbH (Munich, Germany), Thermo Fisher Scientific (Schwerte, Germany) and VWR International GmbH (Darmstadt, Germany).

4.1.2 Buffers and solutions

All buffers and solutions were prepared with double-distilled water (ddH_2O) if not otherwise stated. Buffers and solutions that do not represent a simple solution or dilution of a single stock chemical are listed in Table 4.1. Unless otherwise stated, buffers were stored at room temperature (RT).

Table 4.1: Buffers and solutions used in this study

Buffer/Solution	**Components**
Amido Black staining solution	0.25% (w/v) Naphthol Blue Black
	50% (v/v) MeOH
	10% (v/v) glacial acetic acid
Amido Black washing solution	90% (v/v) MeOH
	10% (v/v) glacial acetic acid

Table 4.1: (continued)

Buffer/Solution	**Components**
10 × Carbonate blotting buffer	0.31% (w/v) $NaCO_3$
	0.84% (w/v) $NaHCO_3$
	0.08% (w/v) SDS
Clearing solution	8 g chloral hydrate
	in 2 ml 50% (v/v) glycerol
Coomassie staining solution	0.25% (w/v) Coomassie Brilliant Blue R250
	50% (v/v) MeOH
	7% (v/v) glacial acetic acid
Coomassie destaining solution	50% (v/v) MeOH
	7% (v/v) glacial acetic acid
DNA extraction buffer (Thompson)	200 mM Tris/HCl pH 7.5
	250 mM NaCl
	25 mM EDTA
	0.5% (w/v) SDS
DNA extraction buffer (fast method)	50 mM Tris/HCl pH7.2
	300 mM NaCl
	10% (w/v) Sucrose
DNA loading dye	0.25% (w/v) Bromophenol Blue
	30% (v/v) glycerol
HONDA buffer[a]	400 mM Sucrose
	25 mM Tris/HCl pH 7.4
	10 mM $MgCl_2$
	2.5% (w/v) Ficoll 400
	5% (w/v) Dextran T40
	10 mM DTT (added freshly)
	1 × protease inhibitor cocktail (added freshly)
5 × Laemmli buffer[b]	310 mM Tris/HCl pH 6.8
	10% (w/v) SDS
	50% (v/v) Glycerol
	0.25% (w/v) Bromophenol Blue
	500 mM DTT
PCR reaction buffer	100 mM Tris/HCl pH 9.0
	500 mM KCl
	15 mM $MgCl_2$
Protein extraction buffer	50 mM Tris/HCl pH 7.5
	150 mM NaCl
	1 mM EDTA
	10% (v/v) glycerol
	0.1% (v/v) Triton™ X-100
	5 mM DTT (added freshly)
	1 × protease inhibitor cocktail (added freshly)
	10 µM MG132 (added freshly)

Table 4.1: (continued)

Buffer/Solution	**Components**
SDS-PAGE resolving gel	7.5-15% (w/v) acrylamide
	375 mM Tris/HCl pH 8.8
	0.1% (w/v) SDS
	0.08% (w/v) APS (added directly before pouring)
	0.08% (v/v) TEMED (added directly before pouring)
SDS-PAGE stacking gel	5% (w/v) acrylamide
	125 mM Tris/HCl pH 6.8
	0.1% (w/v) SDS
	0.05% (w/v) APS (added directly before pouring)
	0.1% (v/v) TEMED (added directly before pouring)
10 × SDS running buffer	1.9 M Glycine
	240 mM Tris
	1% (w/v) SDS
Seed sterilisation solution	20% (v/v) Klorix
	0.03% (v/v) Triton™ X-100
TB buffer[c]	10 mM PIPES/KOH pH 6.7
	15 mM $CaCl_2$
	250 mM KCl
	55 mM $MnCl_2$ (added after pH adjustment)
10 × TBE	890 mM Tris
	890 mM Boric acid
	20 mM EDTA
10 × TBS buffer	200 mM Tris/HCl pH 7.5
	1.37 M NaCl
TBS-T buffer	0.1% (v/v) Tween® 20
	in 1 × TBS
TE buffer	10 mM Tris/HCl pH 8.0
	1 mM EDTA

[a] Solution was autoclaved after preparation.
[b] Solution was stored at −20°C.
[c] Solution was filter-sterilised after preparation.

4.1.3 Antibiotics and growth regulators

Antibiotics and growth regulators added to bacterial or plant growth media are listed in Table 4.2. Stock solutions (usually 1000 × concentrated) were filter-sterilised and stored at −20°C unless otherwise stated.

Table 4.2: Antibiotics and growth regulators used in this study

Chemical	Solvent	Working concentration	Manufacturer
Ampicillin	ddH_2O	100 µg/ml	Duchefa (Haarlem, Netherlands)
Bikinin	DMSO	30 µM	Merck (Darmstadt, Germany)
DEX	DMSO	0.02 µM	Sigma-Aldrich (Munich, Germany)
Gentamycin	ddH_2O	25 µg/ml	Duchefa (Haarlem, Netherlands)
Hygromycin[a]	ddH_2O	15 µg/ml (for plants)	Life Technologies (Karlsruhe, Germany)
		50 µg/ml (for bacteria)	
Kanamycin	ddH_2O	50 µg/ml	Duchefa (Haarlem, Netherlands)
NAA[a,b]	ddH_2O	variable	Sigma-Aldrich (Munich, Germany)
MG132	DMSO	30 µM	Sigma-Aldrich (Munich, Germany)
NPA	DMSO	10 µM	Sigma-Aldrich (Munich, Germany)
Rifampicin[c]	DMSO	25 µg/ml	Duchefa (Haarlem, Netherlands)
Tetracyclin	70% EtOH	10 µg/ml	Duchefa (Haarlem, Netherlands)

[a] Solution was stored at 4°C.

[b] NAA powder was pre-dissolved in a drop of EtOH before being mixed with ddH_2O.

[c] Solution was stored at RT.

4.1.4 Growth media

Media for bacterial and plant growth used in this study are listed in Table 4.3. For preparation of solid media, agar was added to a concentration of 1.5% (LB, YEB) or 1% (MS). All media were autoclaved prior to usage. For some experiments, MS was supplemented with 1% (w/v) sucrose before autoclaving. Any other supplements were added after autoclaving when medium was cooled down to approximately 60°C.

Table 4.3: Growth media used in this study

Medium	Components
Luria-Bertani (LB) broth	10 g/L Tryptone
	5 g/L Yeast extract
	10 g/L NaCl
Murashige and Skoog (MS) medium	4.44 g/L MS salts
	pH was adjusted to 5.8
Yeast extract broth (YEB)	5 g/L Peptone
	5 g/L Beef extract
	5 g/L Yeast extract
	5 g/L Sucrose
	2 mM $MgSO_4$
	pH was adjusted to 7.2

4.1.5 Antibodies

Antibodies used in this study are listed in Table 4.4. Primary antibodies were diluted in TBS containing 3% (w/v) milk powder, horseradish peroxidase (HRP)-coupled secondary antibodies were diluted in TBS containing 5% (w/v) milk powder.

Table 4.4: Antibodies used in this study

Antibody	Source	Dilution	Manufacturer
anti-COP1	Rabbit	1:300	(Balcerowicz et al., 2011)
anti-GFP	Mouse	1:5000	Roche Diagnostics (Mannheim, Germany)
anti-HA	Rat	1:4000	Roche Diagnostics (Mannheim, Germany)
anti-Histone H3	Rabbit	1:5000	Abcam (Cambridge, MA, USA)
anti-HSC70	Mouse	1:20 000	Stressgen Biotechnologies (San Diego, CA, USA)
anti-mouse IgG-HRP	Goat	1:50 000	Sigma-Aldrich (Munich, Germany)
anti-PEPC	Rabbit	1:5000	Rockland (Gilbertsville, PA, USA)
anti-rabbit IgG-HRP	Goat	1:80 000	Sigma-Aldrich (Munich, Germany)
anti-rat IgG-HRP	Goat	1:5000	Santa Cruz Biotechnology (Dallas, TX, USA)
anti-α-Tubulin	Rabbit	1:10 000	Sigma-Aldrich (Munich, Germany)

4.1.6 Enzymes

Enzymes used in this study are listed in Table 4.5. They were stored at −20°C unless otherwise stated. Reaction buffers were provided by the manufacturers along with the respective enzymes.

Table 4.5: Enzymes used in this study

Enzymes	Manufacturer
Gateway® BP Clonase® Mix[a]	Life Technologies (Karlsruhe, Germany)
Gateway® LR Clonase® Mix[a]	Life Technologies (Karlsruhe, Germany)
KAPA™ SYBR® FAST qPCR Mastermix	PEQLAB Biotechnologie (Erlangen, Germany)
Pfu DNA Polymerase	Thermo Fisher Scientific (Schwerte, Germany)
Restriction endonucleases	Thermo Fisher Scientific (Schwerte, Germany)
RevertAid™ H Minus Reverse Transcriptase	Thermo Fisher Scientific (Schwerte, Germany)
Ribonuclease A	Carl Roth (Karlsruhe, Germany)
Shrimp Alkaline Phosphatase	Thermo Fisher Scientific (Schwerte, Germany)

Table 4.5: (continued)

Enzymes	Manufacturer
T4 DNA Ligase	Thermo Fisher Scientific (Schwerte, Germany)
Taq DNA Polymerase	–[b]
TURBO™ DNase	Life Technologies (Karlsruhe, Germany)

[a] The enzyme mix was stored at −80°C.

[b] Recombinant *Taq* DNA polymerase was expressed in and purified from *E. coli*.

4.1.7 Kits for molecular biology

Molecular biology kits used in this study are listed in Table 4.6.

Table 4.6: Molecular biology kits used in this study

Kit	Manufacturer
High Pure PCR Product Purification Kit	Roche Diagnostics (Mannheim, Germany)
Nucleospin® Plasmid Purification Kit	Macherey Nagel (Düren, Germany)
RNeasy® Plant Mini Kit	Qiagen (Hilden, Germany)

4.1.8 Oligonucleotides

Oligonucleotides used in this study were obtained as lyophilised powder from Life Technologies (Karlsruhe, Germany) and Sigma Aldrich (Munich, Germany). They were resuspended in ddH_2O to a concentration of 100 µM and stored at −20°C. Oligonucleotides used for genotyping are listed in Table 4.7, those used for real-time PCR are listed in Table 4.8 and those used for cloning are listed in Table 4.9. Primers were designed using Oligo Explorer 1.1.0 software (Teemu Kulaasma, Kuopio, Finland; http://www.genelink.com/tools/gl-oe.asp), SALK T-DNA Primer Design (Salk Institute; http://signal.salk.edu/tdnaprimers.2.html) and dCAPS Finder 2.0 (Neff et al., 2002; http://helix.wustl.edu/dcaps/dcaps.html).

Table 4.7: Genotyping primers used in this study

Primer	Sequence (5'→ 3')	Reference
AXR2-geno_F2	CAA TAC ATA CAT GCG TAC AAG C	this study
AXR2-geno_R2	ATG ACT CTA ACT CGG TAA GGT TC	this study

Table 4.7: (continued)

Primer	Sequence (5'→3')	Reference
AXR3-geno_F1	TTT TCC ACT CTT CTC TAC TGC TC	this study
AXR3-geno_R1	CTC CGT CCA TTG ATA CCT TC	this study
COP1-geno_F1	GAT GCG CTG AGT GGG CCA	Ruckle et al. (2007)
COP1-geno_R1	TGC CAT TGT CCT TTT ACC ATT TCA GC	Ruckle et al. (2007)
er-105	AGC TGA CTA TAC CCG ATA CTG A	Shpak et al. (2004)
ERg2248	AAG AAG TCA TCT AAA GAT GTG A	Shpak et al. (2004)
ERg3016rc	AGA ATT TTC AGG TTT GGA ATC TGT	Shpak et al. (2004)
ERL1-geno_F2	AGG GAA AAA TAC CAG TTG AGC	this study
ERL1-geno_R2	CGG AGA GAT TGT TGA AGG AG	this study
ERL2-geno_F3	GAA CTA TCC CAG AGA GCA TT	this study
ERL2-geno_R3	TGA TTC AAG GCA GCA CAG	this study
FAMA-geno_F1	TGG TCT TGC TCG TTC TAG CTC	this study
FAMA-geno_R1	CTA TCT TGC ATG TCT TGC GTC	this study
FISH-geno1	CTG GGA ATG GCG AAA TCA AG	Fackendahl (2011)
JL-202	CAT TTT ATA ATA ACG CTG CGG ACA TCT AC	Shpak et al. (2004)
LB-SAIL	TAG CAT CTG AAT TTC ATA ACC A	Fackendahl (2011)
mute-dCAPS_F1	TTC GTT CTT TGA CTC CTT GTT TCT ACC TCA AAA G	this study
mute-dCAPS_R1	CTT CGA GAA AAT AAT TAG GAT TGT GAA TTG AG	this study
SAIL-LB3	TAG CAT CTG AAT TTC ATA ACC AAT CTC GAT ACA C	Salk Institute
SAIL-LB1	GCC TTT TCA GAA ATG GAT AAA TAG CCT TGC TTC C	Salk Institute
SALK-LBa1	TGG TTC ACG TAG TGG GCC ATC G	Salk Institute
SALK-LBb1.3	ATT TTG CCG ATT TCG GAA C	Salk Institute
spa1-100 WT_F1	CAT TCA TAA TAC TAT TCT CAC CAG C	Fackendahl (2011)
spa1-100 WT_R1	GAT TTA AGG TAT GGA GGC TGT AG	Fackendahl (2011)
SPA2-geno_F2	GGG AAA ATG TCT TTG CCT GA	Fackendahl (2011)
SPA2-geno_R2	AGC ACG GCA AAC CAT CAT A	Fackendahl (2011)
SPA3_F2	TTC GGA CTC TGG CTC TGA TTC CTT G	Fackendahl (2011)
SPA3_R4	GTC CTC ATT GAT GGT CGA CAA GTT	Fackendahl (2011)
SPA4-geno_F1	GGT CAA GAA GCT TCC TCG TG	Fackendahl (2011)
SPA4-geno_R1	TCA TCA TCA AGT CCT CCC AAG	Fackendahl (2011)
SPCH-geno_F1	GAA AAA CCT AGA TCC TCC CCC	this study
SPCH-geno_R3	AAC CTG AAG AAT CTC AAG AGC C	this study
tmm-1-dCAPS_F1	AAC GCG TTC AAA GGG CTC AAG AAC GT	this study
tmm-1-dCAPS_R2	AGA CTG TTA TCG TTG AGC C	this study

Table 4.8: Real-time PCR primers used in this study

Primer	Sequence (5'→ 3')	Reference
AXR2-RT_F2	AGA GTC CTG CCA AAT CGG	this study
AXR2-RT_R2	TGA GAT CAA CGG TTT CGG	this study
AXR3-RT_F1	CTC TTT TAC CAT GGG CAA ACA TGG A	Pérez-Pérez et al. (2010)
AXR3-RT_R1	AGG GAA CAT AGT CCC AGC TAT TCA	Pérez-Pérez et al. (2010)
FAMA-RT_F2	CTG CTT TGG AGG ATC TTC ATC TCT	Kang et al. (2009)
FAMA-RT_R2	CTT CTG CCG TAA ACC TCG TTT C	Kang et al. (2009)
HA-RT_fw1	GGC CGC TTA CCC ATA TGA C	Balcerowicz et al. (2011)
HA-RT_rev1	GGT AAG CGT AAT CCG GAA CG	Balcerowicz et al. (2011)
MUTE-RT_F2	GAC GAT CAC TTC ATC AGA CAC AAA G	Kang et al. (2009)
MUTE-RT_R2	CCT CAA TAT TAG TAG CAT GGA GGA GAC T	Kang et al. (2009)
SHY2-RT_F1	CTT AAA GCT TTA GAA GTG ATG TTCA A	Pérez-Pérez et al. (2010)
SHY2-RT_R1	CAC GTA CAT ATG AAC ATC TCC CA	Pérez-Pérez et al. (2010)
SPCH-RT_F2	TTC TGC ACT TAG TTG GCA CTC AAT	Kang et al. (2009)
SPCH-RT_R2	GCT GCT CTT GAA GAT TTG GCT CT	Kang et al. (2009)
UBQ10-RT_F3	CAC ACT CCA CTT GGT CTT GCGT	Czechowski et al. (2005)
UBQ10-RT_R3	TGG TCT TTC CGG TGA GAG TCT TCA	Czechowski et al. (2005)

Table 4.9: Primers used for cloning

Primer	Sequence (5'→ 3')	Reference
AXR3pro-attB-F	GGG GAC AAG TTT GTA CAA AAA AGC AGG CTT GTG GTA GAA TGT TGA GAG TTG TGG C	this study
AXR3pro-attB-R	GGG GAC CAC TTT GTA CAA GAA AGC TGG GTT ATT AAC CTT TCT TCT TCT TTG GTG TTC	this study
AXR3-XhoI-R	CAT GCT CGA GAG CTC TGC TCT TGC ACT TCT CC	this study
HindIII-AXR3-F	CTT GAA GCT TAT GAT GGG CAG TGT CGA GCT G	this study
ICE1pro-attB-F	GGG GAC AAG TTT GTA CAA AAA AGC AGG CTA CCG GAC CAC CGT CAA TAA CAT CG	this study
ICE1pro-attB-R	GGG GAC CAC TTT GTA CAA GAA AGC TGG GTC GCC AAA GTT GAC ACC TTT ACC C	this study
SPCHpro-attB-F	GGG GAC AAG TTT GTA CAA AAA AGC AGG CTC AAG ATC ATC ACT GCG ATA AGG AG	this study
SPCHpro-attB-R	GGG GAC CAC TTT GTA CAA GAA AGC TGG GTC GTG ATT AGA GAT ATA TCC TTC TC	this study
XhoI-YFP-F	GCA TCT CGA GAT GGT GAG CAA GGG CGA GGA G	this study
YFP-SpeI-R	TCA CAC TAG TCT ACT TGT ACA GCT CGT CCA TGC	this study

4.1.9 Molecular markers

GeneRuler™ 1kb DNA Ladder and GeneRuler™ Low Range DNA Ladder for agarose gel electrophoresis as well as PageRuler™ Prestained Protein Ladder for SDS-PAGE were obtained from Thermo Fisher Scientific (Schwerte, Germany).

4.1.10 Plasmids

Plasmid vectors used in this study are listed in Table 4.10.

Table 4.10: Plasmid vectors used in this study

Vector	Description	Reference
pBS-axr3-1	Basic cloning vector containing the *axr3-1* ORF; selection: ampicillin	Ouellet et al. (2001)
pDest-Venus-GW-Ter	Gateway® destination vector for expression of N-terminal Venus-YFP fusion proteins from the *35S* promoter; selection: kanamycin (bacteria and plants)	Hänsch, unpublished
pDONR™207	Gateway® donor vector; selection: gentamycin	Life Technologies
pDONR™207-35Spro	Gateway® entry vector containing the *35S* promoter; selection: gentamycin	An et al. (2004)
pDONR™207-AXR3pro	Gateway® entry vector containing the *AXR3* promoter; selection: gentamycin	this study
pDONR™207-ICE1pro	Gateway® entry vector containing the *ICE1* promoter; selection: gentamycin	this study
pDONR™207-ML1pro	Gateway® entry vector containing the *ML1* promoter; selection: gentamycin	An et al. (2004)
pDONR™207-SPCHpro	Gateway® entry vector containing the *SPCH* promoter; selection: gentamycin	this study
pDONR™221-CAB3pro	Gateway® entry vector containing the *CAB3* promoter; selection: kanamycin	Ranjan et al. (2011)
pJIC30 (GW-MCS-Tnos pGREEN0229)	Gateway®destination vector; selection: kanamycin (bacteria), BASTA (plants)	Corbesier et al. (2007)
pJIC30-axr3-1-YFP	Gateway®destination vector for expression of an axr3-1-YFP fusion protein; selection: kanamycin (bacteria), BASTA (plants)	this study

Table 4.10: (continued)

Vector	Description	Reference
pJIC30-35S::axr3-1-YFP	Gateway® expression vector for expression of an axr3-1-YFP fusion protein from the *35S* promoter; selection: kanamycin (bacteria), BASTA (plants)	this study
pJIC30-AXR3::axr3-1-YFP	Gateway® expression vector for expression of an axr3-1-YFP fusion protein from the *AXR3* promoter; selection: kanamycin (bacteria), BASTA (plants)	this study
pJIC30-CAB3::axr3-1-YFP	Gateway® expression vector for expression of an axr3-1-YFP fusion protein from the *CAB3* promoter; selection: kanamycin (bacteria), BASTA (plants)	this study
pJIC30-ICE1::axr3-1-YFP	Gateway® expression vector for expression of an axr3-1-YFP fusion protein from the *ICE1* promoter; selection: kanamycin (bacteria), BASTA (plants)	this study
pJIC30-ML1::axr3-1-YFP	Gateway® expression vector for expression of an axr3-1-YFP fusion protein from the *ML1* promoter; selection: kanamycin (bacteria), BASTA (plants)	this study
pJIC30-SPCH::axr3-1-YFP	Gateway® expression vector for expression of an axr3-1-YFP fusion protein from the *SPCH* promoter; selection: kanamycin (bacteria), BASTA (plants)	this study
pJIC30-YFP	Gateway® destination vector for expression of C-terminal Venus-YFP fusion proteins; selection: kanamycin (bacteria), BASTA (plants)	this study
pSoup	Helper plasmid for replication of pGreen-based vectors in Agrobacteria; selection: tetracyclin	Hellens et al. (2000)

4.1.11 Bacterial strains

The *E. coli* strain DH5α was used for standard cloning, the ccdB-resistant *E. coli* strain DB3.1 was used for cloning and propagating Gateway® vectors (both Life Technologies, Karlsruhe, Germany). The *Agrobacterium tumefaciens* strain GV3101::pMP90 (Koncz and Schell, 1986) was used for stable transformation of Arabidopsis.

4.1.12 Plant material

Arabidopsis mutant lines used in this study are listed in Table 4.11, transgenic lines used in this study are listed in Table 4.12. Columbia-0 (Col-0) is the corresponding wild type for all mutants except *shy2-2*, which is in the Landsberg *erecta* (Ler) background.

Table 4.11: Arabidopsis mutants used in this study

Mutant	Mutagen	Reference
axr2-1	EMS	Timpte et al. (1994)
axr2-1 axr3-1	EMS	this study
axr3-1	EMS	Leyser et al. (1996)
axr3-1 cop1-4	EMS	this study
axr3-1 er-105	EMS, FNB	this study
axr3-1 er-105 erl2-1	EMS, FNB, T-DNA	this study
axr3-1 er-105 erl1-2 erl2-1	EMS, FNB, T-DNA	this study
axr3-1 erl1-2	EMS, T-DNA	this study
axr3-1 erl1-2 erl2-1	EMS, T-DNA	this study
axr3-1 fama-1	EMS, T-DNA	this study
axr3-1 mute-1	EMS	this study
axr3-1 spch-3	EMS, T-DNA	this study
axr3-1 tmm-1	EMS	this study
cop1-4	EMS	Deng and Quail (1992)
det2-1	EMS	Chory et al. (1991)
epf1-1 epf2-3	T-DNA	Hara et al. (2009)
er-105	FNB	Torii et al. (1996)
er-105 erl2-1	FNB, T-DNA	Shpak et al. (2004)
er-105 erl1-2 erl2-1	FNB, T-DNA	Shpak et al. (2004)
erl1-2	T-DNA	Shpak et al. (2004)
erl1-2 erl2-1	T-DNA	Shpak et al. (2004)
fama-1	T-DNA	Ohashi-Ito and Bergmann (2006)
mute-1	EMS	Pillitteri et al. (2007)
shy2-2	EMS	Reed et al. (1998)
spa1-7 spa2-1 spa3-1	T-DNA	Balcerowicz et al. (2011)
spa1-7 spa3-1 spa4-1	T-DNA	Fittinghoff et al. (2006)
spa1-7 spa2-1 spa3-1 spa4-1 (spa-Q)	T-DNA	Balcerowicz et al. (2011)
spa2-1 spa3-1 spa4-1	T-DNA	Fittinghoff et al. (2006)
spa1-100 spa2-2 spa3-1 spa4-3 (spa-nQ)	T-DNA	Fackendahl (2011)
spch-3	T-DNA	MacAlister et al. (2007)
tir1-1	EMS	Ruegger et al. (1998)
tir1-1 afb2-3 afb3-4	EMS, T-DNA	Parry et al. (2009)

Table 4.11: (continued)

Mutant	Mutagen	Reference
tmm-1	EMS	Yang and Sack (1995)
wei8-1	T-DNA	Stepanova et al. (2008)
wei8-1 tar2-1	T-DNA	Stepanova et al. (2008)
yda-10	T-DNA	Kang et al. (2009)

FNB fast neutron bombardment

Table 4.12: Arabidopsis transgenic lines used in this study

Line	Background	Reference
35S::axr3-1-YFP	Col-0	this study
35S::YFP-COP1	Col-0	Subramanian et al. (2006)
35S::YFP-COP1	*spa-nQ*	this study
AXR3::axr3-1-YFP	Col-0	this study
CAB3::axr3-1-YFP	Col-0	this study
FAMA::FAMA-GFP	Col-0	Pillitteri et al. (2007)
FAMA::FAMA-GFP	*axr3-1*	this study
GVG-Nt-$MEK2^{DD}$	Col-0	Ren et al. (2002)
GVG-Nt-$MEK2^{DD}$	*axr3-1*	this study
ICE1::axr3-1-YFP	Col-0	this study
ML1::axr3-1-YFP	Col-0	this study
MUTE::MUTE-GFP	Col-0	Pillitteri et al. (2007)
MUTE::MUTE-GFP	*axr3-1*	this study
MUTE::GFP	Col-0	MacAlister et al. (2007)
MUTE::GFP	*axr3-1*	this study
SPA1::SPA1-HA	*spa1-7 spa2-1 spa3-1*	Balcerowicz et al. (2011)
SPA1::SPA1-HA	*spa-Q*	Balcerowicz et al. (2011)
SPA1::SPA2-HA	*spa1-7 spa2-1 spa3-1*	Balcerowicz et al. (2011)
SPA1::SPA2-HA	*spa-Q*	Balcerowicz et al. (2011)
SPA2::SPA1-HA	*spa1-7 spa2-1 spa3-1*	Balcerowicz et al. (2011)
SPA2::SPA1-HA	*spa-Q*	Balcerowicz et al. (2011)
SPA2::SPA2-HA	*spa1-7 spa2-1 spa3-1*	Balcerowicz et al. (2011)
SPA2::SPA2-HA	*spa-Q*	Balcerowicz et al. (2011)
SPCH::axr3-1-YFP	Col-0	this study
SPCH::nucGFP	Col-0	MacAlister et al. (2007)
SPCH::nucGFP	*axr3-1*	this study
TMM::TMM-GFP	Col-0	Nadeau and Sack (2002a)
TMM::TMM-GFP	*axr3-1*	this study

4.2 Methods for plant growth

4.2.1 Seed sterilisation

For sterile growth of Arabidopsis seedlings on MS plates, seeds were surface-sterilised prior to plating. For liquid sterilisation, seeds were incubated in seed sterilisation solution for 10 min and then washed four times with autoclaved ddH_2O. Alternatively, seeds were incubated in a chlorine gas atmosphere (produced by adding 2.5 ml 37% HCl to 80 ml NaClO) for 3 h, which was subsequently evaporated in a sterile hood for at least 1 h.

4.2.2 General plant growth

For growth on soil, seeds were stratified at 4°C for 3 d in 0.1% agarose before sowing. A mixture of three parts soil and one part vermiculite was used as substrate. Plants were grown in the greenhouse under long day conditions (16 h light, 8 h darkness) at approximately 40% humidity and a temperature cycle of 21°C during the day and 18°C during the night. For phenotypic analysis, plants were grown in walk-in growth chambers (Johnson Controls, Milwaukee, WI, USA) under short day (8 h light, 16 h darkness) or long day conditions (16 h light, 8 h dark) at 21°C and 60% humidity. They were grown at light intensities of approximately 100 µmol m^{-2} s^{-1} generated by Lumilux L36W/840 cool white fluorescent tubes (Osram, Munich, Germany).

For sterile growth, sterilised seeds were plated on MS medium without sucrose; for analysis of stomatal development, MS medium was supplemented with 1% (w/v) sucrose due to the longer growth period in darkness. Plated seeds were stratified at 4°C for 3 d before germination was induced by 3 h treatment with white light (approximately 25 µmol m^{-2} s^{-1}). Plates were then either kept in Wc, moved to continuous darkness or incubated in the dark for 21 h before being shifted to monochromatic FR. In each case, plates were incubated in growth chambers (CLF Plant Climatics, Wertingen, Germany) at 21°C. White light was produced by Fluora L58W/77 fluorescent tubes (Osram, Munich, Germany), monochromatic FR was produced by LED light sources (Quantum Devices, Barneveld, WI, USA).

4.2.3 Crossing of Arabidopsis plants

Flowers that had a well-developed stigma, but immature stamina, were emasculated under a stereomicroscope using fine tweezers. For crossing, pollen from donor stamina was then dabbed on the stigma of the emasculated flower. Mature siliques resulting from these crosses were harvested separately and allowed to dry. Three to four seeds per cross were used to grow the F1 generation, which was allowed to self-fertilise. Selection was then carried out in the F2 generation.

4.2.4 Selection of transgenic plants

Transgenic plants were selected for their respective resistance genes on MS plates containing 25 µg/ml gentamycin, 15 µg/ml hygromycin, 50 µg/ml kanamycin or 10 µg/ml DL-phosphinotricin (BASTA).

4.2.5 Chemical and hormonal treatments

Treatments with NAA, NPA, DEX and bikinin were carried out on seedlings grown on solid MS medium containing 1% sucrose. For NAA treatment, medium was supplemented with various concentrations of NAA given in the results section. For treatment with NPA, DEX and bikinin, medium was supplemented with 10 µM NPA, 0.02 µM DEX and 30 µM bikinin, respectively, or the equivalent amount of DMSO for mock treatment.

For MG132 treatment, seedlings were grown on solid MS medium in darkness for 4 d. Under green safety light, they were then transferred to liquid MS medium containing 50 µM MG132 or 0.5% DMSO for mock treatment and vacuum-infiltrated for 10 min at 100 mbar using a BA-VC-300H vacuum concentrator (Saur, Reutlingen, Germany). Afterwards, they were kept in darkness for 15 min before being shifted to FR.

4.3 Methods for phenotypic analysis

4.3.1 Brightfield microscopy

For observation by brightfield microscopy, seedlings were preserved in 95% alcohol for at least 12 h. They were then rehydrated by subsequent incubation in 70%, 50%, 30% and 0% ethanol for 1-2 h each. Rehydrated seedlings were dissected under a stereomicroscope and the parts to be analysed were then mounted in freshly prepared clearing solution. Samples were left to clear at RT for at least 12 h. They were analysed on the next day using an Eclipse E800 compound light microscope (Nikon Instruments, Amsterdam, Germany) and Diskus software (Hilgers, Königswinter, Germany).

4.3.2 Fluorescence and confocal microscopy

Fluorescing reporter dyes and proteins were observed either by a DM5000 B fluorescent microscope or a DM5500 Q confocal laser-scanning microscope using LAS AF software (Leica Microsystems, Wetzlar, Germany). For counterstaining of cell outlines, samples were stained in 50 µg/ml PI for several minutes, rinsed briefly with water and then mounted in water for microscopy. PI fluorescence was detected between 580 and 650 nm, GFP fluoresence between 480 and 530 nm and YFP fluorescence between 500 and 550 nm.

4.3.3 Measurement of hypocotyl length

To determine hypocotyl length, 4-d-old seedlings were pressed lengthwise on MS plates and were subsequently documented with a digital camera. Measurements of hypocotyl length were conducted on digital images using ImageJ 1.43u software (Wayne Rasband, NIH, Bethesda, USA). 25 seedlings were measured per genotype.

4.3.4 Quantification of epidermal cell types

To quantify the proportion of stomata and stomatal precursors in the epidermis, bright field images of cleared cotyledons or leaves were analysed using ImageJ 1.43u software (Wayne Rasband, NIH, Bethesda, USA). Depending on cotyledon or leaf size, up to three areas were selected, avoiding the margin and the central area close to the petiole, and cell types in these areas were counted. Area size was 250 µm × 250 µm in cotyledons of light-grown seedlings and 100 µm × 100 µm in cotyledons of dark-grown seedlings. Epidermal cells were classified as stomata (i.e. pairs of guard cells), stomatal precursors (i.e. meristemoids and GMCs) or other epidermal cells according to morphological differences described in Nadeau and Sack (2002b). Percentages of stomata and stomatal precursors were calculated according to Formulas 4.1 and 4.2, respectively. Stomata were considered to be clustered when their guard cells shared a common cell wall. Ten cotyledons or leaves of individual seedlings and plants, respectively, were analysed per genotype and condition. Percentages of stomata and stomatal precursors were calculated for each cotyledon or leaf individually before mean and SEM were calculated from these data.

$$(4.1)\ \%\ \text{Stomata (SI)} = \frac{\text{stomata}}{\text{stomata} + \text{stomatal precursors} + \text{other epidermal cells}}$$

$$(4.2)\ \%\ \text{Stomatal precursors} = \frac{\text{stomatal precursors}}{\text{stomata} + \text{stomatal precursors} + \text{other epidermal cells}}$$

4.3.5 Quantification of total epidermal cell number

To quantify the total number of epidermal cells per cotyledon, cell outlines were stained in 50 µg/ml PI for 10-15 min and observed by confocal microscopy. Digital images of a Z stack through the cotyledon were combined into a single image of the whole epidermis by maximum projection using LAS AF software (Leica Microsystems, Wetzlar, Germany). Cells were then counted using ImageJ 1.43u software (Wayne Rasband, NIH, Bethesda, USA).

4.4 Molecular biology methods

4.4.1 Agarose gel electrophoresis

DNA was separated by agarose gel electrophoresis in 0.5% TBE according to standard protocols (Sambrook et al., 2001). Agarose gels were supplemented with 0.25 µg/ml ethidium bromide for visualisation of DNA bands on a GEL Stick "Touch" imager (INTAS Science Imaging Instruments, Göttingen, Germany).

4.4.2 Polymerase chain reaction (PCR)

Standard PCR was carried out with 1 µl *Taq* DNA polymerase in a mixture of 1 × PCR reaction buffer, 0.5 µM forward and reverse primers and 125 µM dNTPs in a 20 µl reaction. In case of genomic DNA, 1-2 µl were used as template. The standard PCR program consisted of 3 min initial denaturation at 95°C, 40 cycles of 30 s denaturation at 95°C, 30 s annealing at 54°C and 1 min per kb elongation at 72°C and a final elongation step of 10 min at 72°C. In case of colony PCR, a small portion of a bacterial colony was used as template and the initial denaturation step was extended to 5 min. For cloning, PCR was carried out in a 50 µl reaction using *Pfu* DNA polymerase (Thermo Fisher Scientific, Schwerte, Germany) according to the manufacturer's instructions.

4.4.3 DNA sequencing

Plasmids and PCR products were sequenced by GATC Biotech (Konstanz, Germany). Sequences were analysed using Lasergene® SeqMan Pro™ software (DNASTAR, Madison, WI, USA).

4.4.4 Cloning

Conventional cloning including restriction digestion, vector dephosphorylation and ligation was carried out according to standard protocols (Sambrook et al., 2001). Gateway® cloning was carried out according to the manufacturer's instructions with the following modifications: BP and LR reactions were scaled down to 10 µl and only 0.5 µl of the respective enzyme (BP or LR clonase) were used. PCR products and digested DNA fragments used for cloning were purified from agarose gels or directly from the PCR mixtures using the Nucleospin® Plasmid Purification Kit (Macherey Nagel, Düren, Germany). Plasmids were isolated from *E. coli* cells using the High Pure PCR Product Purification Kit (Roche Diagnostics, Mannheim, Germany). Positive clones were selected by colony PCR, DNA sequences were verified by appropriate restriction digests and sequencing.

4.4.5 Cloning strategy for generation of *promoter::axr3-1-YFP* constructs

Promoter::axr3-1-YFP constructs were generated from the pJIC30 vector (Corbesier et al., 2007; Figure 4.1 A). To this end, the *Venus-YFP* sequence was PCR-amplified from the pDEST-Venus-GW-Ter vector (R. Hänsch, unpublished) with primers introducing XhoI and SpeI restriction sites (XhoI-YFP-F and YFP-SpeI-R). The purified *Venus-YFP* PCR product was digested with XhoI and SpeI and ligated into pJIC30, thereby generating pJIC30-YFP. The *axr3-1* ORF was PCR-amplified from the pBS-axr3-1 vector (Ouellet et al., 2001) with primers introducing HindIII and XhoI restriction sites (HindIII-AXR3-F and AXR3-XhoI-R). The purified *axr3-1* PCR product was digested with HindIII and XhoI and ligated into pJIC30-YFP, thereby generating pJIC30-axr3-1-YFP (Figure 4.1 B).

Promoter fragments 2421 bp upstream of the *AXR3* ORF, 2581 bp upstream of the *ICE1* ORF and 2574 bp upstream of the *SPCH* ORF were amplified from Col-0 genomic DNA using the primers AXR3pro-attB-F and AXR3pro-attB-R, ICE1pro-attB-F and ICE1pro-attB-R and SPCHpro-attB-F and SPCHpro-attB-R, respectively. The purified PCR products were cloned into pDONR™207 using GATEWAY® BP technology, thereby generating the promoter entry clones pDONR™207-AXR3pro, pDONR™207-

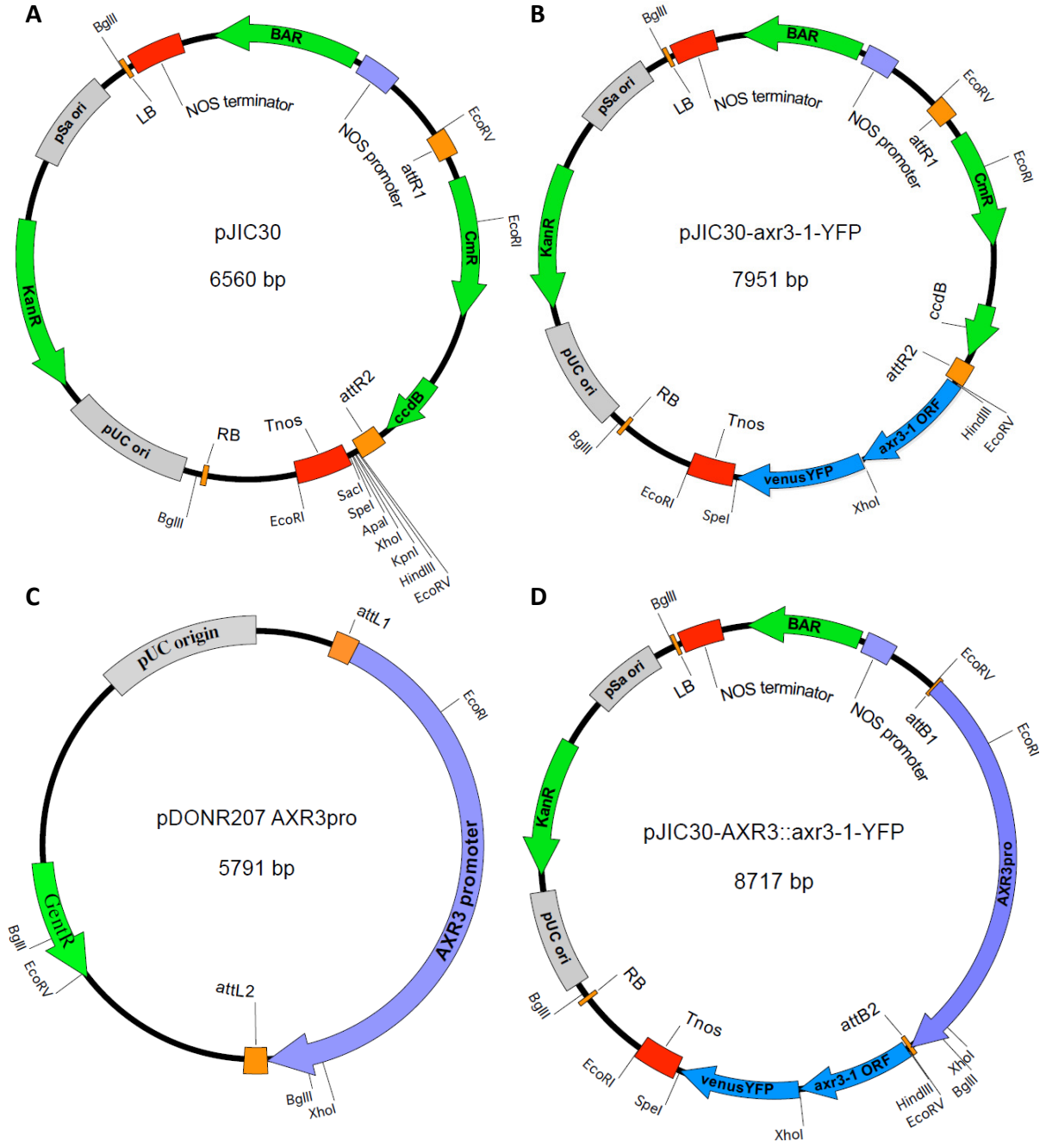

Figure 4.1: Plasmid vectors used in this study.
A: pJIC30 destination vector. **B:** pJIC30-axr3-1-YFP destination vector. **C:** Representative promoter entry clone containing the *AXR3* promoter. **D:** Representative *promoter::axr3-1-YFP* expression clone for expression of an axr3-1-YFP fusion protein from the *AXR3* promoter.

ICE1pro and pDONR™207-SPCHpro (Figure 4.1 C). The entry clones pDONR™207-35Spro, pDONR™207-ML1 and pDONR™221-CAB3 have been described previously (An et al., 2004; Ranjan et al., 2011). *Promoter::axr3-1-YFP* constructs (Figure 4.1 D) were generated by GATEWAY® LR reactions between these promoter entry clones and the pJIC30-axr3-1-YFP destination vector.

Cloning strategies and constructs were designed using Lasergene® SeqBuilder™ software (DNASTAR, Madison, WI, USA).

4.4.6 Preparation and transformation of chemically competent *E. coli*

For preparation of chemically competent *E. coli*, a single colony was used for inoculation of a 250 ml culture. The culture was grown at 18°C until an OD_{600} of 0.6 was reached and then centrifuged for 10 min at 2500 *g* and 4°C. After removal of the supernatant, the pellet was resuspended in 80 ml ice-cold TB buffer and incubated on ice for 10 min. The suspension was centrifuged again for 10 min at 2500 *g* and 4°C and the pellet was subsequently resuspended in 20 ml ice-cold TB buffer. DMSO was added to a final concentration of 7% (v/v) and the mixture was incubated on ice for 10 min. The cell suspension was then split into 50 µl aliquots that were snap-frozen in liquid nitrogen and stored at −80°C.

For transformation, a 50 µl aliquot of chemically competent *E. coli* cells was thawed on ice, mixed with 50-100 ng plasmid DNA and heat-shocked for 90 s at 42°C. Subsequently, 500 µl LB medium were added, the mixture was cooled briefly on ice and then incubated at 37°C for 45-60 min before being plated on solid LB medium containing the appropriate antibiotics for selection of transformed cells.

4.4.7 Preparation and transformation of electro-competent *Agrobacterium tumefaciens*

For preparation of electro-competent Agrobacteria, three to four single colonies were used to inoculate a 250 ml culture. The culture was grown at 28°C until an OD_{600} of 0.5 was reached and then centrifuged for 10 min at 4000 *g* and 4°C. After removal of the supernatant, the pellet was resuspended in 300 ml ice-cold water and centrifuged again for 10 min at 4000 *g* and 4°C. The supernatant was removed and the pellet was rinsed with 300 ml ice-cold 10% (v/v) glycerol and centrifuged again for 10 min at 4000 *g* and 4°C. This wash step was repeated twice before the pellet was resuspended in 1-2 ml 10% (v/v) glycerol. The cell suspension was split into 40 µl aliquots that were snap-frozen in liquid nitrogen and stored at −80°C.

For transformation, a 40 µl aliquot of electro-competent Agrobacteria was mixed with 100-250 ng plasmid, incubated for 30 min on ice and then electroporated using the Micro-Pulser™ electroporator (Bio-Rad Laboratories, Munich, Germany) according to the manufacturer's instructions. Transformed cells were immediately mixed with 500 µl YEB medium and incubated at 28°C for 3-4 h before being plated on solid LB medium containing appropriate antibiotics.

4.4.8 Stable transformation of Arabidopsis by floral dipping

Arabidopsis plants were stably transformed using the floral dip method (Clough and Bent, 1998). Briefly, a 5 ml LB pre-culture of agrobacteria containing the plasmid with the T-DNA to be transformed was used to inoculate a 250 ml LB culture that was grown at 28°C for 8-10 h. The culture was then centrifuged for 20 min at 4000 *g* and 4°C, the supernatant was removed and the pellet was resuspended in ice-cold 5% (w/v) sucrose to an OD_{600} of 0.8. Silwet L-77 was added to a final concentration of 0.05% (v/v). Inflorescences of the plants to be transformed were submerged into the solution and slowly agitated for 5 s before they were removed from the suspension. The dipped plants were then kept under low light and high humidity for 24 h.

4.4.9 Isolation of genomic DNA from Arabidopsis

Single leaves or five to ten seedlings were snap-frozen in liquid nitrogen, ground to a fine powder and mixed with 400 µl Thompson DNA extraction buffer by vortexing. Samples were centrifuged at 20 000 *g* for 3 min, 200 µl of the supernatant were transferred to a new tube, mixed with 200 µl isopropanol and incubated at RT for 2 min. Samples were then centrifuged at 20 000 *g* for 10 min, the supernatant was removed and the pellets were air-dried for 15 min before being resuspended in 30-50 µl TE buffer or ddH_2O.

For high-throughput genotyping, single leaves were transferred to racked collection microtubes (Qiagen, Hilden, Germany) containing stainless steel beads (5 mm diameter). After addition of 300 µl DNA extraction buffer, the tissue was disrupted in a MM301 tissue lyser (Retsch, Haan, Germany) by shaking at 30 Hz for 3 min.

DNA was kept at 4°C or −20°C for long-term storage.

4.4.10 Genotyping of Arabidopsis mutants

Genomic DNA prepared from leaves was used to genotype Arabidopsis plants. To genotype T-DNA insertion mutants, presence of the wild-type and the mutant allele was tested by two PCR reactions containing combinations of two wild-type-specific or a wild-type-specific and a T-DNA-specific primer. Primer combinations used for genotyping T-DNA insertion mutants are given in Table 4.13. To genotype EMS mutants, CAPS or dCAPS primers were used for amplification of the locus of interest; wild-type and mutant locus were subsequently distinguished by different restriction patterns. In some cases, the respective allele was also verified by sequencing of the purified PCR product. Primer combinations as well as restriction enzymes used for genotyping of EMS mutants are given in Table 4.14.

Table 4.13: Primer combinations used for genotyping of T-DNA insertion mutants

Mutant	**Primer combination**	**Product size**
er-105 [a]	wt: ERg2248 + ERg3016rc	770 bp
	er-105: ERg2248 + er-105	ca. 750 bp
erl1-2	wt: ERL1-geno_F2 + ERL1-geno_R2	ca. 750 bp
	erl1-2: ERL1-geno_F2 + JL-202	ca. 350 bp
erl2-1	wt: ERL2-geno_F3 + ERL2-geno_R3	ca. 800 bp
	erl2-1: ERL2-geno_R3 + JL-202	ca. 350 bp
fama-1	wt: FAMA-geno_F1 + FAMA-geno_R1	965 bp
	fama-1: FAMA-geno_R1 + SALK-LBb1.3	ca. 600 bp
spa1-100	wt: spa1-100-WT_F1 + spa1-100-WT_R1	700 bp
	spa1-100: spa1-100 WT_R1 + LB-SAIL	ca. 550 bp
spa2-2	SPA2-geno_F2 + SPA2-geno_R2	360 bp
	spa2-2: SPA2-geno_F2 + FISH-geno1	ca. 600 bp
spa3-1	SPA3-F2 + SPA3-R4	600 bp
	spa3-1: SPA3-F2 + LB-SAIL	ca. 400 bp
spa4-3	SPA4-geno_F1 + SPA4-geno_R1	380 bp
	spa4-3: SPA4-geno_F1 + FISH-geno1	ca. 380 bp
spch-3	wt: SPCH-geno_F1 + SPCH-geno_R3	1600 bp
	spch-3: SPCH-geno_R3 + SAIL-LB1	ca. 1200 bp

[a] *er-105* is not a T-DNA insertion mutant, but contains a genomic rearrangement induced by fast neutron bombardment that allowed for identification of the mutant allele by PCR.

Table 4.14: Primer combinations used for genotyping of EMS mutants

Mutant	Primer combination	Restriction enzyme	Restriction fragments
axr2-1	AXR2-geno_F2 + AXR2-geno_R2	MslI	wt: 205 bp, 155 bp, 145 bp *axr2-1*: 360 bp, 145 bp
axr3-1	AXR3-geno_F1 + AXR3-geno_R1	BshTI	wt: 300 bp, 100 bp *axr3-1*: 400 bp
cop1-4	COP1-geno_F1 + COP1-geno_R1	HpyF10VI	wt: 125 bp, 15 bp *cop1-4*: 140 bp
mute-1	mute-dCAPS_F1 + mute-dCAPS_R1	BslI	wt: 110 bp, 30 bp *mute-1*: 140 bp
tmm-1	tmm-1-dCAPS_F1 + tmm-1-dCAPS_R2	AclI	wt: 200 bp *tmm-1*: 175 bp, 25 bp

wt wild-type allele

4.4.11 Isolation of total RNA from Arabidopsis

Total RNA was isolated from 50-100 ng of snap-frozen seedlings using the RNeasy® Plant Mini Kit (Qiagen, Hilden, Germany) according to the manufacturer's instructions. RNA concentrations were measured using a Nanodrop® ND-1000 spectrophotometer (Thermo Fisher Scientific, Schwerte, Germany). Integrity of RNA was analysed on a 1% agarose gel by checking the presence of clear $28S$ and $18S$ rRNA bands. RNA samples were stored at −80°C.

4.4.12 DNase treatment of RNA

To remove copurified DNA, 1 µg of total RNA was treated with 0.5 µl TURBO™ DNase (Life Technologies, Karlsruhe, Germany) in a 20 µl reaction containing 1 × TURBO™ DNase buffer and incubated at 37°C for 30 min. Afterwards, 2 µl 50 mM EDTA were added and the samples were incubated at 75°C for 10 min to inactivate the DNase. If not used immediately, DNase-treated RNA samples were stored at −80°C.

4.4.13 Reverse transcription of Arabidopsis mRNA

Reverse transcription of mRNA into cDNA was carried out in a reaction mix containing 1 µg DNase-treated RNA, 0.5 µM oligo$(dT)_{18}$ primers (Thermo Fisher Scientific, Schwerte, Germany), 1 mM dNTPs, 1 × RevertAid™ H Minus reaction buffer and RevertAid™ H Minus Reverse Transcriptase (Thermo Fisher Scientific, Schwerte, Germany). First, DNase-treated RNA was supplemented with oligo-$(dT)_{18}$ primers and denatured at 65°C for 5 min. After a short incubation on ice, dNTPs, reaction buffer and 1 µl reverse transcriptase were added and the volume was filled up to 40 µl with RNase-free water. The mixture was incubated at 42°C for 1 h to allow first strand cDNA synthesis and the reverse transcriptase was subsequently inactivated at 70°C for 10 min. The obtained cDNA samples were stored at −20°C.

4.4.14 Real-time PCR

Real-time PCR was used to determine transcript levels. To this end, 1 µl cDNA was used as template in a 20 µl reaction mix containing 1 × KAPA™ SYBR® FAST qPCR Mastermix (PEQLAB Biotechnologie, Erlangen, Germany) and 125 nM forward and reverse primers. Real-time PCR was performed on an Applied Biosystems® 7300 Real-time PCR system (Life Technologies, Karlsruhe, Germany). The PCR program consisted of an initial denaturation step at 95°C for 2 min, followed by 40 cycles of a denaturation step at 95°C for 2 s and a combined annealing and elongation step at 60°C for 30 s. For melting curve analysis, a dissociation stage consisting of two cycles of 60°C for 15 s and 95°C for 15 s was performed at the end of each run. Relative transcript levels were calculated using the $2^{\Delta\Delta C_T}$ method (Livak and Schmittgen, 2001) with minor modifications according to Bookout and Mangelsdorf (2003). Two to three biological replicates were analysed, and each of them was analysed in technical duplicates.

4.5 Biochemical methods

4.5.1 Isolation of total protein from Arabidopsis

For preparation of total protein extracts from seedlings or leaves, 200 mg tissue were snap-frozen in liquid nitrogen, ground to a fine powder and mixed with 300 µl protein extraction buffer until completely thawed. Extracts were then centrifuged at 20 000 *g* and 4°C for 12 min and the supernatant was transferred to a new tube. Part of the supernatant was used for measurement of protein concentration by the Bradford assay, while the remainder was supplemented with Laemmli buffer and boiled for 5 min at 92°C. Samples were stored at −20°C.

4.5.2 Nuclear fractionation

Nuclear fractionation was performed according to Xia et al. (1997) with minor modifications. Briefly, 1.5 g tissue were snap-frozen in liquid nitrogen, ground to a fine powder and mixed with 3 ml HONDA buffer. All subsequent steps were carried out at 4^4∘C or on ice. Extracts were filtered through a 62 µm (pore size) nylon mesh by centrifugation at 400 *g* for 5 min, supplemented with Triton X-100 to a final concentration of 0.5% (v/v) and incubated on ice for 15 min. Extracts were then centrifuged at 1500 *g* for 5 min, the supernatant was removed and the pellet was washed with 2.5 ml pre-cooled HONDA buffer containing 0.1% (v/v) Triton X-100 before being centrifuged again at 1500 *g* for 5 min. After removal of the supernatant, the pellet was resuspended in 2.5 ml pre-cooled HONDA buffer, the suspension was split into four aliquots and centrifuged at 100 *g* for 5 min to pellet starch and cell debris. The supernatant was transferred to a new tube and centrifuged at 2000 *g* for 5 min to pellet the nuclei. After removal of the supernatant, the pellets were resuspended in 200 µl 2 x Laemmli buffer. Samples of total protein extracts were taken after addition of Triton X-100, samples of nuclei-depleted fractions were taken from the supernatant after the first centrifugation step at 1500 *g* and both were supplemented with Laemmli buffer. All samples were boiled at 92°C for 5 min and stored at −20°C. Protein concentration was determined by the amido black assay.

4.5.3 Bradford assay

Protein concentration in total protein extracts was determined by the Bradford Assay (Bio-Rad Laboratories, Munich, Germany) prior to addition of Laemmli buffer. Extracts were diluted 1:5 or 1:10 and 10 µl of the diluted extracts were mixed with 190 µl 1:5 diluted Bradford reagent (Bio-Rad Laboratories, Munich, Germany). Samples were incubated for at least 5 min at RT and then the OD_{595} was measured in an Infinite® M200 plate reader (Tecan, Männedorf, Switzerland). Protein concentration was calculated from the OD_{595} using a bovine serum albumin (BSA) calibration curve.

4.5.4 Amido Black assay

Protein concentration of samples obtained by nuclear fractionation was determined by the amido black assay. Of these samples, 10 µl were mixed with 500 µl Amido Black staining solution by vortexing and the mixture was centrifuged at 20 000 *g* for 10 min. After removal of the supernatant, the pellet was washed with 1 ml Amido Black wash solution and centrifuged again at 20 000 *g* for 10 min. The washing step was repeated once more and the pellet was then air-dried for 10 min. The dried pellet was resuspended in 250 µl 0.2 M NaOH and centrifuged at 20 000 *g* for 1 min. The OD_{595} was measured in 100 µl of the suspension using an Infinite® M200 plate reader (Tecan, Männedorf, Switzerland). Protein concentration was calculated from OD_{595} using a BSA calibration curve.

4.5.5 SDS polyacrylamide gel electrophoresis (SDS-PAGE)

SDS-PAGE was performed using the Mini PROTEAN® Tetra cell electrophoresis system (Bio-Rad Laboratories, Munich, Germany). Protein samples were separated in a discontinuous gel system according to Laemmli (1970). Stacking gels containing 5% acrylamide and resolving gels containing acrylamide concentrations of 7.5%, 10%, 12.5% or 15% were used.

4.5.6 Western blotting

Proteins separated by SDS-PAGE were blotted on a polyvinyledene difluoride (PVDF) membrane that had been activated in MeOH prior to transfer. Blotting was carried out in carbonate blotting buffer at a current of 0.35 mA cm^{-2} membrane for 70 min using the Mini PROTEAN® Tetra cell wet blot system (Bio-Rad Laboratories, Munich, Germany). After transfer, the membrane was blocked by incubation in Roti®-Block (Roth, Karlsruhe, Germany) for 1 h at RT or for at least 12 h at 4°C.

4.5.7 Immunodetection of blotted proteins

Membranes were incubated with the primary antibody for at least 12 h 4°C or for 1 h at RT, washed three times with TBS-T for 5 min and then incubated with the HRP-coupled secondary antibody for 1 h at RT. After three additional washing steps with TBS-T for 5 min each, HRP activity was detected with the ECL Plus™ Western Blotting kit (GE Healthcare, Piscataway, USA) or the SuperSignal® West Femto Maximum Sensitivity kit (Thermo Fisher Scientific, Schwerte, Germany) according to the manufacturer's instructions and visualised in an ImageQuant™ LAS 4000 mini imaging system (GE Healthcare, Piscataway, USA). Protein bands were quantified using MultiGauge Software (Fujifilm, Tokyo, Japan).

4.5.8 Coomassie staining of PVDF membranes

PVDF membranes were stained for 2-3 min with Coomassie staining solution followed by 15-20 min washing in Coomassie destaining solution.

References

Abel, S., Nguyen, M.D. and Theologis, A. (1995) The *PS-IAA4/5-like* family of early auxin-inducible mRNAs in *Arabidopsis thaliana*. *J. Mol. Biol.* **251**, 533–549.

Abrash, E.B. and Bergmann, D.C. (2010) Regional specification of stomatal production by the putative ligand CHALLAH. *Development* **137**, 447–455.

Abrash, E.B., Davies, K.A. and Bergmann, D.C. (2011) Generation of signaling specificity in *Arabidopsis* by spatially restricted buffering of ligand-receptor interactions. *Plant Cell* **23**, 2864–2879.

Ahmad, M. and Cashmore, A.R. (1993) *HY4* gene of *A. thaliana* encodes a protein with characteristics of a blue-light photoreceptor. *Nature* **366**, 162–166.

Al-Sady, B., Ni, W., Kircher, S., Schäfer, E. and Quail, P.H. (2006) Photoactivated phytochrome induces rapid PIF3 phosphorylation prior to proteasome-mediated degradation. *Mol. Cell* **23**, 439–446.

An, H., Roussot, C., Suárez-López, P., Corbesier, L., Vincent, C., Piñeiro, M., Hepworth, S., Mouradov, A., Justin, S., Turnbull, C. and Coupland, G. (2004) CONSTANS acts in the phloem to regulate a systemic signal that induces photoperiodic flowering of *Arabidopsis*. *Development* **131**, 3615–3626.

Ang, L.H., Chattopadhyay, S., Wei, N., Oyama, T., Okada, K., Batschauer, A. and Deng, X.W. (1998) Molecular interaction between COP1 and HY5 defines a regulatory switch for light control of *Arabidopsis* development. *Mol. Cell* **1**, 213–222.

Balcerowicz, M., Fittinghoff, K., Wirthmueller, L., Maier, A., Fackendahl, P., Fiene, G., Koncz, C. and Hoecker, U. (2011) Light exposure of arabidopsis seedlings causes rapid de-stabilization as well as selective post-translational inactivation of the repressor of photomorphogenesis SPA2. *Plant J.* **65**, 712–723.

Bandyopadhyay, A., Blakeslee, J.J., Lee, O.R., Mravec, J., Sauer, M., Titapiwatanakun, B., Makam, S.N., Bouchard, R., Geisler, M., Martinoia, E., Friml, J., Peer, W.A. and Murphy, A.S. (2007) Interactions of PIN and PGP auxin transport mechanisms. *Biochem. Soc. Trans.* **35**, 137–141.

Bao, F., Shen, J., Brady, S.R., Muday, G.K., Asami, T. and Yang, Z. (2004) Brassinosteroids interact with auxin to promote lateral root development in arabidopsis. *Plant Physiol.* **134**, 1624–1631.

Bauer, D., Viczián, A., Kircher, S., Nobis, T., Nitschke, R., Kunkel, T., Panigrahi, K.C.S., Adám, E., Fejes, E., Schäfer, E. and Nagy, F. (2004) Constitutive photomorphogenesis 1 and multiple photoreceptors control degradation of phytochrome interacting factor 3, a transcription factor required for light signaling in arabidopsis. *Plant Cell* **16**, 1433–1445.

Baumgardt, R.L., Oliverio, K.A., Casal, J.J. and Hoecker, U. (2002) SPA1, a component of phytochrome a signal transduction, regulates the light signaling current. *Planta* **215**, 745–753.

Benková, E., Michniewicz, M., Sauer, M., Teichmann, T., Seifertová, D., Jürgens, G. and Friml, J. (2003) Local, efflux-dependent auxin gradients as a common module for plant organ formation. *Cell* **115**, 591–602.

Bergmann, D.C., Lukowitz, W. and Somerville, C.R. (2004) Stomatal development and pattern controlled by a MAPKK kinase. *Science* **304**, 1494–1497.

Berleth, T. and Jurgens, G. (1993) The role of the *monopteros* gene in organising the basal body region of the *Arabidopsis* embryo. *Development* **118**, 575–587.

Bhalerao, R.P., Eklöf, J., Ljung, K., Marchant, A., Bennett, M. and Sandberg, G. (2002) Shoot-derived auxin is essential for early lateral root emergence in *Arabidopsis* seedlings. *Plant J.* **29**, 325–332.

Bhave, N.S., Veley, K.M., Nadeau, J.A., Lucas, J.R., Bhave, S.L. and Sack, F.D. (2009) TOO MANY MOUTHS promotes cell fate progression in stomatal development of *Arabidopsis* stems. *Planta* **229**, 357–367.

Biedermann, S. and Hellmann, H. (2011) WD40 and CUL4-based e3 ligases: lubricating all aspects of life. *Trends Plant Sci.* **16**, 38–46.

Boccalandro, H.E., Rugnone, M.L., Moreno, J.E., Ploschuk, E.L., Serna, L., Yanovsky, M.J. and Casal, J.J. (2009) Phytochrome b enhances photosynthesis at the expense of water-use efficiency in arabidopsis. *Plant Physiol.* **150**, 1083–1092.

Bookout, A.L. and Mangelsdorf, D.J. (2003) Quantitative real-time PCR protocol for analysis of nuclear receptor signaling pathways. *Nucl Recept Signal* **1**, e012.

Botto, J.F., Sanchez, R.A., Whitelam, G.C. and Casal, J.J. (1996) Phytochrome a mediates the promotion of seed germination by very low fluences of light and canopy shade light in arabidopsis. *Plant Physiol.* **110**, 439–444.

Brunoud, G., Wells, D.M., Oliva, M., Larrieu, A., Mirabet, V., Burrow, A.H., Beeckman, T., Kepinski, S., Traas, J., Bennett, M.J. and Vernoux, T. (2012) A novel sensor to map auxin response and distribution at high spatio-temporal resolution. *Nature* **482**, 103–106.

Casal, J.J., Sánchez, R.A. and Botto, J.F. (1998) Modes of action of phytochromes. *J. Exp. Bot.* **49**, 127–138.

Casson, S. and Gray, J.E. (2008) Influence of environmental factors on stomatal development. *New Phytol.* **178**, 9–23.

Casson, S.A., Franklin, K.A., Gray, J.E., Grierson, C.S., Whitelam, G.C. and Hetherington, A.M. (2009) phytochrome b and *PIF4* regulate stomatal development in response to light quantity. *Curr. Biol.* **19**, 229–234.

Casson, S.A. and Hetherington, A.M. (2010) Environmental regulation of stomatal development. *Curr. Opin. Plant Biol.* **13**, 90–95.

Castillon, A., Shen, H. and Huq, E. (2007) Phytochrome interacting factors: central players in phytochrome-mediated light signaling networks. *Trends Plant Sci.* **12**, 514–521.

Chamovitz, D.A., Wei, N., Osterlund, M.T., von Arnim, A.G., Staub, J.M., Matsui, M. and Deng, X.W. (1996) The COP9 complex, a novel multisubunit nuclear regulator involved in light control of a plant developmental switch. *Cell* **86**, 115–121.

Chapman, E.J. and Estelle, M. (2009) Mechanism of auxin-regulated gene expression in plants. *Annu. Rev. Genet.* **43**, 265–285.

Chaves, I., Pokorny, R., Byrdin, M., Hoang, N., Ritz, T., Brettel, K., Essen, L.O., van der Horst, G.T.J., Batschauer, A. and Ahmad, M. (2011) The cryptochromes: blue light photoreceptors in plants and animals. *Annu Rev Plant Biol* **62**, 335–364.

Chen, H., Huang, X., Gusmaroli, G., Terzaghi, W., Lau, O.S., Yanagawa, Y., Zhang, Y., Li, J., Lee, J.H., Zhu, D. and Deng, X.W. (2010) *Arabidopsis* CULLIN4-damaged DNA binding protein 1 interacts with CONSTITUTIVELY PHOTOMORPHOGENIC1-SUPPRESSOR OF PHYA complexes to regulate photomorphogenesis and flowering time. *Plant Cell* **22**, 108–123.

Chory, J., Nagpal, P. and Peto, C.A. (1991) Phenotypic and genetic analysis of *det2*, a new mutant that affects light-regulated seedling development in *Arabidopsis*. *Plant Cell* **3**, 445–459.

Christie, J.M. (2007) Phototropin blue-light receptors. *Annu Rev Plant Biol* **58**, 21–45.

Chung, Y., Maharjan, P.M., Lee, O., Fujioka, S., Jang, S., Kim, B., Takatsuto, S., Tsujimoto, M., Kim, H., Cho, S., Park, T., Cho, H., Hwang, I. and Choe, S. (2011) Auxin stimulates *DWARF4* expression and brassinosteroid biosynthesis in arabidopsis. *Plant J.* **66**, 564–578.

Clack, T., Mathews, S. and Sharrock, R.A. (1994) The phytochrome apoprotein family in *Arabidopsis* is encoded by five genes: the sequences and expression of *PHYD* and *PHYE*. *Plant Mol. Biol.* **25**, 413–427.

Clough, S.J. and Bent, A.F. (1998) Floral dip: a simplified method for *Agrobacterium*-mediated transformation of *Arabidopsis thaliana*. *Plant J.* **16**, 735–743.

Cluis, C.P., Mouchel, C.F. and Hardtke, C.S. (2004) The *Arabidopsis* transcription factor HY5 integrates light and hormone signaling pathways. *Plant J.* **38**, 332–347.

Colón-Carmona, A., Chen, D.L., Yeh, K.C. and Abel, S. (2000) Aux/IAA proteins are phosphorylated by phytochrome in vitro. *Plant Physiol.* **124**, 1728–1738.

Corbesier, L., Vincent, C., Jang, S., Fornara, F., Fan, Q., Searle, I., Giakountis, A., Farrona, S., Gissot, L., Turnbull, C. and Coupland, G. (2007) FT protein movement contributes to long-distance signaling in floral induction of *Arabidopsis*. *Science* **316**, 1030–1033.

Cruz-Ramírez, A., Díaz-Triviño, S., Blilou, I., Grieneisen, V.A., Sozzani, R., Zamioudis, C., Miskolczi, P., Nieuwland, J., Benjamins, R., Dhonukshe, P., Caballero-Pérez, J., Horvath, B., Long, Y., Mähönen, A.P., Zhang, H., Xu, J., Murray, J.A.H., Benfey, P.N., Bako, L., Marée, A.F.M. and Scheres, B. (2012) A bistable circuit involving SCARECROW-RETINOBLASTOMA integrates cues to inform asymmetric stem cell division. *Cell* **150**, 1002–1015.

Czechowski, T., Stitt, M., Altmann, T., Udvardi, M.K. and Scheible, W.R. (2005) Genome-wide identification and testing of superior reference genes for transcript normalization in arabidopsis. *Plant Physiol.* **139**, 5–17.

Datta, S., Johansson, H., Hettiarachchi, C., Irigoyen, M.L., Desai, M., Rubio, V. and Holm, M. (2008) LZF1/SALT TOLERANCE HOMOLOG3, an *Arabidopsis* b-box protein involved in light-dependent development and gene expression, undergoes COP1-mediated ubiquitination. *Plant Cell* **20**, 2324–2338.

De Rybel, B., Audenaert, D., Vert, G., Rozhon, W., Mayerhofer, J., Peelman, F., Coutuer, S., Denayer, T., Jansen, L., Nguyen, L., Vanhoutte, I., Beemster, G.T.S., Vleminckx, K., Jonak, C., Chory, J., Inzé, D., Russinova, E. and Beeckman, T. (2009) Chemical inhibition of a subset of *Arabidopsis thaliana* GSK3-like kinases activates brassinosteroid signaling. *Chem. Biol.* **16**, 594–604.

Dehesh, K., Franci, C., Parks, B.M., Seeley, K.A., Short, T.W., Tepperman, J.M. and Quail, P.H. (1993) Arabidopsis *HY8* locus encodes phytochrome a. *Plant Cell* **5**, 1081–1088.

Delarue, M., Prinsen, E., Onckelen, H.V., Caboche, M. and Bellini, C. (1998) *Sur2* mutations of *Arabidopsis thaliana* define a new locus involved in the control of auxin homeostasis. *Plant J.* **14**, 603–611.

Demarsy, E. and Fankhauser, C. (2009) Higher plants use LOV to perceive blue light. *Curr. Opin. Plant Biol.* **12**, 69–74.

Deng, X.W., Caspar, T. and Quail, P.H. (1991) *cop1*: a regulatory locus involved in light-controlled development and gene expression in *Arabidopsis*. *Genes Dev.* **5**, 1172–1182.

Deng, X.W. and Quail, P.H. (1992) Genetic and phenotypic characterization of *cop1* mutants of *Arabidopsis thaliana*. *Plant J.* **2**, 83–95.

Deshaies, R.J. and Joazeiro, C.A.P. (2009) RING domain e3 ubiquitin ligases. *Annu. Rev. Biochem.* **78**, 399–434.

Devlin, P.F., Yanovsky, M.J. and Kay, S.A. (2003) A genomic analysis of the shade avoidance response in arabidopsis. *Plant Physiol* **133**, 1617–1629.

Deyholos, M.K., Cordner, G., Beebe, D. and Sieburth, L.E. (2000) The *SCARFACE* gene is required for cotyledon and leaf vein patterning. *Development* **127**, 3205–3213.

Dharmasiri, N., Dharmasiri, S. and Estelle, M. (2005a) The f-box protein TIR1 is an auxin receptor. *Nature* **435**, 441–445.

Dharmasiri, N., Dharmasiri, S., Weijers, D., Lechner, E., Yamada, M., Hobbie, L., Ehrismann, J.S., Jürgens, G. and Estelle, M. (2005b) Plant development is regulated by a family of auxin receptor f box proteins. *Dev. Cell* **9**, 109–119.

Dong, J., MacAlister, C.A. and Bergmann, D.C. (2009) BASL controls asymmetric cell division in *Arabidopsis*. *Cell* **137**, 1320–1330.

Fackendahl, P.C. (2011) *Functional analysis of Arabidopsis SPA proteins in plant growth control.* Ph.D. thesis, Universität zu Köln.

Falke, C. (2009) *Biochemical and molecular analysis of the light signal transduction in Arabidopsis thaliana.* Master's thesis, Universität zu Köln.

Favory, J.J., Stec, A., Gruber, H., Rizzini, L., Oravecz, A., Funk, M., Albert, A., Cloix, C., Jenkins, G.I., Oakeley, E.J., Seidlitz, H.K., Nagy, F. and Ulm, R. (2009) Interaction of COP1 and UVR8 regulates UV-B-induced photomorphogenesis and stress acclimation in *Arabidopsis*. *EMBO J.* **28**, 591–601.

Feraru, E. and Friml, J. (2008) PIN polar targeting. *Plant Physiol.* **147**, 1553–1559.

Fittinghoff, K., Laubinger, S., Nixdorf, M., Fackendahl, P., Baumgardt, R.L., Batschauer, A. and Hoecker, U. (2006) Functional and expression analysis of arabidopsis *SPA* genes during seedling photomorphogenesis and adult growth. *Plant J.* **47**, 577–590.

Folta, K.M. and Spalding, E.P. (2001) Unexpected roles for cryptochrome 2 and phototropin revealed by high-resolution analysis of blue light-mediated hypocotyl growth inhibition. *Plant J.* **26**, 471–478.

Franklin, K.A., Davis, S.J., Stoddart, W.M., Vierstra, R.D. and Whitelam, G.C. (2003a) Mutant analyses define multiple roles for phytochrome c in arabidopsis photomorphogenesis. *Plant Cell* **15**, 1981–1989.

Franklin, K.A., Praekelt, U., Stoddart, W.M., Billingham, O.E., Halliday, K.J. and Whitelam, G.C. (2003b) Phytochromes b, d, and e act redundantly to control multiple physiological responses in arabidopsis. *Plant Physiol.* **131**, 1340–1346.

Franklin, K.A. and Quail, P.H. (2010) Phytochrome functions in *Arabidopsis* development. *J. Exp. Bot.* **61**, 11–24.

Franks, P.J. and Farquhar, G.D. (2001) The effect of exogenous abscisic acid on stomatal development, stomatal mechanics, and leaf gas exchange in *Tradescantia virginiana*. *Plant Physiol.* **125**, 935–942.

Friml, J. (2010) Subcellular trafficking of PIN auxin efflux carriers in auxin transport. *Eur. J. Cell Biol.* **89**, 231–235.

Friml, J., Vieten, A., Sauer, M., Weijers, D., Schwarz, H., Hamann, T., Offringa, R. and Jürgens, G. (2003) Efflux-dependent auxin gradients establish the apical-basal axis of arabidopsis. *Nature* **426**, 147–153.

Friml, J., Wiśniewska, J., Benková, E., Mendgen, K. and Palme, K. (2002) Lateral relocation of auxin efflux regulator PIN3 mediates tropism in *Arabidopsis*. *Nature* **415**, 806–809.

Geisler, M., Nadeau, J. and Sack, F.D. (2000) Oriented asymmetric divisions that generate the stomatal spacing pattern in arabidopsis are disrupted by the *too many mouths* mutation. *Plant Cell* **12**, 2075–2086.

Genoud, T., Schweizer, F., Tscheuschler, A., Debrieux, D., Casal, J.J., Schäfer, E., Hiltbrunner, A. and Fankhauser, C. (2008) FHY1 mediates nuclear import of the light-activated phytochrome a photoreceptor. *PLoS Genet.* **4**, e1000143.

Gray, J.E., Holroyd, G.H., van der Lee, F.M., Bahrami, A.R., Sijmons, P.C., Woodward, F.I., Schuch, W. and Hetherington, A.M. (2000) The *HIC* signalling pathway links CO_2 perception to stomatal development. *Nature* **408**, 713–716.

Gray, W.M., Kepinski, S., Rouse, D., Leyser, O. and Estelle, M. (2001) Auxin regulates SCF^{TIR1}-dependent degradation of AUX/IAA proteins. *Nature* **414**, 271–276.

Gu, N.N., Zhang, Y.C. and Yang, H.Q. (2012) Substitution of a conserved glycine in the PHR domain of *Arabidopsis* cryptochrome 1 confers a constitutive light response. *Mol Plant* **5**, 85–97.

Gudesblat, G.E., Schneider-Pizoń, J., Betti, C., Mayerhofer, J., Vanhoutte, I., van Dongen, W., Boeren, S., Zhiponova, M., de Vries, S., Jonak, C. and Russinova, E. (2012) SPEECHLESS integrates brassinosteroid and stomata signalling pathways. *Nat. Cell Biol.* **14**, 548–554.

Guo, H., Yang, H., Mockler, T.C. and Lin, C. (1998) Regulation of flowering time by *Arabidopsis* photoreceptors. *Science* **279**, 1360–1363.

Halliday, K.J., Martínez-García, J.F. and Josse, E.M. (2009) Integration of light and auxin signaling. *Cold Spring Harb Perspect Biol* **1**, a001586.

Hamann, T., Benkova, E., Bäurle, I., Kientz, M. and Jürgens, G. (2002) The *Arabidopsis BODENLOS* gene encodes an auxin response protein inhibiting MONOPTEROS-mediated embryo patterning. *Genes Dev.* **16**, 1610–1615.

Hamann, T., Mayer, U. and Jürgens, G. (1999) The auxin-insensitive *bodenlos* mutation affects primary root formation and apical-basal patterning in the *Arabidopsis* embryo. *Development* **126**, 1387–1395.

Hara, K., Kajita, R., Torii, K.U., Bergmann, D.C. and Kakimoto, T. (2007) The secretory peptide gene *EPF1* enforces the stomatal one-cell-spacing rule. *Genes Dev.* **21**, 1720–1725.

Hara, K., Yokoo, T., Kajita, R., Onishi, T., Yahata, S., Peterson, K.M., Torii, K.U. and Kakimoto, T. (2009) Epidermal cell density is autoregulated via a secretory peptide, EPIDERMAL PATTERNING FACTOR 2 in arabidopsis leaves. *Plant Cell Physiol.* **50**, 1019–1031.

Hay, A., Barkoulas, M. and Tsiantis, M. (2006) ASYMMETRIC LEAVES1 and auxin activities converge to repress *BREVIPEDICELLUS* expression and promote leaf development in *Arabidopsis*. *Development* **133**, 3955–3961.

Hayashi, K.I. (2012) The interaction and integration of auxin signaling components. *Plant Cell Physiol.* **53**, 965–975.

Hellens, R.P., Edwards, E.A., Leyland, N.R., Bean, S. and Mullineaux, P.M. (2000) pGreen: a versatile and flexible binary ti vector for *Agrobacterium*-mediated plant transformation. *Plant Mol. Biol.* **42**, 819–832.

Henderson, J., Bauly, J.M., Ashford, D.A., Oliver, S.C., Hawes, C.R., Lazarus, C.M., Venis, M.A. and Napier, R.M. (1997) Retention of maize auxin-binding protein in the endoplasmic reticulum: quantifying escape and the role of auxin. *Planta* **202**, 313–323.

Hennig, L., Stoddart, W.M., Dieterle, M., Whitelam, G.C. and Schäfer, E. (2002) Phytochrome e controls light-induced germination of arabidopsis. *Plant Physiol.* **128**, 194–200.

Hiltbrunner, A., Tscheuschler, A., Viczián, A., Kunkel, T., Kircher, S. and Schäfer, E. (2006) FHY1 and FHL act together to mediate nuclear accumulation of the phytochrome a photoreceptor. *Plant Cell Physiol.* **47**, 1023–1034.

Hoecker, U. (2005) Regulated proteolysis in light signaling. *Curr. Opin. Plant Biol.* **8**, 469–476.

Hoecker, U. and Quail, P.H. (2001) The phytochrome a-specific signaling intermediate SPA1 interacts directly with COP1, a constitutive repressor of light signaling in *Arabidopsis*. *J. Biol. Chem.* **276**, 38173–38178.

Hoecker, U., Tepperman, J.M. and Quail, P.H. (1999) SPA1, a WD-repeat protein specific to phytochrome a signal transduction. *Science* **284**, 496–499.

Hoecker, U., Toledo-Ortiz, G., Bender, J. and Quail, P.H. (2004) The photomorphogenesis-related mutant *red1* is defective in *CYP83B1*, a red light-induced gene encoding a cytochrome p450 required for normal auxin homeostasis. *Planta* **219**, 195–200.

Hoecker, U., Xu, Y. and Quail, P.H. (1998) *SPA1*: a new genetic locus involved in phytochrome a-specific signal transduction. *Plant Cell* **10**, 19–33.

Holm, M., Ma, L.G., Qu, L.J. and Deng, X.W. (2002) Two interacting bZIP proteins are direct targets of COP1-mediated control of light-dependent gene expression in *Arabidopsis*. *Genes Dev.* **16**, 1247–1259.

Hunt, L., Bailey, K.J. and Gray, J.E. (2010) The signalling peptide EPFL9 is a positive regulator of stomatal development. *New Phytol.* **186**, 609–614.

Hunt, L. and Gray, J.E. (2009) The signaling peptide EPF2 controls asymmetric cell divisions during stomatal development. *Curr. Biol.* **19**, 864–869.

Imaizumi, T., Schultz, T.F., Harmon, F.G., Ho, L.A. and Kay, S.A. (2005) FKF1 f-box protein mediates cyclic degradation of a repressor of *CONSTANS* in *Arabidopsis*. *Science* **309**, 293–297.

Imaizumi, T., Tran, H.G., Swartz, T.E., Briggs, W.R. and Kay, S.A. (2003) FKF1 is essential for photoperiodic-specific light signalling in *Arabidopsis*. *Nature* **426**, 302–306.

Ito, S., Song, Y.H. and Imaizumi, T. (2012) LOV domain-containing f-box proteins: light-dependent protein degradation modules in *Arabidopsis*. *Mol Plant* **5**, 573–582.

Jang, I.C., Henriques, R., Seo, H.S., Nagatani, A. and Chua, N.H. (2010) Arabidopsis PHYTOCHROME INTERACTING FACTOR proteins promote phytochrome b polyubiquitination by COP1 e3 ligase in the nucleus. *Plant Cell* **22**, 2370–2383.

Jang, I.C., Yang, J.Y., Seo, H.S. and Chua, N.H. (2005) HFR1 is targeted by COP1 e3 ligase for post-translational proteolysis during phytochrome a signaling. *Genes Dev.* **19**, 593–602.

Jang, S., Marchal, V., Panigrahi, K.C.S., Wenkel, S., Soppe, W., Deng, X.W., Valverde, F. and Coupland, G. (2008) *Arabidopsis* COP1 shapes the temporal pattern of CO accumulation conferring a photoperiodic flowering response. *EMBO J.* **27**, 1277–1288.

Jensen, P.J., Hangarter, R.P. and Estelle, M. (1998) Auxin transport is required for hypocotyl elongation in light-grown but not dark-grown arabidopsis. *Plant Physiol.* **116**, 455–462.

Jewaria, P.K., Hara, T., Tanaka, H., Kondo, T., Betsuyaku, S., Sawa, S., Sakagami, Y., Aimoto, S. and Kakimoto, T. (2013) Differential effects of the peptides stomagen, EPF1 and EPF2 on activation of MAP kinase MPK6 and the SPCH protein level. *Plant Cell Physiol.* **54**, 1253–1262.

Jiao, Y., Lau, O.S. and Deng, X.W. (2007) Light-regulated transcriptional networks in higher plants. *Nat. Rev. Genet.* **8**, 217–230.

Jiao, Y., Ma, L., Strickland, E. and Deng, X.W. (2005) Conservation and divergence of light-regulated genome expression patterns during seedling development in rice and arabidopsis. *Plant Cell* **17**, 3239–3256.

Jiao, Y., Yang, H., Ma, L., Sun, N., Yu, H., Liu, T., Gao, Y., Gu, H., Chen, Z., Wada, M., Gerstein, M., Zhao, H., Qu, L.J. and Deng, X.W. (2003) A genome-wide analysis of blue-light regulation of arabidopsis transcription factor gene expression during seedling development. *Plant Physiol.* **133**, 1480–1493.

Jones, A.M. and Herman, E.M. (1993) KDEL-Containing auxin-binding protein is secreted to the plasma membrane and cell wall. *Plant Physiol.* **101**, 595–606.

Jones, A.M. and Venis, M.A. (1989) Photoaffinity labeling of indole-3-acetic acid-binding proteins in maize. *Proc. Natl. Acad. Sci. U.S.A.* **86**, 6153–6156.

Kanaoka, M.M., Pillitteri, L.J., Fujii, H., Yoshida, Y., Bogenschutz, N.L., Takabayashi, J., Zhu, J.K. and Torii, K.U. (2008) *SCREAM/ICE1* and *SCREAM2* specify three cell-state transitional steps leading to *Arabidopsis* stomatal differentiation. *Plant Cell* **20**, 1775–1785.

Kang, C.Y., Lian, H.L., Wang, F.F., Huang, J.R. and Yang, H.Q. (2009) Cryptochromes, phytochromes, and COP1 regulate light-controlled stomatal development in *Arabidopsis*. *Plant Cell* **21**, 2624–2641.

Keller, M.M., Jaillais, Y., Pedmale, U.V., Moreno, J.E., Chory, J. and Ballaré, C.L. (2011) Cryptochrome 1 and phytochrome b control shade-avoidance responses in arabidopsis via partially independent hormonal cascades. *Plant J.* **67**, 195–207.

Kepinski, S. and Leyser, O. (2005) The *Arabidopsis* f-box protein TIR1 is an auxin receptor. *Nature* **435**, 446–451.

Khan, M., Rozhon, W., Bigeard, J., Pflieger, D., Husar, S., Pitzschke, A., Teige, M., Jonak, C., Hirt, H. and Poppenberger, B. (2013) Brassinosteroid-regulated GSK3/Shaggy-like kinases phosphorylate mitogen-activated protein (MAP) kinase kinases, which control stomata development in *Arabidopsis thaliana*. *J. Biol. Chem.* **288**, 7519–7527.

Kieber, J.J., Rothenberg, M., Roman, G., Feldmann, K.A. and Ecker, J.R. (1993) *CTR1*, a negative regulator of the ethylene response pathway in arabidopsis, encodes a member of the raf family of protein kinases. *Cell* **72**, 427–441.

Kim, T.W., Michniewicz, M., Bergmann, D.C. and Wang, Z.Y. (2012) Brassinosteroid regulates stomatal development by GSK3-mediated inhibition of a MAPK pathway. *Nature* **482**, 419–422.

Kim, W.Y., Fujiwara, S., Suh, S.S., Kim, J., Kim, Y., Han, L., David, K., Putterill, J., Nam, H.G. and Somers, D.E. (2007) ZEITLUPE is a circadian photoreceptor stabilized by GIGANTEA in blue light. *Nature* **449**, 356–360.

Kinoshita, T., Doi, M., Suetsugu, N., Kagawa, T., Wada, M. and Shimazaki, K. (2001) Phot1 and phot2 mediate blue light regulation of stomatal opening. *Nature* **414**, 656–660.

Kircher, S., Gil, P., Kozma-Bognár, L., Fejes, E., Speth, V., Husselstein-Muller, T., Bauer, D., Adám, E., Schäfer, E. and Nagy, F. (2002) Nucleocytoplasmic partitioning of the plant photoreceptors phytochrome a, b, c, d, and e is regulated differentially by light and exhibits a diurnal rhythm. *Plant Cell* **14**, 1541–1555.

Kircher, S., Kozma-Bognar, L., Kim, L., Adam, E., Harter, K., Schäfer, E. and Nagy, F. (1999) Light quality-dependent nuclear import of the plant photoreceptors phytochrome a and b. *Plant Cell* **11**, 1445–1456.

Koncz, C. and Schell, J. (1986) The promoter of T_L-DNA gene 5 controls the tissue-specific expression of chimaeric genes carried by a novel type of *Agrobacterium* binary vector. *Molec. Gen. Genet.* **204**, 383–396.

Kovtun, Y., Chiu, W.L., Zeng, W. and Sheen, J. (1998) Suppression of auxin signal transduction by a MAPK cascade in higher plants. *Nature* **395**, 716–720.

Kwok, S.F., Piekos, B., Misera, S. and Deng, X.W. (1996) A complement of ten essential and pleiotropic arabidopsis *COP/DET/FUS* genes is necessary for repression of photomorphogenesis in darkness. *Plant Physiol.* **110**, 731–742.

Laemmli, U.K. (1970) Cleavage of structural proteins during the assembly of the head of bacteriophage t4. *Nature* **227**, 680–685.

Lai, L.B., Nadeau, J.A., Lucas, J., Lee, E.K., Nakagawa, T., Zhao, L., Geisler, M. and Sack, F.D. (2005) The *Arabidopsis* R2R3 MYB proteins FOUR LIPS and MYB88 restrict divisions late in the stomatal cell lineage. *Plant Cell* **17**, 2754–2767.

Lampard, G.R., Lukowitz, W., Ellis, B.E. and Bergmann, D.C. (2009) Novel and expanded roles for MAPK signaling in *Arabidopsis* stomatal cell fate revealed by cell type-specific manipulations. *Plant Cell* **21**, 3506–3517.

Lampard, G.R., MacAlister, C.A. and Bergmann, D.C. (2008) *Arabidopsis* stomatal initiation is controlled by MAPK-mediated regulation of the bHLH SPEECHLESS. *Science* **322**, 1113–1116.

Lau, O.S. and Bergmann, D.C. (2012) Stomatal development: a plant's perspective on cell polarity, cell fate transitions and intercellular communication. *Development* **139**, 3683–3692.

Lau, O.S. and Deng, X.W. (2012) The photomorphogenic repressors COP1 and DET1: 20 years later. *Trends Plant Sci.* **17**, 584–593.

Laubinger, S., Fittinghoff, K. and Hoecker, U. (2004) The SPA quartet: a family of WD-repeat proteins with a central role in suppression of photomorphogenesis in arabidopsis. *Plant Cell* **16**, 2293–2306.

Laubinger, S. and Hoecker, U. (2003) The SPA1-like proteins SPA3 and SPA4 repress photomorphogenesis in the light. *Plant J.* **35**, 373–385.

Laubinger, S., Marchal, V., Le Gourrierec, J., Gentilhomme, J., Wenkel, S., Adrian, J., Jang, S., Kulajta, C., Braun, H., Coupland, G. and Hoecker, U. (2006) *Arabidopsis* SPA proteins regulate photoperiodic flowering and interact with the floral inducer CONSTANS to regulate its stability. *Development* **133**, 3213–3222.

Laxmi, A., Pan, J., Morsy, M. and Chen, R. (2008) Light plays an essential role in intracellular distribution of auxin efflux carrier PIN2 in *Arabidopsis thaliana*. *PLoS ONE* **3**, e1510.

Lee, J., He, K., Stolc, V., Lee, H., Figueroa, P., Gao, Y., Tongprasit, W., Zhao, H., Lee, I. and Deng, X.W. (2007) Analysis of transcription factor HY5 genomic binding sites revealed its hierarchical role in light regulation of development. *Plant Cell* **19**, 731–749.

Lee, J.S., Kuroha, T., Hnilova, M., Khatayevich, D., Kanaoka, M.M., McAbee, J.M., Sarikaya, M., Tamerler, C. and Torii, K.U. (2012) Direct interaction of ligand-receptor pairs specifying stomatal patterning. *Genes Dev.* **26**, 126–136.

Leivar, P. and Quail, P.H. (2011) PIFs: pivotal components in a cellular signaling hub. *Trends Plant Sci.* **16**, 19–28.

Leyser, H.M., Pickett, F.B., Dharmasiri, S. and Estelle, M. (1996) Mutations in the *AXR3* gene of *Arabidopsis* result in altered auxin response including ectopic expression from the *SAUR-AC1* promoter. *Plant J.* **10**, 403–413.

Li, J., Li, G., Gao, S., Martinez, C., He, G., Zhou, Z., Huang, X., Lee, J.H., Zhang, H., Shen, Y., Wang, H. and Deng, X.W. (2010) *Arabidopsis* transcription factor ELONGATED HYPOCOTYL5 plays a role in the feedback regulation of phytochrome a signaling. *Plant Cell* **22**, 3634–3649.

Li, J., Li, G., Wang, H. and Wang Deng, X. (2011) Phytochrome signaling mechanisms. *The Arabidopsis Book* **9**, e0148.

Li, J., Nagpal, P., Vitart, V., McMorris, T.C. and Chory, J. (1996) A role for brassinosteroids in light-dependent development of *Arabidopsis*. *Science* **272**, 398–401.

Lian, H.L., He, S.B., Zhang, Y.C., Zhu, D.M., Zhang, J.Y., Jia, K.P., Sun, S.X., Li, L. and Yang, H.Q. (2011) Blue-light-dependent interaction of cryptochrome 1 with SPA1 defines a dynamic signaling mechanism. *Genes Dev.* **25**, 1023–1028.

Lin, C., Yang, H., Guo, H., Mockler, T., Chen, J. and Cashmore, A.R. (1998) Enhancement of blue-light sensitivity of arabidopsis seedlings by a blue light receptor cryptochrome 2. *Proc. Natl. Acad. Sci. U.S.A.* **95**, 2686–2690.

Liscum, E. and Briggs, W.R. (1995) Mutations in the *NPH1* locus of arabidopsis disrupt the perception of phototropic stimuli. *Plant Cell* **7**, 473–485.

Liscum, E. and Reed, J.W. (2002) Genetics of Aux/IAA and ARF action in plant growth and development. *Plant Mol. Biol.* **49**, 387–400.

Liu, B., Zuo, Z., Liu, H., Liu, X. and Lin, C. (2011a) *Arabidopsis* cryptochrome 1 interacts with SPA1 to suppress COP1 activity in response to blue light. *Genes Dev.* **25**, 1029–1034.

Liu, H., Yu, X., Li, K., Klejnot, J., Yang, H., Lisiero, D. and Lin, C. (2008a) Photoexcited CRY2 interacts with CIB1 to regulate transcription and floral initiation in *Arabidopsis*. *Science* **322**, 1535–1539.

Liu, L.J., Zhang, Y.C., Li, Q.H., Sang, Y., Mao, J., Lian, H.L., Wang, L. and Yang, H.Q. (2008b) COP1-mediated ubiquitination of CONSTANS is implicated in cryptochrome regulation of flowering in *Arabidopsis*. *Plant Cell* **20**, 292–306.

Liu, X., Cohen, J.D. and Gardner, G. (2011b) Low-fluence red light increases the transport and biosynthesis of auxin. *Plant Physiol.* **157**, 891–904.

Livak, K.J. and Schmittgen, T.D. (2001) Analysis of relative gene expression data using real-time quantitative PCR and the $2^{\Delta\Delta\ C_T}$ method. *Methods* **25**, 402–408.

Ljung, K. (2013) Auxin metabolism and homeostasis during plant development. *Development* **140**, 943–950.

Ljung, K., Bhalerao, R.P. and Sandberg, G. (2001) Sites and homeostatic control of auxin biosynthesis in *Arabidopsis* during vegetative growth. *Plant J.* **28**, 465–474.

Ma, L., Li, J., Qu, L., Hager, J., Chen, Z., Zhao, H. and Deng, X.W. (2001) Light control of arabidopsis development entails coordinated regulation of genome expression and cellular pathways. *Plant Cell* **13**, 2589–2607.

MacAlister, C.A., Ohashi-Ito, K. and Bergmann, D.C. (2007) Transcription factor control of asymmetric cell divisions that establish the stomatal lineage. *Nature* **445**, 537–540.

Maier, A. (2011) *Genetic and biochemical characterization of COP1/SPA function in Arabidopsis photomorphogenesis.* Ph.D. thesis, Universität zu Köln.

Maier, A., Schrader, A., Kokkelink, L., Falke, C., Welter, B., Iniesto, E., Rubio, V., Uhrig, J.F., Hülskamp, M. and Hoecker, U. (2013) Light and the e3 ubiquitin ligase COP1/SPA control the protein stability of the MYB transcription factors PAP1 and PAP2 involved in anthocyanin accumulation in arabidopsis. *Plant J.* **74**, 638–651.

Marine, J.C. (2012) Spotlight on the role of COP1 in tumorigenesis. *Nat. Rev. Cancer* **12**, 455–464.

Más, P., Kim, W.Y., Somers, D.E. and Kay, S.A. (2003) Targeted degradation of TOC1 by ZTL modulates circadian function in *Arabidopsis thaliana*. *Nature* **426**, 567–570.

Mashiguchi, K., Tanaka, K., Sakai, T., Sugawara, S., Kawaide, H., Natsume, M., Hanada, A., Yaeno, T., Shirasu, K., Yao, H., McSteen, P., Zhao, Y., Hayashi, K.i., Kamiya, Y. and Kasahara, H. (2011) The main auxin biosynthesis pathway in *Arabidopsis*. *Proc. Natl. Acad. Sci. U.S.A.* **108**, 18512–18517.

Mattsson, J., Sung, Z.R. and Berleth, T. (1999) Responses of plant vascular systems to auxin transport inhibition. *Development* **126**, 2979–2991.

McNellis, T.W., von Arnim, A.G., Araki, T., Komeda, Y., Miséra, S. and Deng, X.W. (1994) Genetic and molecular analysis of an allelic series of *cop1* mutants suggests functional roles for the multiple protein domains. *Plant Cell* **6**, 487–500.

Mockaitis, K. and Estelle, M. (2008) Auxin receptors and plant development: a new signaling paradigm. *Annu. Rev. Cell Dev. Biol.* **24**, 55–80.

Mockaitis, K. and Howell, S.H. (2000) Auxin induces mitogenic activated protein kinase (MAPK) activation in roots of arabidopsis seedlings. *Plant J.* **24**, 785–796.

Mockler, T., Yang, H., Yu, X., Parikh, D., Cheng, Y., Dolan, S. and Lin, C. (2003) Regulation of photoperiodic flowering by *Arabidopsis* photoreceptors. *Proc. Natl. Acad. Sci. U.S.A.* **100**, 2140–2145.

Mockler, T.C., Guo, H., Yang, H., Duong, H. and Lin, C. (1999) Antagonistic actions of *Arabidopsis* cryptochromes and phytochrome b in the regulation of floral induction. *Development* **126**, 2073–2082.

Nadeau, J.A. and Sack, F.D. (2002a) Control of stomatal distribution on the *Arabidopsis* leaf surface. *Science* **296**, 1697–1700.

Nadeau, J.A. and Sack, F.D. (2002b) Stomatal development in arabidopsis. *The Arabidopsis Book* **1**, e0066.

Nagashima, A., Suzuki, G., Uehara, Y., Saji, K., Furukawa, T., Koshiba, T., Sekimoto, M., Fujioka, S., Kuroha, T., Kojima, M., Sakakibara, H., Fujisawa, N., Okada, K. and Sakai, T. (2008) Phytochromes and cryptochromes regulate the differential growth of arabidopsis hypocotyls in both a PGP19-dependent and a PGP19-independent manner. *Plant J.* **53**, 516–529.

Nagatani, A., Chory, J. and Furuya, M. (1991) Phytochrome b is not detectable in the *hy3* mutant of *Arabidopsis*, which is deficient in responding to end-of-day far-red light treatments. *Plant Cell Physiol* **32**, 1119–1122.

Nagatani, A., Reed, J.W. and Chory, J. (1993) Isolation and initial characterization of *Arabidopsis* mutants that are deficient in phytochrome a. *Plant Physiol.* **102**, 269–277.

Neff, M.M., Fankhauser, C. and Chory, J. (2000) Light: an indicator of time and place. *Genes Dev.* **14**, 257–271.

Neff, M.M., Turk, E. and Kalishman, M. (2002) Web-based primer design for single nucleotide polymorphism analysis. *Trends Genet.* **18**, 613–615.

Nemhauser, J.L., Mockler, T.C. and Chory, J. (2004) Interdependency of brassinosteroid and auxin signaling in *Arabidopsis*. *PLoS Biol.* **2**, E258.

Ohashi-Ito, K. and Bergmann, D.C. (2006) *Arabidopsis* FAMA controls the final proliferation/differentiation switch during stomatal development. *Plant Cell* **18**, 2493–2505.

Ohgishi, M., Saji, K., Okada, K. and Sakai, T. (2004) Functional analysis of each blue light receptor, cry1, cry2, phot1, and phot2, by using combinatorial multiple mutants in *Arabidopsis*. *Proc. Natl. Acad. Sci. U.S.A.* **101**, 2223–2228.

Osterlund, M.T. and Deng, X.W. (1998) Multiple photoreceptors mediate the light-induced reduction of GUS-COP1 from arabidopsis hypocotyl nuclei. *Plant J.* **16**, 201–208.

Osterlund, M.T., Hardtke, C.S., Wei, N. and Deng, X.W. (2000) Targeted destabilization of HY5 during light-regulated development of *Arabidopsis*. *Nature* **405**, 462–466.

Ouellet, F., Overvoorde, P.J. and Theologis, A. (2001) IAA17/AXR3: biochemical insight into an auxin mutant phenotype. *Plant Cell* **13**, 829–841.

Ouyang, J., Shao, X. and Li, J. (2000) Indole-3-glycerol phosphate, a branchpoint of indole-3-acetic acid biosynthesis from the tryptophan biosynthetic pathway in *Arabidopsis thaliana*. *Plant J.* **24**, 327–333.

Overvoorde, P.J., Okushima, Y., Alonso, J.M., Chan, A., Chang, C., Ecker, J.R., Hughes, B., Liu, A., Onodera, C., Quach, H., Smith, A., Yu, G. and Theologis, A. (2005) Functional genomic analysis of the *AUXIN/INDOLE-3-ACETIC ACID* gene family members in *Arabidopsis thaliana*. *Plant Cell* **17**, 3282–3300.

Parry, G., Calderon-Villalobos, L.I., Prigge, M., Peret, B., Dharmasiri, S., Itoh, H., Lechner, E., Gray, W.M., Bennett, M. and Estelle, M. (2009) Complex regulation of the TIR1/AFB family of auxin receptors. *Proc. Natl. Acad. Sci. U.S.A.* **106**, 22540–22545.

Pekker, I., Alvarez, J.P. and Eshed, Y. (2005) Auxin response factors mediate *Arabidopsis* organ asymmetry via modulation of KANADI activity. *Plant Cell* **17**, 2899–2910.

Pérez-Pérez, J.M., Candela, H., Robles, P., López-Torrejón, G., del Pozo, J.C. and Micol, J.L. (2010) A role for *AUXIN RESISTANT3* in the coordination of leaf growth. *Plant Cell Physiol.* **51**, 1661–1673.

Perrot-Rechenmann, C. (2010) Cellular responses to auxin: division versus expansion. *Cold Spring Harb. Perspect. Biol.* **2**, a001446.

Peterson, K.M., Rychel, A.L. and Torii, K.U. (2010) Out of the mouths of plants: the molecular basis of the evolution and diversity of stomatal development. *Plant Cell* **22**, 296–306.

Petrásek, J. and Friml, J. (2009) Auxin transport routes in plant development. *Development* **136**, 2675–2688.

Pierik, R., Djakovic-Petrovic, T., Keuskamp, D.H., de Wit, M. and Voesenek, L.A.C.J. (2009) Auxin and ethylene regulate elongation responses to neighbor proximity signals independent of gibberellin and della proteins in arabidopsis. *Plant Physiol.* **149**, 1701–1712.

Pillitteri, L.J., Peterson, K.M., Horst, R.J. and Torii, K.U. (2011) Molecular profiling of stomatal meristemoids reveals new component of asymmetric cell division and commonalities among stem cell populations in *Arabidopsis*. *Plant Cell* **23**, 3260–3275.

Pillitteri, L.J., Sloan, D.B., Bogenschutz, N.L. and Torii, K.U. (2007) Termination of asymmetric cell division and differentiation of stomata. *Nature* **445**, 501–505.

Pillitteri, L.J. and Torii, K.U. (2012) Mechanisms of stomatal development. *Annu. Rev. Plant Biol.* **63**, 591–614.

Popescu, S.C., Popescu, G.V., Bachan, S., Zhang, Z., Gerstein, M., Snyder, M. and Dinesh-Kumar, S.P. (2009) MAPK target networks in *Arabidopsis thaliana* revealed using functional protein microarrays. *Genes Dev.* **23**, 80–92.

Ranjan, A. (2010) *The role of COP1/SPA in light signaling: Growth control, cell-cell communication and functional conservation in plants*. Ph.D. thesis, Universität zu Köln.

Ranjan, A., Fiene, G., Fackendahl, P. and Hoecker, U. (2011) The *Arabidopsis* repressor of light signaling SPA1 acts in the phloem to regulate seedling de-etiolation, leaf expansion and flowering time. *Development* **138**, 1851–1862.

Rausenberger, J., Tscheuschler, A., Nordmeier, W., Wüst, F., Timmer, J., Schäfer, E., Fleck, C. and Hiltbrunner, A. (2011) Photoconversion and nuclear trafficking cycles determine phytochrome a's response profile to far-red light. *Cell* **146**, 813–825.

Raven, J.A. (1975) Transport of indoleacetic acid in plant cells in relation to ph and electrical potential gradients, and its significance for polar IAA transport. *New Phytol.* **74**, 163âĂŞ172.

Reed, J.W. (2001) Roles and activities of Aux/IAA proteins in *Arabidopsis*. *Trends Plant Sci.* **6**, 420–425.

Reed, J.W., Elumalai, R.P. and Chory, J. (1998) Suppressors of an *Arabidopsis thaliana phyB* mutation identify genes that control light signaling and hypocotyl elongation. *Genetics* **148**, 1295–1310.

Reed, J.W., Nagpal, P., Poole, D.S., Furuya, M. and Chory, J. (1993) Mutations in the gene for the red/far-red light receptor phytochrome b alter cell elongation and physiological responses throughout arabidopsis development. *Plant Cell* **5**, 147–157.

Reinhardt, D., Pesce, E.R., Stieger, P., Mandel, T., Baltensperger, K., Bennett, M., Traas, J., Friml, J. and Kuhlemeier, C. (2003) Regulation of phyllotaxis by polar auxin transport. *Nature* **426**, 255–260.

Ren, D., Yang, H. and Zhang, S. (2002) Cell death mediated by MAPK is associated with hydrogen peroxide production in *Arabidopsis*. *J. Biol. Chem.* **277**, 559–565.

Rizzini, L., Favory, J.J., Cloix, C., Faggionato, D., O'Hara, A., Kaiserli, E., Baumeister, R., Schäfer, E., Nagy, F., Jenkins, G.I. and Ulm, R. (2011) Perception of UV-B by the *Arabidopsis* UVR8 protein. *Science* **332**, 103–106.

Robert, S., Kleine-Vehn, J., Barbez, E., Sauer, M., Paciorek, T., Baster, P., Vanneste, S., Zhang, J., Simon, S., Čovanová, M., Hayashi, K., Dhonukshe, P., Yang, Z., Bednarek, S.Y., Jones, A.M., Luschnig, C., Aniento, F., Zažímalová, E. and Friml, J. (2010) ABP1 mediates auxin inhibition of clathrin-dependent endocytosis in *Arabidopsis*. *Cell* **143**, 111–121.

Rockwell, N.C., Su, Y.S. and Lagarias, J.C. (2006) Phytochrome structure and signaling mechanisms. *Annu Rev Plant Biol* **57**, 837–858.

Rolauffs, S., Fackendahl, P., Sahm, J., Fiene, G. and Hoecker, U. (2012) Arabidopsis *COP1* and *SPA* genes are essential for plant elongation but not for acceleration of flowering time in response to a low red light to far-red light ratio. *Plant Physiol.* **160**, 2015–2027.

Rubery, P.H. and Sheldrake, A.R. (1974) Carrier-mediated auxin transport. *Planta* **118**, 101–121.

Ruckle, M.E., DeMarco, S.M. and Larkin, R.M. (2007) Plastid signals remodel light signaling networks and are essential for efficient chloroplast biogenesis in *Arabidopsis*. *Plant Cell* **19**, 3944–3960.

Ruegger, M., Dewey, E., Gray, W.M., Hobbie, L., Turner, J. and Estelle, M. (1998) The TIR1 protein of *Arabidopsis* functions in auxin response and is related to human SKP2 and yeast grr1p. *Genes Dev* **12**, 198–207.

Rychel, A.L., Peterson, K.M. and Torii, K.U. (2010) Plant twitter: ligands under 140 amino acids enforcing stomatal patterning. *J. Plant Res.* **123**, 275–280.

Sachs, T. (1991) Cell polarity and tissue patterning in plants. *Development* **113**, 83–93.

Saibo, N.J.M., Vriezen, W.H., Beemster, G.T.S. and Van Der Straeten, D. (2003) Growth and stomata development of *Arabidopsis* hypocotyls are controlled by gibberellins and modulated by ethylene and auxins. *Plant J.* **33**, 989–1000.

Saijo, Y., Sullivan, J.A., Wang, H., Yang, J., Shen, Y., Rubio, V., Ma, L., Hoecker, U. and Deng, X.W. (2003) The COP1-SPA1 interaction defines a critical step in phytochrome a-mediated regulation of HY5 activity. *Genes Dev.* **17**, 2642–2647.

Sakai, T., Kagawa, T., Kasahara, M., Swartz, T.E., Christie, J.M., Briggs, W.R., Wada, M. and Okada, K. (2001) *Arabidopsis* nph1 and npl1: blue light receptors that mediate both phototropism and chloroplast relocation. *Proc. Natl. Acad. Sci. U.S.A.* **98**, 6969–6974.

Sakamoto, K. and Briggs, W.R. (2002) Cellular and subcellular localization of phototropin 1. *Plant Cell* **14**, 1723–1735.

Sakamoto, K. and Nagatani, A. (1996) Nuclear localization activity of phytochrome b. *Plant J.* **10**, 859–868.

Sambrook, J., Fritsch, E.F. and Maniatis, T. (2001) *Molecular cloning: a laboratory manual.* Cold Spring Harbor Laboratory Press, Cold Spring Harbor, NY.

Sassi, M., Lu, Y., Zhang, Y., Wang, J., Dhonukshe, P., Blilou, I., Dai, M., Li, J., Gong, X., Jaillais, Y., Yu, X., Traas, J., Ruberti, I., Wang, H., Scheres, B., Vernoux, T. and Xu, J. (2012) COP1 mediates the coordination of root and shoot growth by light through modulation of PIN1- and PIN2-dependent auxin transport in *Arabidopsis*. *Development* **139**, 3402–3412.

Sauer, M. and Kleine-Vehn, J. (2011) AUXIN BINDING PROTEIN1: the outsider. *Plant Cell* **23**, 2033–2043.

Sawa, M., Nusinow, D.A., Kay, S.A. and Imaizumi, T. (2007) FKF1 and GIGANTEA complex formation is required for day-length measurement in *Arabidopsis*. *Science* **318**, 261–265.

Schwechheimer, C., Serino, G., Callis, J., Crosby, W.L., Lyapina, S., Deshaies, R.J., Gray, W.M., Estelle, M. and Deng, X.W. (2001) Interactions of the COP9 signalosome with the e3 ubiquitin ligase SCF^{TIR1} in mediating auxin response. *Science* **292**, 1379–1382.

Seo, H.S., Watanabe, E., Tokutomi, S., Nagatani, A. and Chua, N.H. (2004) Photoreceptor ubiquitination by COP1 e3 ligase desensitizes phytochrome a signaling. *Genes Dev.* **18**, 617–622.

Seo, H.S., Yang, J.Y., Ishikawa, M., Bolle, C., Ballesteros, M.L. and Chua, N.H. (2003) LAF1 ubiquitination by COP1 controls photomorphogenesis and is stimulated by SPA1. *Nature* **423**, 995–999.

Serna, L. (2009) Cell fate transitions during stomatal development. *Bioessays* **31**, 865–873.

Serna, L. and Fenoll, C. (1996) Ethylene induces stomata differentiation in arabidopsis. *Int. J. Dev. Biol.* **Suppl 1**, 123S–124S.

Sessions, A., Weigel, D. and Yanofsky, M.F. (1999) The *Arabidopsis thaliana MERISTEM LAYER 1* promoter specifies epidermal expression in meristems and young primordia. *Plant J.* **20**, 259–263.

Shalitin, D., Yang, H., Mockler, T.C., Maymon, M., Guo, H., Whitelam, G.C. and Lin, C. (2002) Regulation of *Arabidopsis* cryptochrome 2 by blue-light-dependent phosphorylation. *Nature* **417**, 763–767.

Sharrock, R.A. and Quail, P.H. (1989) Novel phytochrome sequences in *Arabidopsis thaliana*: structure, evolution, and differential expression of a plant regulatory photoreceptor family. *Genes Dev.* **3**, 1745–1757.

Shen, H., Moon, J. and Huq, E. (2005) PIF1 is regulated by light-mediated degradation through the ubiquitin-26S proteasome pathway to optimize photomorphogenesis of seedlings in arabidopsis. *Plant J.* **44**, 1023–1035.

Shen, H., Zhu, L., Castillon, A., Majee, M., Downie, B. and Huq, E. (2008) Light-induced phosphorylation and degradation of the negative regulator PHYTOCHROME-INTERACTING FACTOR1 from *Arabidopsis* depend upon its direct physical interactions with photoactivated phytochromes. *Plant Cell* **20**, 1586–1602.

Shen, Y., Khanna, R., Carle, C.M. and Quail, P.H. (2007) Phytochrome induces rapid PIF5 phosphorylation and degradation in response to red-light activation. *Plant Physiol.* **145**, 1043–1051.

Shinomura, T., Nagatani, A., Chory, J. and Furuya, M. (1994) The induction of seed germination in *Arabidopsis thaliana* is regulated principally by phytochrome b and secondarily by phytochrome a. *Plant Physiol.* **104**, 363–371.

Shpak, E.D., Berthiaume, C.T., Hill, E.J. and Torii, K.U. (2004) Synergistic interaction of three ERECTA-family receptor-like kinases controls *Arabidopsis* organ growth and flower development by promoting cell proliferation. *Development* **131**, 1491–1501.

Shpak, E.D., McAbee, J.M., Pillitteri, L.J. and Torii, K.U. (2005) Stomatal patterning and differentiation by synergistic interactions of receptor kinases. *Science* **309**, 290–293.

Sibout, R., Sukumar, P., Hettiarachchi, C., Holm, M., Muday, G.K. and Hardtke, C.S. (2006) Opposite root growth phenotypes of *hy5* versus *hy5 hyh* mutants correlate with increased constitutive auxin signaling. *PLoS Genet.* **2**, e202.

Sieburth, L.E. (1999) Auxin is required for leaf vein pattern in arabidopsis. *Plant Physiol.* **121**, 1179–1190.

Simillion, C., Vandepoele, K., Van Montagu, M.C.E., Zabeau, M. and Van de Peer, Y. (2002) The hidden duplication past of *Arabidopsis thaliana*. *Proc. Natl. Acad. Sci. U.S.A.* **99**, 13627–13632.

Somers, D.E., Sharrock, R.A., Tepperman, J.M. and Quail, P.H. (1991) The *hy3* long hypocotyl mutant of arabidopsis is deficient in phytochrome b. *Plant Cell* **3**, 1263–1274.

Stacey, M.G., Hicks, S.N. and von Arnim, A.G. (1999) Discrete domains mediate the light-responsive nuclear and cytoplasmic localization of arabidopsis COP1. *Plant Cell* **11**, 349–364.

Stacey, M.G., Kopp, O.R., Kim, T.H. and von Arnim, A.G. (2000) Modular domain structure of arabidopsis COP1. reconstitution of activity by fragment complementation and mutational analysis of a nuclear localization signal in planta. *Plant Physiol.* **124**, 979–990.

Staswick, P.E., Serban, B., Rowe, M., Tiryaki, I., Maldonado, M.T., Maldonado, M.C. and Suza, W. (2005) Characterization of an arabidopsis enzyme family that conjugates amino acids to indole-3-acetic acid. *Plant Cell* **17**, 616–627.

Stepanova, A.N., Robertson-Hoyt, J., Yun, J., Benavente, L.M., Xie, D.Y., Dolezal, K., Schlereth, A., Jürgens, G. and Alonso, J.M. (2008) *TAA1*-mediated auxin biosynthesis is essential for hormone crosstalk and plant development. *Cell* **133**, 177–191.

Stepanova, A.N., Yun, J., Robles, L.M., Novak, O., He, W., Guo, H., Ljung, K. and Alonso, J.M. (2011) The *Arabidopsis* YUCCA1 flavin monooxygenase functions in the indole-3-pyruvic acid branch of auxin biosynthesis. *Plant Cell* **23**, 3961–3973.

Stratmann, J.W. and Gusmaroli, G. (2012) Many jobs for one good cop - the COP9 signalosome guards development and defense. *Plant Sci.* **185-186**, 50–64.

Subramanian, C., Kim, B.H., Lyssenko, N.N., Xu, X., Johnson, C.H. and von Arnim, A.G. (2004) The *Arabidopsis* repressor of light signaling, COP1, is regulated by nuclear exclusion: mutational analysis by bioluminescence resonance energy transfer. *Proc. Natl. Acad. Sci. U.S.A.* **101**, 6798–6802.

Subramanian, C., Woo, J., Cai, X., Xu, X., Servick, S., Johnson, C.H., Nebenführ, A. and von Arnim, A.G. (2006) A suite of tools and application notes for *in vivo* protein interaction assays using bioluminescence resonance energy transfer (BRET). *Plant J.* **48**, 138–152.

Sugano, S.S., Shimada, T., Imai, Y., Okawa, K., Tamai, A., Mori, M. and Hara-Nishimura, I. (2010) Stomagen positively regulates stomatal density in *Arabidopsis*. *Nature* **463**, 241–244.

Susek, R.E., Ausubel, F.M. and Chory, J. (1993) Signal transduction mutants of arabidopsis uncouple nuclear *CAB* and *RBCS* gene expression from chloroplast development. *Cell* **74**, 787–799.

Swarup, R., Friml, J., Marchant, A., Ljung, K., Sandberg, G., Palme, K. and Bennett, M. (2001) Localization of the auxin permease AUX1 suggests two functionally distinct hormone transport pathways operate in the *Arabidopsis* root apex. *Genes Dev.* **15**, 2648–2653.

Szemenyei, H., Hannon, M. and Long, J.A. (2008) TOPLESS mediates auxin-dependent transcriptional repression during *Arabidopsis* embryogenesis. *Science* **319**, 1384–1386.

Tan, X., Calderon-Villalobos, L.I.A., Sharon, M., Zheng, C., Robinson, C.V., Estelle, M. and Zheng, N. (2007) Mechanism of auxin perception by the TIR1 ubiquitin ligase. *Nature* **446**, 640–645.

Tanaka, H., Dhonukshe, P., Brewer, P.B. and Friml, J. (2006) Spatiotemporal asymmetric auxin distribution: a means to coordinate plant development. *Cell. Mol. Life Sci.* **63**, 2738–2754.

Tanaka, Y., Nose, T., Jikumaru, Y. and Kamiya, Y. (2013) ABA inhibits entry into stomatal-lineage development in arabidopsis leaves. *Plant J.* **74**, 448–457.

Tao, Y., Ferrer, J.L., Ljung, K., Pojer, F., Hong, F., Long, J.A., Li, L., Moreno, J.E., Bowman, M.E., Ivans, L.J., Cheng, Y., Lim, J., Zhao, Y., Ballaré, C.L., Sandberg, G., Noel, J.P. and Chory, J. (2008) Rapid synthesis of auxin via a new tryptophan-dependent pathway is required for shade avoidance in plants. *Cell* **133**, 164–176.

Teale, W.D., Paponov, I.A. and Palme, K. (2006) Auxin in action: signalling, transport and the control of plant growth and development. *Nat. Rev. Mol. Cell Biol.* **7**, 847–859.

Tepperman, J.M., Hudson, M.E., Khanna, R., Zhu, T., Chang, S.H., Wang, X. and Quail, P.H. (2004) Expression profiling of *phyB* mutant demonstrates substantial contribution of other phytochromes to red-light-regulated gene expression during seedling de-etiolation. *Plant J.* **38**, 725–739.

Tepperman, J.M., Zhu, T., Chang, H.S., Wang, X. and Quail, P.H. (2001) Multiple transcription-factor genes are early targets of phytochrome a signaling. *Proc. Natl. Acad. Sci. U.S.A.* **98**, 9437–9442.

Tian, Q., Nagpal, P. and Reed, J.W. (2003) Regulation of *Arabidopsis* SHY2/IAA3 protein turnover. *Plant J.* **36**, 643–651.

Timpte, C., Wilson, A.K. and Estelle, M. (1994) The *axr2-1* mutation of *Arabidopsis thaliana* is a gain-of-function mutation that disrupts an early step in auxin response. *Genetics* **138**, 1239–1249.

Tiwari, S.B., Hagen, G. and Guilfoyle, T. (2003) The roles of auxin response factor domains in auxin-responsive transcription. *Plant Cell* **15**, 533–543.

Tiwari, S.B., Wang, X.J., Hagen, G. and Guilfoyle, T.J. (2001) AUX/IAA proteins are active repressors, and their stability and activity are modulated by auxin. *Plant Cell* **13**, 2809–2822.

Torii, K.U., McNellis, T.W. and Deng, X.W. (1998) Functional dissection of *Arabidopsis* COP1 reveals specific roles of its three structural modules in light control of seedling development. *EMBO J.* **17**, 5577–5587.

Torii, K.U., Mitsukawa, N., Oosumi, T., Matsuura, Y., Yokoyama, R., Whittier, R.F. and Komeda, Y. (1996) The arabidopsis *ERECTA* gene encodes a putative receptor protein kinase with extracellular leucine-rich repeats. *Plant Cell* **8**, 735–746.

Ulmasov, T., Hagen, G. and Guilfoyle, T.J. (1997a) ARF1, a transcription factor that binds to auxin response elements. *Science* **276**, 1865–1868.

Ulmasov, T., Hagen, G. and Guilfoyle, T.J. (1999) Activation and repression of transcription by auxin-response factors. *Proc. Natl. Acad. Sci. U.S.A.* **96**, 5844–5849.

Ulmasov, T., Murfett, J., Hagen, G. and Guilfoyle, T.J. (1997b) Aux/IAA proteins repress expression of reporter genes containing natural and highly active synthetic auxin response elements. *Plant Cell* **9**, 1963–1971.

Umbrasaite, J., Schweighofer, A., Kazanaviciute, V., Magyar, Z., Ayatollahi, Z., Unterwurzacher, V., Choopayak, C., Boniecka, J., Murray, J.A.H., Bogre, L. and Meskiene, I. (2010) MAPK phosphatase AP2C3 induces ectopic proliferation of epidermal cells leading to stomata development in arabidopsis. *PLoS ONE* **5**, e15357.

Valverde, F., Mouradov, A., Soppe, W., Ravenscroft, D., Samach, A. and Coupland, G. (2004) Photoreceptor regulation of CONSTANS protein in photoperiodic flowering. *Science* **303**, 1003–1006.

Vanneste, S. and Friml, J. (2009) Auxin: a trigger for change in plant development. *Cell* **136**, 1005–1016.

von Arnim, A. and Deng, X.W. (1996) Light control of seedling development. *Annu. Rev. Plant Physiol. Plant Mol. Biol.* **47**, 215–243.

von Arnim, A.G. and Deng, X.W. (1994) Light inactivation of arabidopsis photomorphogenic repressor COP1 involves a cell-specific regulation of its nucleocytoplasmic partitioning. *Cell* **79**, 1035–1045.

von Arnim, A.G., Osterlund, M.T., Kwok, S.F. and Deng, X.W. (1997) Genetic and developmental control of nuclear accumulation of COP1, a repressor of photomorphogenesis in arabidopsis. *Plant Physiol.* **114**, 779–788.

Wang, H., Ma, L.G., Li, J.M., Zhao, H.Y. and Deng, X.W. (2001) Direct interaction of *Arabidopsis* cryptochromes with COP1 in light control development. *Science* **294**, 154–158.

Wang, H., Ngwenyama, N., Liu, Y., Walker, J.C. and Zhang, S. (2007) Stomatal development and patterning are regulated by environmentally responsive mitogen-activated protein kinases in *Arabidopsis*. *Plant Cell* **19**, 63–73.

Wang, X., Li, W., Piqueras, R., Cao, K., Deng, X.W. and Wei, N. (2009) Regulation of COP1 nuclear localization by the COP9 signalosome via direct interaction with CSN1. *Plant J.* **58**, 655–667.

Wargent, J.J., Gegas, V.C., Jenkins, G.I., Doonan, J.H. and Paul, N.D. (2009) UVR8 in *Arabidopsis thaliana* regulates multiple aspects of cellular differentiation during leaf development in response to ultraviolet b radiation. *New Phytol.* **183**, 315–326.

Whitelam, G.C., Johnson, E., Peng, J., Carol, P., Anderson, M.L., Cowl, J.S. and Harberd, N.P. (1993) Phytochrome a null mutants of arabidopsis display a wild-type phenotype in white light. *Plant Cell* **5**, 757–768.

Woo, E.J., Marshall, J., Bauly, J., Chen, J.G., Venis, M., Napier, R.M. and Pickersgill, R.W. (2002) Crystal structure of auxin-binding protein 1 in complex with auxin. *EMBO J.* **21**, 2877–2885.

Woodward, A.W. and Bartel, B. (2005) Auxin: regulation, action, and interaction. *Ann. Bot.* **95**, 707–735.

Worley, C.K., Zenser, N., Ramos, J., Rouse, D., Leyser, O., Theologis, A. and Callis, J. (2000) Degradation of Aux/IAA proteins is essential for normal auxin signalling. *Plant J.* **21**, 553–562.

Wu, G. and Spalding, E.P. (2007) Separate functions for nuclear and cytoplasmic cryptochrome 1 during photomorphogenesis of arabidopsis seedlings. *Proc. Natl. Acad. Sci. U.S.A.* **104**, 18813–18818.

Xia, Y., Nikolau, B.J. and Schnable, P.S. (1997) Developmental and hormonal regulation of the arabidopsis *CER2* gene that codes for a nuclear-localized protein required for the normal accumulation of cuticular waxes. *Plant Physiol.* **115**, 925–937.

Yang, H.Q., Tang, R.H. and Cashmore, A.R. (2001) The signaling mechanism of arabidopsis CRY1 involves direct interaction with COP1. *Plant Cell* **13**, 2573–2587.

Yang, J., Lin, R., Sullivan, J., Hoecker, U., Liu, B., Xu, L., Deng, X.W. and Wang, H. (2005) Light regulates COP1-mediated degradation of HFR1, a transcription factor essential for light signaling in arabidopsis. *Plant Cell* **17**, 804–821.

Yang, J. and Wang, H. (2006) The central coiled-coil domain and carboxyl-terminal WD-repeat domain of arabidopsis SPA1 are responsible for mediating repression of light signaling. *Plant J.* **47**, 564–576.

Yang, M. and Sack, F.D. (1995) The *too many mouths* and *four lips* mutations affect stomatal production in arabidopsis. *Plant Cell* **7**, 2227–2239.

Yi, C. and Deng, X.W. (2005) COP1 – from plant photomorphogenesis to mammalian tumorigenesis. *Trends Cell Biol.* **15**, 618–625.

Yi, C., Wang, H., Wei, N. and Deng, X.W. (2002) An initial biochemical and cell biological characterization of the mammalian homologue of a central plant developmental switch, COP1. *BMC Cell Biol.* **3**, 30.

Yu, X., Klejnot, J., Zhao, X., Shalitin, D., Maymon, M., Yang, H., Lee, J., Liu, X., Lopez, J. and Lin, C. (2007) *Arabidopsis* cryptochrome 2 completes its posttranslational life cycle in the nucleus. *Plant Cell* **19**, 3146–3156.

Yu, X., Liu, H., Klejnot, J. and Lin, C. (2010) The cryptochrome blue light receptors. *The Arabidopsis Book* **8**, e0135.

Zazímalová, E., Murphy, A.S., Yang, H., Hoyerová, K. and Hosek, P. (2010) Auxin transporters–why so many? *Cold Spring Harb Perspect Biol* **2**, a001552.

Zheng, X., Wu, S., Zhai, H., Zhou, P., Song, M., Su, L., Xi, Y., Li, Z., Cai, Y., Meng, F., Yang, L., Wang, H. and Yang, J. (2013) *Arabidopsis* phytochrome b promotes SPA1 nuclear accumulation to repress photomorphogenesis under far-red light. *Plant Cell* **25**, 115–133.

Zhu, D., Maier, A., Lee, J.H., Laubinger, S., Saijo, Y., Wang, H., Qu, L.J., Hoecker, U. and Deng, X.W. (2008) Biochemical characterization of *Arabidopsis* complexes containing CONSTITUTIVELY PHOTOMORPHOGENIC1 and SUPPRESSOR OF PHYA proteins in light control of plant development. *Plant Cell* **20**, 2307–2323.

Zuo, Z., Liu, H., Liu, B., Liu, X. and Lin, C. (2011) Blue light-dependent interaction of CRY2 with SPA1 regulates COP1 activity and floral initiation in arabidopsis. *Curr. Biol.* **21**, 841–847.

Supplement

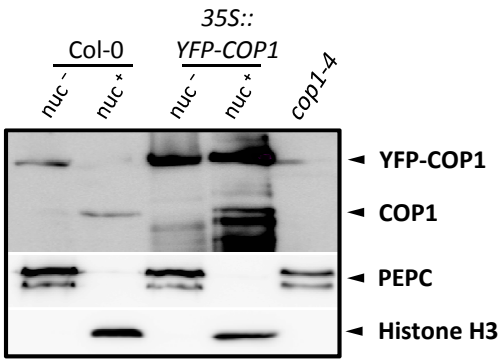

Supplemental Figure S1: YFP-COP1 is present both in the cytosol and in the nucleus. Immunodetection of YFP-COP1 and native COP1 protein in nuclei-depleted (nuc^-) and nuclei-enriched (nuc^+) protein fractions of 4-d-old dark-grown Col-0 and *35S::YFP-COP1* seedlings. Both proteins were detected using an anti-COP1 antibody. PEPC was used as a cytosolic marker, Histone H3 was used as a nuclear marker. The nuclei-enriched fractions were 15 × concentrated compared to the nuclei-depleted fractions.

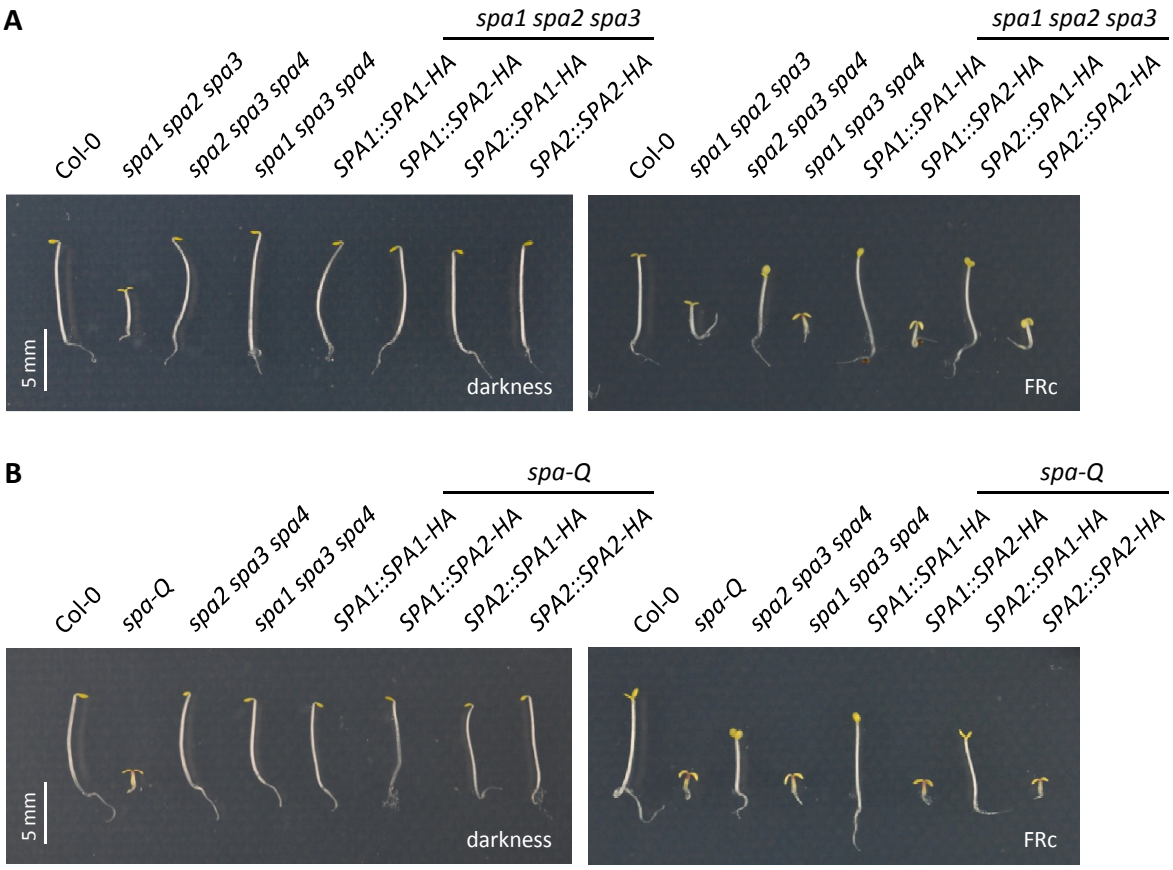

Supplemental Figure S2: The *SPA1* and *SPA2* ORFs confer different repressor functions in light-grown seedlings.
A: Visual phenotype of 4-d-old transgenic *spa1 spa2 spa3* seedlings expressing the chimeric *SPA1*/*SPA2* constructs shown in Figure 1.4 A. Seedlings were grown in darkness or FRc ($0.35\,\mu mol\,m^{-2}\,s^{-1}$). Col-0 and *spa* triple mutant seedlings are shown as controls. **B:** Visual phenotype of 4-d-old transgenic *spa-Q* seedlings expressing the chimeric *SPA1*/*SPA2* constructs shown in Figure 1.4 A. Seedlings were grown in darkness or FRc ($0.35\,\mu mol\,m^{-2}\,s^{-1}$). Col-0, *spa-Q* and *spa* triple mutant seedlings are shown as controls.

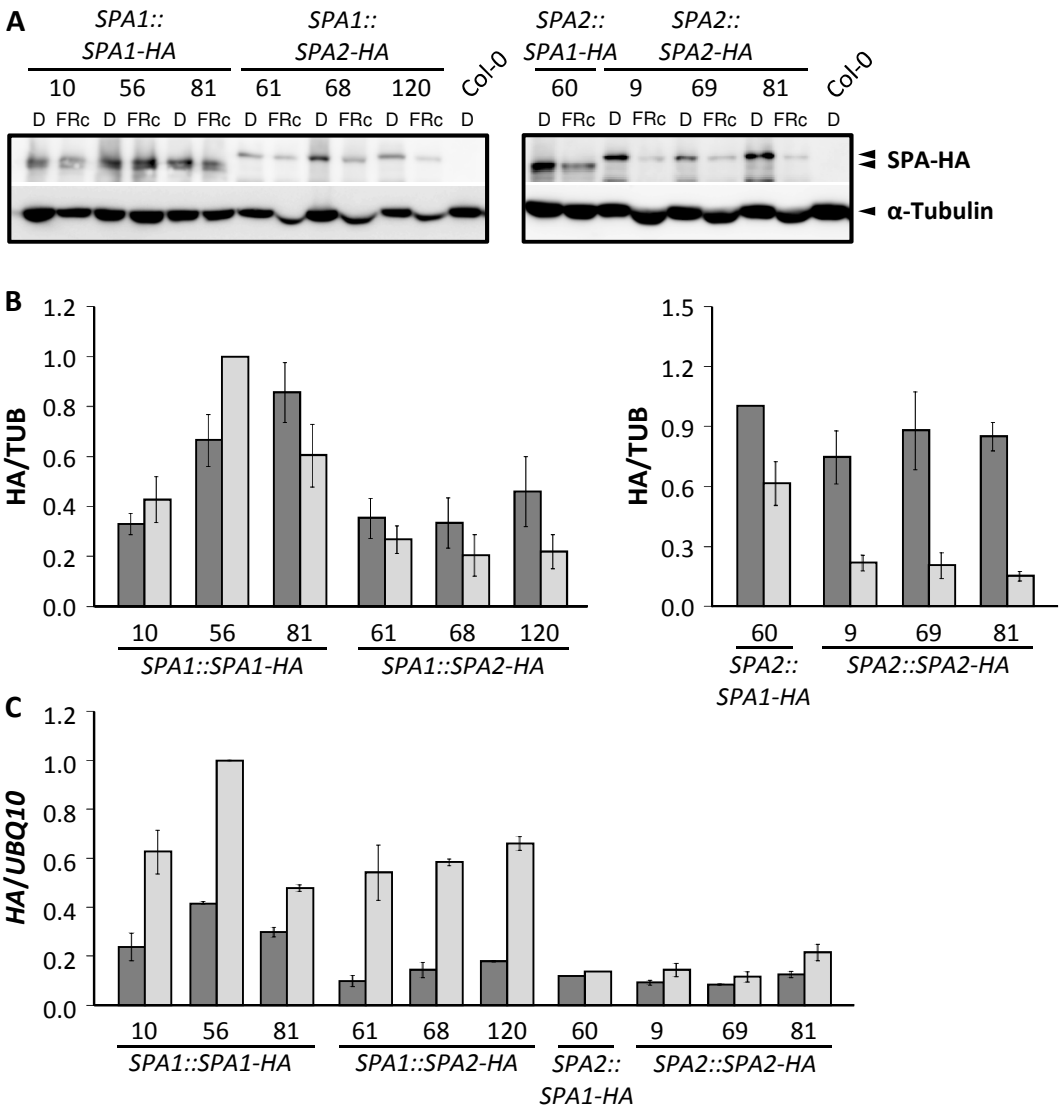

Supplemental Figure S3: SPA2-HA protein accumulates to lower levels than SPA1-HA protein in the *spa-Q* mutant background.
A, B: Immunodetection (A) and quantification (B) of SPA1-HA and SPA2-HA protein levels in 4-d-old transgenic *spa-Q* mutant seedlings grown in darkness or FRc ($0.35\,\mu mol\,m^{-2}\,s^{-1}$). SPA1-HA and SPA2-HA were expressed from the *SPA1* promoter (left) and *SPA2* promoter (right), respectively, and detected using an anti-HA antibody. Numbers indicate independent transgenic lines. Tubulin levels are shown as loading control. Protein levels were normalised to tubulin levels and expressed relative to the respective highest-accumulating line. **C:** Transcript levels of *SPA1-HA* and *SPA2-HA* in darkness or FRc in the lines shown in A. Transcript levels were normalised to *UBQ10* and calibrated to the highest-expressing line.
Error bars represent the SEM.

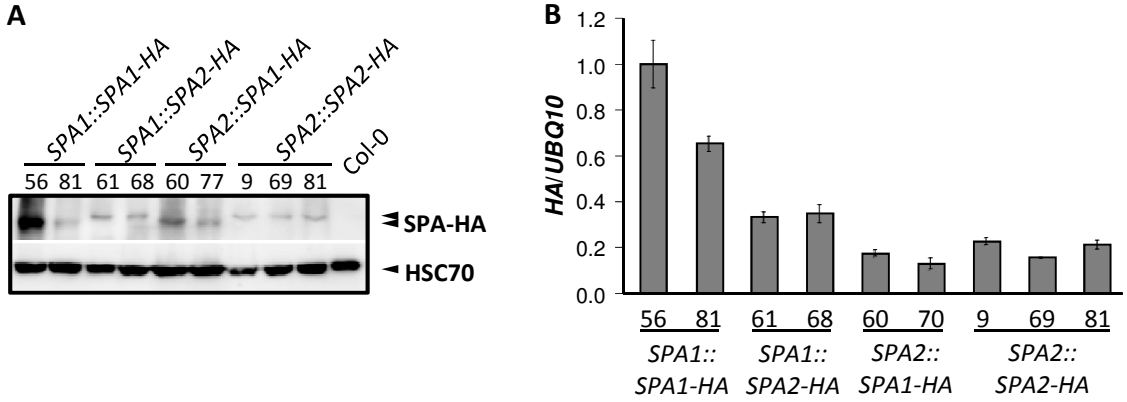

Supplemental Figure S4: SPA2-HA protein accumulates to lower levels than SPA1-HA protein in adult transgenic *spa-Q* plants. A: Immunodetection of SPA1-HA and SPA2-HA proteins in 33-d-old transgenic *spa-Q* plants grown in short day. SPA1-HA and SPA2-HA were detected using an anti-HA antibody. Numbers indicate independent transgenic lines. HSC70 levels are shown as loading control. **B:** Transcript levels of *SPA1-HA* and *SPA2-HA* in the lines shown in A. Transcript levels were normalised to *UBQ10* and calibrated to the highest-expressing line.
Error bars represent the SEM.

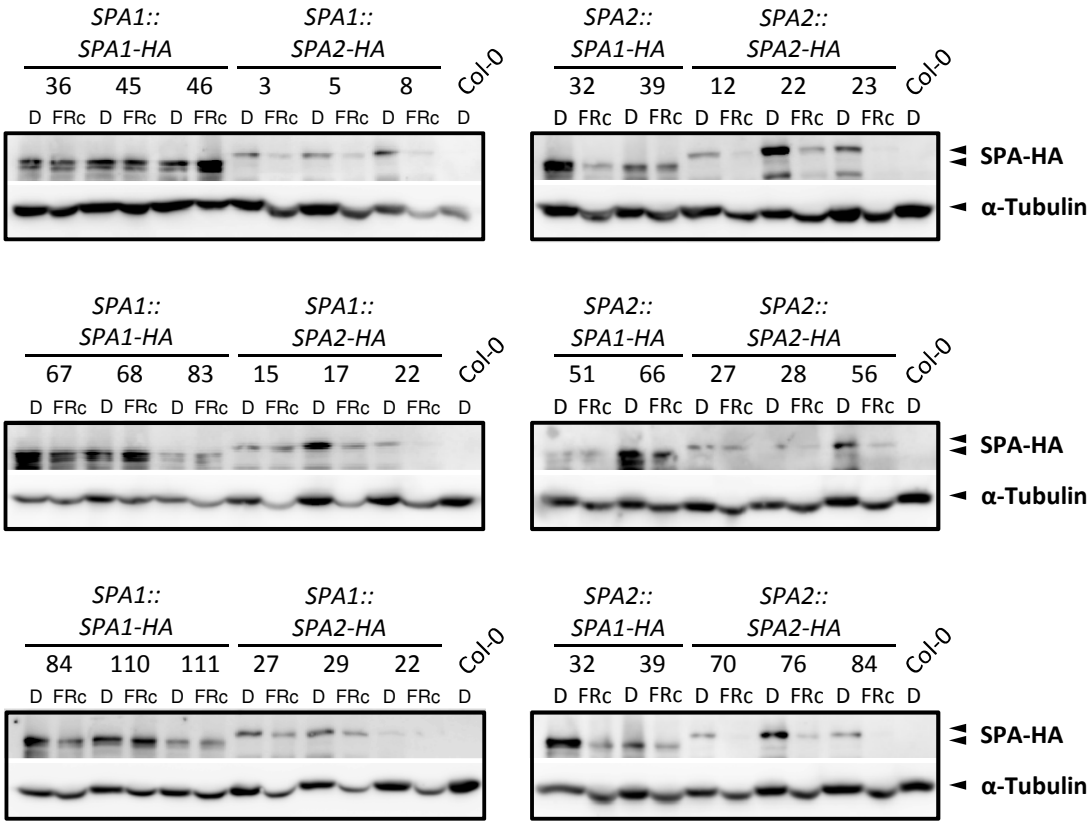

Supplemental Figure S5: SPA1-HA and SPA2-HA protein levels in dark- and FRc-grown seedlings of additional transgenic lines expressing the chimeric *SPA1/SPA2* constructs. Imunodetection of SPA1-HA and SPA2-HA protein levels in 4-d-old transgenic *spa1 spa2 spa3* seedlings grown in darkness or FRc ($0.35\,\mu mol\,m^{-2}\,s^{-1}$). Independent transgenic lines expressing SPA1-HA or SPA2-HA from the *SPA1* promoter (left) and *SPA2* promoter (right), respectively, were analysed. SPA-HA proteins were detected using an anti-HA antibody. Numbers indicate independent transgenic lines. Tubulin levels are shown as loading control.

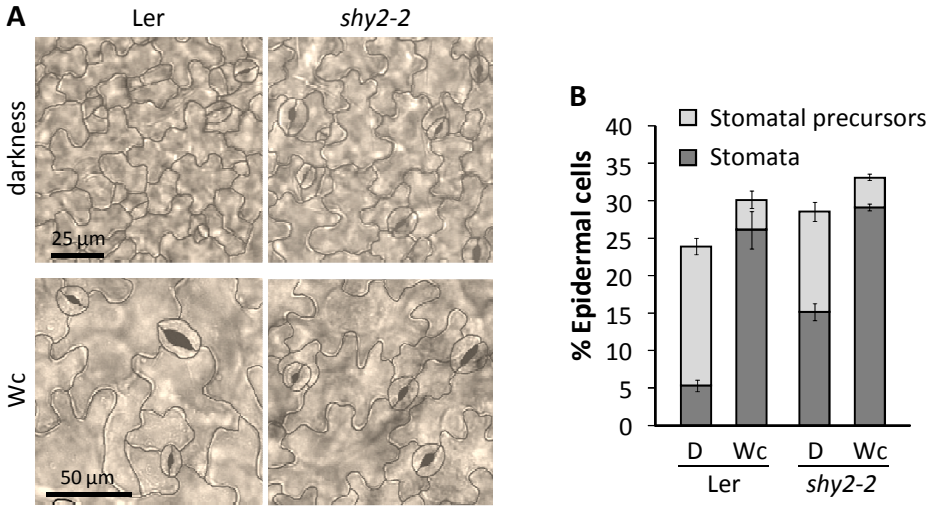

Supplemental Figure S6: The *shy2-2* mutant shows increased stomata formation in darkness. **A:** Brightfield images of the abaxial cotyledon epidermis of 10-d-old seedlings of the indicated genotypes grown in darkness or Wc ($25\,\mu mol\,m^{-2}\,s^{-1}$). Cell outlines were traced in dark grey. **B:** Quantification of stomata and stomatal precursors of the genotypes shown in A. Error bars represent the SEM (n = 10).

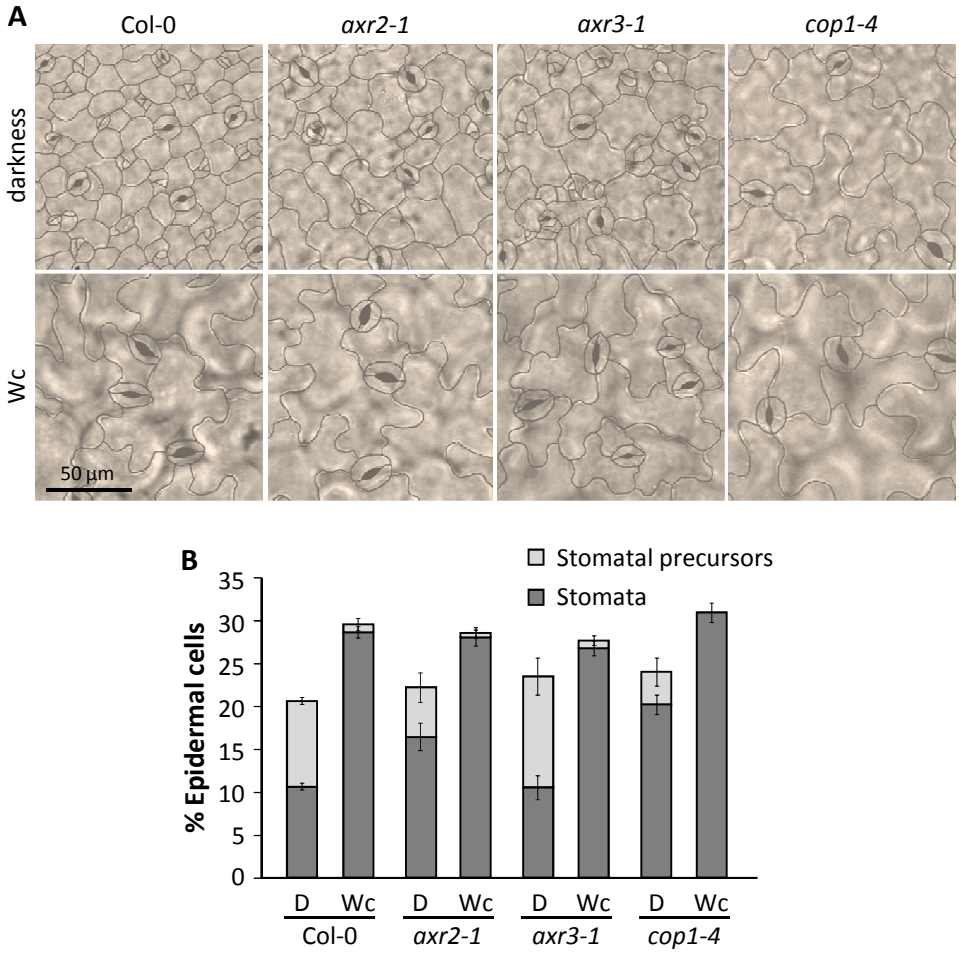

Supplemental Figure S7: *axr2-1*, but not *axr3-1*, shows an increased SI in the adaxial epidermis.
A: Brightfield images of the adaxial epidermis of 10-d-old seedlings of the indicated genotypes grown in darkness or Wc (25 µmol m^{-2} s^{-1}). Cell outlines were traced in dark grey. **B:** Quantification of stomata and stomatal precursors of the genotypes shown in A. Error bars represent the SEM (n = 10).

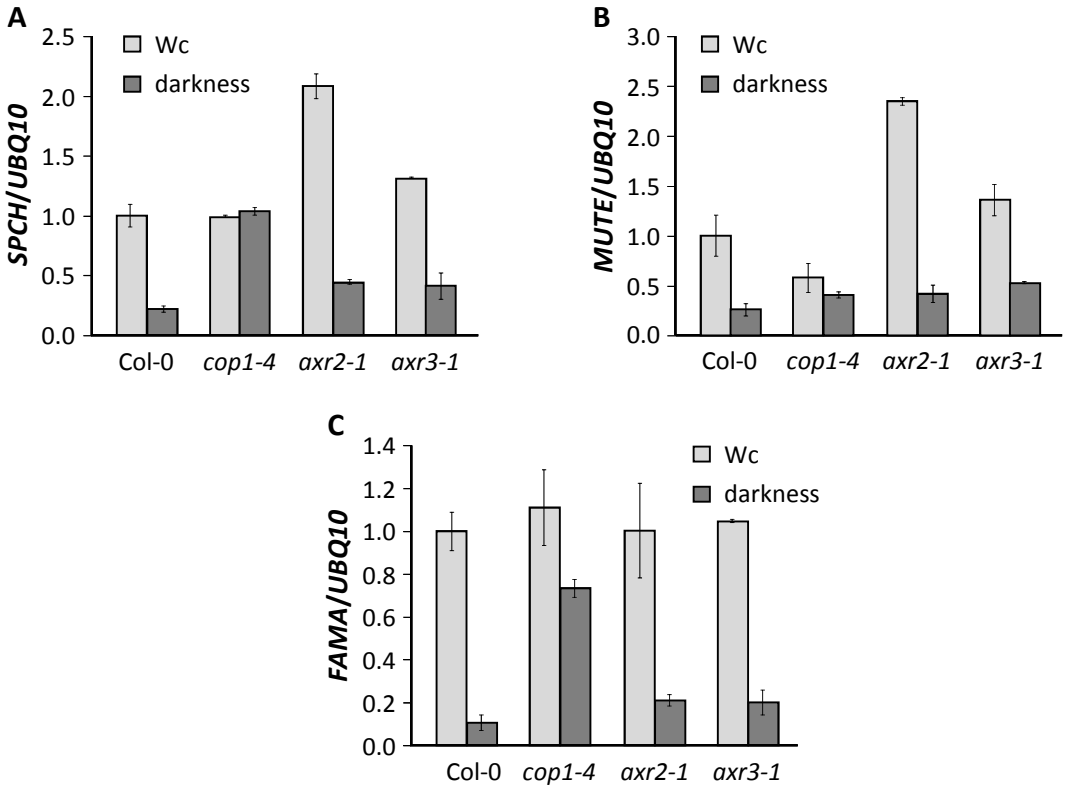

Supplemental Figure S8: Expression of *SPCH*, *MUTE* and *FAMA* is not strongly altered in dark-grown *axr2-1* and *axr3-1* seedlings.
Transcript levels of *SPCH* (A), *MUTE* (B) and *FAMA* (C) in 5-d-old dark- and Wc-grown seedlings of the indicated genotypes. Transcript levels were normalised to *UBQ10* and calibrated to the levels of Wc-grown Col-0 seedlings. Error bars represent the SEM of three biological replicates.

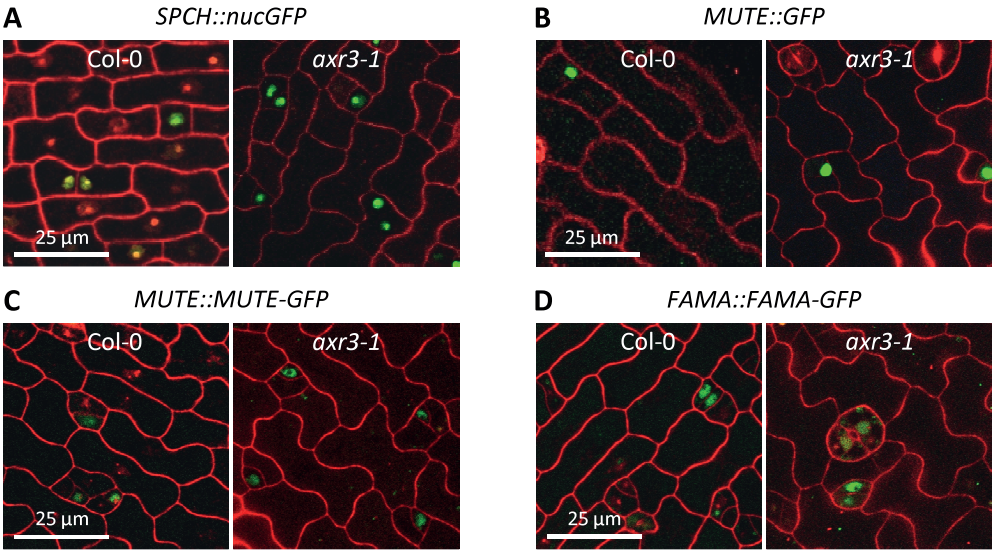

Supplemental Figure S9: Expression and localisation of transcriptional and translational reporters of *SPCH*, *MUTE* and *FAMA* are not altered in *axr3-1*.
A: Confocal images of the abaxial cotyledon epidermis of 3-d-old dark-grown Col-0 and *axr3-1* seedlings expressing a *SPCH::nucGFP* construct. **B:** Confocal images of the abaxial cotyledon epidermis of 5-d-old dark-grown Col-0 and *axr3-1* seedlings expressing a *MUTE::GFP* construct. **C, D:** Confocal images of the abaxial cotyledon epidermis of 5-d-old dark-grown Col-0 and *axr3-1* seedlings expressing a *MUTE::MUTE-GFP* (C) or a *FAMA::FAMA-GFP* (D) construct.
Cell outlines were visualised by PI staining.

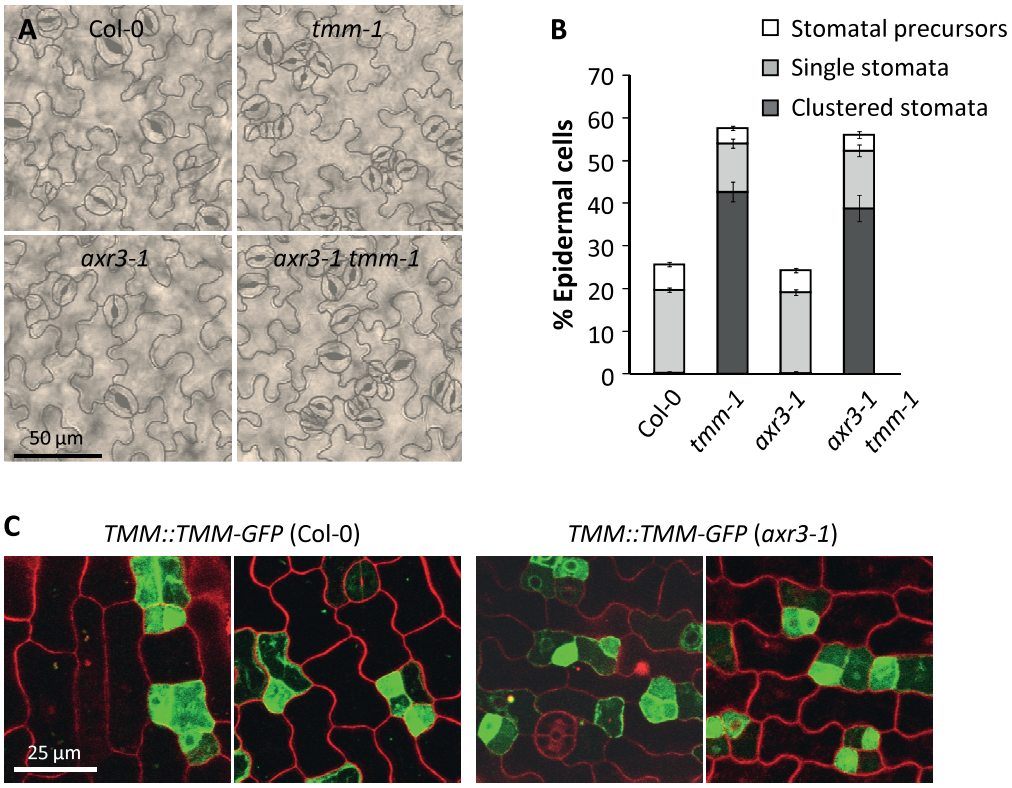

Supplemental Figure S10: The *axr3-1* mutation has no effect on the phenotype of Wc-grown *tmm-1* mutant seedlings, nor on the expression and localisation of TMM-GFP.
A: Brightfield images of the abaxial cotyledon epidermis of 10-d-old seedlings of the indicated genotypes grown in Wc (25 µmol m^{-2} s^{-1}). Cell outlines were traced in dark grey. **B:** Quantification of stomata and stomatal precursors of the genotypes shown in A. Error bars represent the SEM (n = 10). **C:** Confocal images of the abaxial cotyledon epidermis of 5-d-old dark-grown Col-0 and *axr3-1* seedlings expressing a *TMM::TMM-GFP* construct. Cell outlines were visualised by PI staining.

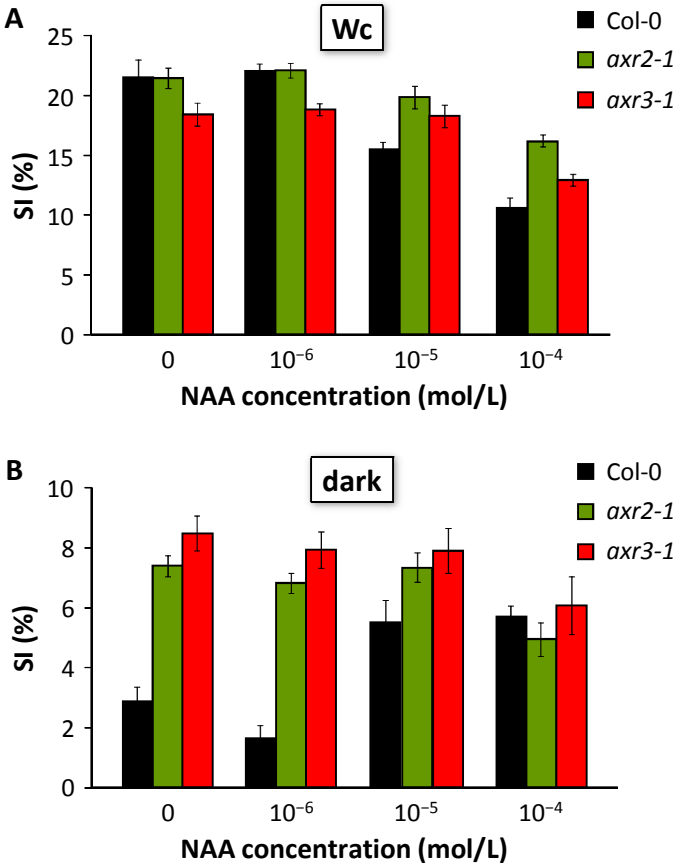

Supplemental Figure S11: NAA treatment affects stomatal development in dark- and light-grown seedlings.
SI of the abaxial cotyledon epidermis of 10-d-old Col-0, *axr2-1* and *axr3-1* seedlings grown in Wc (25 µmol m^{-2} s^{-1}) (A) or darkness (B) when treated with different concentrations of NAA. Error bars represent the SEM (n = 10).

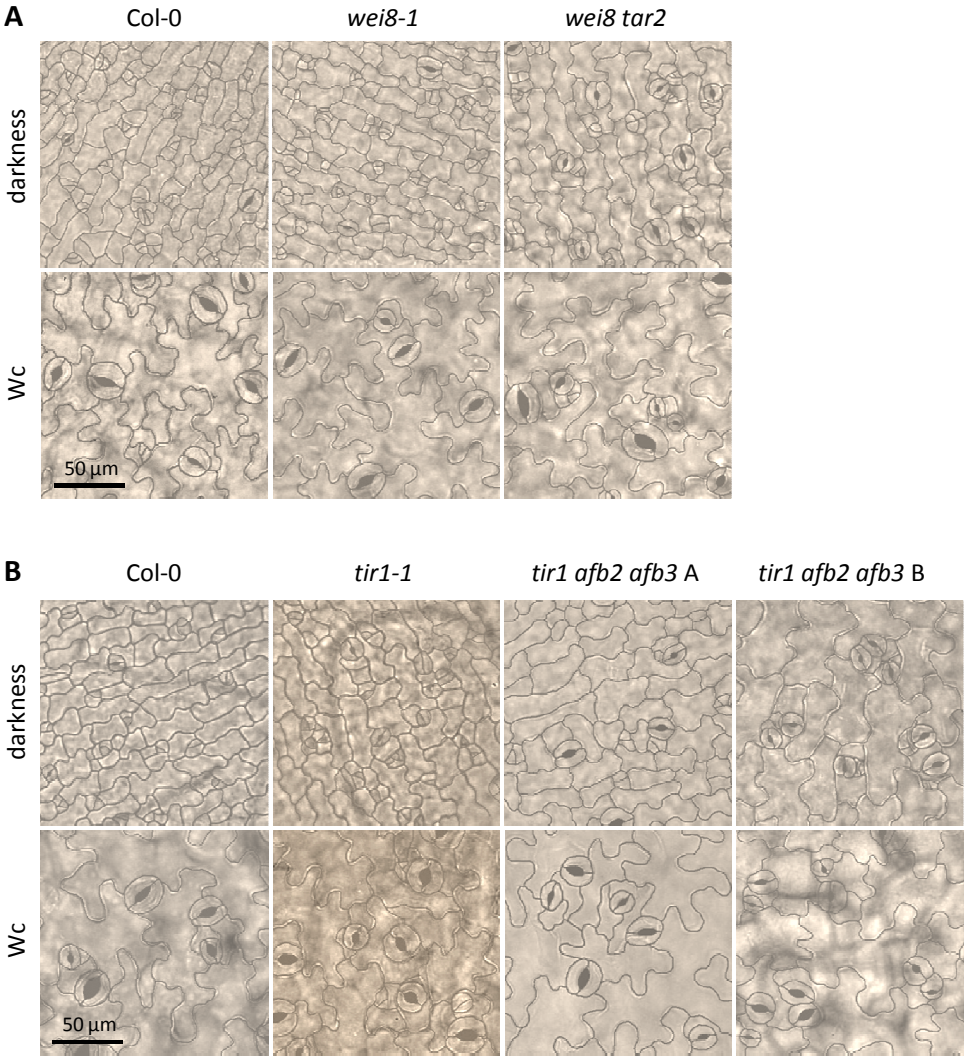

Supplemental Figure S12: Auxin mutants show altered stomatal phenotypes.
Brightfield images of the abaxial cotyledon epidermis of 10-d-old seedlings of auxin biosynthesis (A) and auxin receptor mutants (B) grown in darkness or Wc (25 µmol m^{-2} s^{-1}). Cell outlines were traced in dark grey.

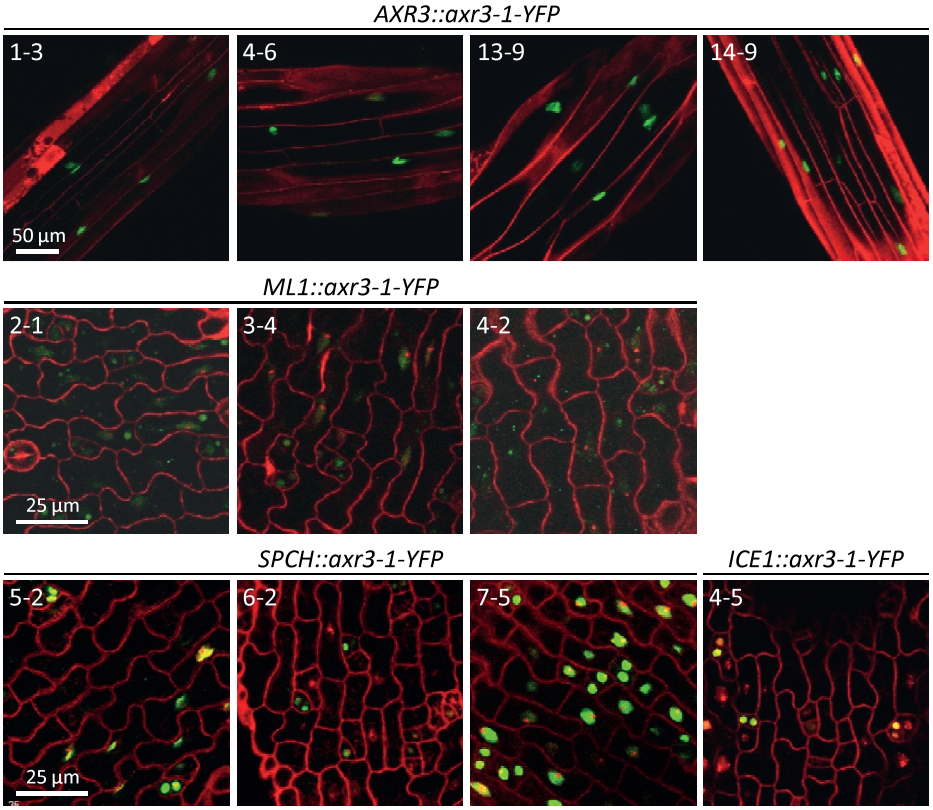

Supplemental Figure S13: Accumulation of axr3-1-YFP protein in dark-grown seedlings of additional *promoter::axr3-1-YFP* lines.
Confocal images of the hypocotyl of Col-0 seedlings expressing axr3-1-YFP from the *AXR3* promoter (5 dpg, upper panel) and of the abaxial cotyledon epidermis of Col-0 seedlings expressing axr3-1-YFP from the *ML1* (5 dpg, middle panel), *SPCH* (3 dpg, lower panel) and *ICE1* (5 dpg, lower panel) promoters. Cell outlines were visualised by PI staining.

Acknowledgements

First and foremost, I want to thank Prof. Dr. Ute Höcker for her excellent supervision during the last four years. I especially appreciate that she not only supported me with persistent help and advice but also encouraged me to think and work independently; this is something I will always benefit from in the future. I am also grateful to Prof. Dr. Martin Hülskamp for being the second examiner of my thesis and to Prof. Dr. Wolfgang Werr for being the head of my examination committee.

I want to thank all past and present members of the Höcker lab. Special thanks go to Kirsten, Alex, Petra, Aashish, Sebastian and Gabi for their warm welcome and for getting me started in the lab. But thanks also go to Leonie, Stefan, Xu, Stephen, Song, Natalia, Lisa and Eva for being not only great colleagues, but also good friends. I really enjoyed all our scientific (and non-scientific) discussions, lab outings, conference visits, parties and "thirsty Thursdays". I want to thank all "Hiwis" for helping me a lot with my work, especially Laura, who also worked with me as a Master student on the stomata project. I would also like to acknowledge the greenhouse staff for their help with growing plants and the workshop staff for keeping all our equipment running.

I would like to extend my "thank you" to the co-workers of the Bucher, Flügge and Hülskamp labs, who were very supportive in any kind of way. In particular, I would like to mention Benni, Karl and Nils, who already were or became close friends during the last years and made every day at work enjoyable. Karl as well as Leonie are also duly acknowledged for their help in correcting my thesis.

Furthermore, I want to thank those of my friends that I have not mentioned so far, especially Alex, Andrea, Christian, Melvin, Nicole, Paul, Philipp and Steffen. The last four years have not always been easy, but you guys made these years a great time nonetheless!

Finally, I wish to express my deepest gratitude to my parents, who always supported me and encouraged me to do the things in life I want to do. My father passed away before his time, but both he and my mother made me the person I am today, and I am truly thankful for that.

Erklärung

Ich versichere, dass ich die von mir vorgelegte Dissertation selbständig angefertigt, die benutzten Quellen und Hilfsmittel vollständig angegeben und die Stellen der Arbeit – einschließlich Tabellen, Karten und Abbildungen –, die anderen Werken im Wortlaut oder dem Sinn nach entnommen sind, in jedem Einzelfall als Entlehnung kenntlich gemacht habe; dass diese Dissertation noch keiner anderen Fakultät oder Universität zur Prüfung vorgelegen hat; dass sie – abgesehen von unten angegebenen Teilpublikationen – noch nicht veröffentlicht worden ist sowie dass ich eine solche Veröffentlichung vor Abschluss des Promotionsverfahrens nicht vornehmen werde.

Die von mir vorgelegte Dissertation ist von Prof. Dr. Ute Höcker betreut worden.

Martin Balcerowicz

Teilpublikationen:

Balcerowicz, M., Fittinghoff, K., Wirthmueller, L., Maier, A., Fackendahl, P., Fiene, G., Koncz, C. and Hoecker, U. (2011) Light exposure of Arabidopsis seedlings causes rapid de-stabilization as well as selective post-translational inactivation of the repressor of photomorphogenesis SPA2. *Plant J.* **65**, 712-723.

Lebenslauf

Martin Balcerowicz

Lothringer Straße 85
50677 Köln
Tel. (mobil): 0171 7249323
E-mail: martin.balcerowicz@gmx.de

Persönliche Daten

◆ Geburtsdatum	23.09.1984
◆ Geburtsort	Neuss

Schulausbildung

◆ 1995-2004	Norbert Gymnasium Knechtsteden, Dormagen
◆ 26.06.2004	Abschluss: Allgemeine Hochschulreife

Hochschulausbildung

◆ 10/2004-08/2009	Studium der Biologie (Diplom) an der Universität zu Köln
◆ 11/2008-08/2009	Externe Diplomarbeit in der School of Biological Sciences, Auckland, Neuseeland, unter Betreuung von Prof. Dr. Joanna Putterill Titel: "Analysis of the Genetic Regulation of Photoperiodic Flowering in the Model Legume *Medicago truncatula*"
◆ 11.08.2009	Abschluss: Diplom in Biologie (Gesamtnote: sehr gut)
◆ seit 10/2009	Promotion am Botanischen Institut der Universität zu Köln unter Betreuung von Prof. Dr. Ute Höcker Titel: "Genetic and Biochemical Characterisation of Light Signalling Events during Arabidopsis Seedling and Stomata Development"

Berufliche Erfahrungen

◆ 01/2002	Betriebspraktikum im UVE Labor für Umweltanalytik, Neuss
◆ 10/2005-01/2008	Nachhilfetätigkeit beim ABACUS Nachhilfeinstitut, Wuppertal
◆ 03/2007-07/2008	Studentische Hilfskraft am Botanischen Institut der Universität zu Köln
◆ seit 01/2010	Wissenschaftlicher Mitarbeiter an der Universität zu Köln
◆ 26.05.2011	Organisation des Botanischen Forschungskolloquiums 2011 der Universität zu Köln

Publikationen

- **Balcerowicz, M.**, Fittinghoff, K., Wirthmueller, L., Maier, A., Fackendahl, P., Fiene, G., Koncz, C. and Hoecker, U. (2011) Light exposure of Arabidopsis seedlings causes rapid de-stabilization as well as selective post-translational inactivation of the repressor of photomorphogenesis SPA2. *Plant J.* 65, 712-723.
- Yeoh, C.C., **Balcerowicz, M.**, Laurie, R., Macknight, R., Putterill, J. (2011) Developing a method for customized induction of flowering. *BMC Biotechnol.* 11: 11-36.
- Yeoh, C.C., **Balcerowicz, M.**, Zhang, L., Jaudal, M., Brocard, L., Ratet, P., Putterill, J. (2013) Fine mapping links the *FTa1* flowering time regulator to the dominant *spring1* locus in Medicago. *PLoS One* 8: e53467.

Teilnahme an wissenschaftlichen Konferenzen

09/2010	9th Tri-National Arabidopsis Meeting, Salzburg, Österreich
07/2011	2011 International Symposium on Plant Photobiology, Peking, China
07/2012	23rd International Conference on Arabidopsis Research, Wien, Österreich
06/2013	2013 International Symposium on Plant Photobiology, Edinburgh, Schottland

Preise

09/2010	Posterpreis des 9th Tri-National Arabidopsis Meeting, Salzburg, Österreich
06/2013	Posterpreis des International Symposium on Plant Photobiology, Edinburgh, Schottland

Weiterbildungen

04/2012	Scientific Writing Kurs, BioScript, Graduate School for Biological Sciences, Universität zu Köln

Persönliche Qualifikationen

Fremdsprachen	Englisch fließend in Wort und Schrift Grundkenntnisse in Französisch und Spanisch
EDV-Kenntnisse	MS Office, LaTeX, R

Interessen

Privat	Literatur, Zeichnen, Reisen, Schwimmen, Schach
Berufsbezogen	Molekularbiologie, Biochemie